ORIGIN AND DEVELOPMENT OF

THE APALACHICOLA BASIN

by

IAN HUNTER

DELORES M. ROBINSON, COMMITTEE CHAIR
ANDREW M. GOODLIFFE
IBRAHIM ÇEMEN
AMY WEISLOGEL

A THESIS

Submitted in partial fulfillment of the requirements
for the degree of Master of Science
in the Department of Geological Sciences
in the Graduate School of
The University of Alabama

TUSCALOOSA, ALABAMA

2014

ABSTRACT

Seismic mapping, restorations and subsidence analysis suggest an initial phase of rifting created the Apalachicola Basin during Late Triassic-Middle Jurassic time. A later period of rifting occurred during Late Jurassic-Early Cretaceous time, extending the basin towards the southwest. Subsidence analysis implies that tectonic hinge zones do not mark crustal boundaries; however, they may be tilted crustal blocks associated with reactivation of a pre-existing Paleozoic lineament or fault.

Basin restorations demonstrate that since Late Jurassic time, the two major controls on basin paleogeography are salt movement and subsidence. A massive differential sediment load between the northeastern and southwestern Apalachicola Basin enabled updip migration of salt into the large Destin Dome salt anticline and the surrounding diapir field. Comparison of restorations with expulsion timing from Upper Jurassic and Lower Cretaceous source rocks indicates that structural traps against salt were in place prior to the expulsion of hydrocarbons.

Formation of the Apalachicola Basin is consistent with the steer's head model of basin formation that invokes a simple two layer stretching model. Overall similarities in basin geometry, orientation, sedimentation and subsidence indicate that the Apalachicola Basin and the Tampa Embayment formed in a similar manner. Determining the extent of these basins helps to determine the geometry and distribution of Triassic and Jurassic sedimentary rocks.

LIST OF ABBREVIATIONS AND SYMBOLS

<	Less than
>	Greater than
B	Beta (extension factor)
BOEM	Bureau of Ocean Energy Management
BSE	Base of Salt or Equivalent
DD	Destin Dome
ft	Feet
K/P	Cretaceous/Paleogene
Km	Kilometer
Ma.	Million Years Ago
m	Meter
MCSB	Mid Cretaceous Sequence Boundary
MCU	Mid Cretaceous Unconformity
mm	millimeter
PSTM	Pre Stack Time Migrated
PSDM	Pre Stack Depth Migrated
s	second
SDR	Seaward Dipping Reflector

TTS	Total Tectonic Subsidence
WDMA	World Digital Magnetic Anomaly
GoM	Gulf of Mexico
EGoM	Eastern Gulf of Mexico
yr	Year

ACKNOWLEDGEMENTS

I definitely wouldn't have completed this thesis without the support of my advisor, Dr. Delores Robinson. The many talks we have had were as much about life as about geology. Her advice kept me sane throughout a process that was frustrating at times. I would also like to thank my other advisors Drs. Andrew Goodliffe, Ibrahim Cemen and Amy Weislogel for their constructive critiques during the past two years.

This project is funded by Murphy Oil Corporation whom I had the pleasure of interning with during the summer of 2013. I would particularly like to thank Mike Harbin, Alex Blacque and Adam Seitchik for taking me under their wing. Talks with Lance Wilson provided me with many useful ideas and inspiration for this project. The seismic data that made this project possible were donated by Spectrum Seismic and well data were donated by TGS. The University of Alabama Research and Travel Fund and The Department of Geological Sciences' Johnson Fund were a great asset that allowed me to attend multiple meetings, conferences, and training sessions. The Department of Geological Sciences provided support through graduate research and teaching assistantships.

I would also like to thank my fellow lab mates and friends Andrea Gregg, Subhadip Mandal, Subodha Khanal, Will Jackson, Craig Cato, Levi Crooke, Joel Legg, Jordan Graw, Lindsey Kenyon, Doug Mateas, Ryan Feiner, Aycan Yildirim and Jason Ng for being so supportive and for answering even my dumbest questions. Connie and Tom Hunter were considerate enough to let me rant to them and tell me they like me! Talks with them always help

boost my self-esteem.

Finally, thanks to Chipotle for making an outstanding burrito at a price that is quite reasonable, The University of Alabama Dining Halls which helped satiate my hunger for knowledge as well as endless pizza, and Publix for always having bananas available.

CONTENTS

LIST OF TABLES

LIST OF FIGURES

1. INTRODUCTION

The geologic history of the Eastern Gulf of Mexico (EGoM) is not as thoroughly studied as the rest of the Gulf of Mexico (GoM) because of a ban on commercial drilling until the year 2022 within the federal waters of Florida. However, recent successful exploration wells in the northern EGoM have incentivized further geologic investigation. The Apalachicola Basin is located 10 km east of the drilling moratorium boundary. The commercial successes of the Appomattox (MC 392), Vicksburg (DC 353), Shiloh (DC 269) and Antietam (DC 268) wells make the Apalachicola Basin appealing.

Throughout the GoM, debate continues over rift timing and mechanisms, crustal boundaries, emplacement of oceanic crust, subsalt tectonics and distribution of basin subsidence. Because of a 3-4 km thick salt layer and up to 10 km of Cenozoic overburden on top of Jurassic and Cretaceous rocks in much of the northern GoM, analysis of subsalt events is difficult (Martin, 1978, 1980). The EGoM however, has relatively thin salt and less overburden, making it an ideal location to study Early Mesozoic tectonics.

This study focuses on the Apalachicola Basin, a northeast-southwest trending basin formed during rifting of the Pangean supercontinent (Winkler and Buffler, 1988; Salvador, 1991; Sawyer et al., 1991) (Fig. 1). The Apalachicola Basin is a sub-basin of the GoM and one of a series of basement basins and arches that bound the EGoM from the foothills of the Ouachita Mountains to South Florida. The Apalachicola Basin encompasses an area approximately 225 km long and 150 km wide.

The data set includes a series of PSTM (pre-stack time migrated) and PSDM (pre-stack depth migrated) seismic reflection lines and public well data. Three seismic lines are restored to identify distinct patterns of sedimentation and relate them to subsidence. Subsidence and sedimentation rates are calculated and aid in identifying a model for extension across the Apalachicola Basin. The model accounts for seismic observations within the Apalachicola Basin including Triassic grabens, uplifted rift flanks, patterns of Upper Jurassic sedimentary onlap onto adjacent arches and basin deposits. In addition, this study examines the relationship between crustal boundaries, tectonic hinge zones, salt tectonics and the Cretaceous carbonate shelf. Finally, the evolution of the Apalachicola Basin is compared with the neighboring Tampa Embayment by examining the faulting, sedimentary overburden and basement elevation to identify the timing of rifting and basement geometry within each basin.

1.1 Tectonic Setting

During Paleozoic time, the supercontinent of Pangea was formed through collisions between Gondwana and Laurentia (Thomas, 1976; Salvador, 1987), which ended by Late Permian time. This was followed by a period of relative stability until rifting began in the proto GoM during Late Triassic time (Salvador, 1987). Evidence for rifting exists in widespread basins and arches that rim the GoM basin along both the southern United States and the northern margin of Mexico (Galloway, 2008).

The GoM underwent two phases of rifting (Sawyer et al., 1991). The initial phase of rifting occurred from Late Triassic time to Late Middle Jurassic time as Gondwana separated from Laurentia. Extension in a northwest- southeast direction produced upper crustal to mid crustal thinning (Pindell, 1985; Buffler and Sawyer, 1985; Dunbar and Sawyer, 1987). In the EGoM, this phase of rifting is characterized by large, northeast trending normal faults and their

associated grabens and half grabens that are filled with non-marine red beds and volcanic rocks of the Eagle Mills Formation (Barnett, 1975; MacRae, 1993). The second phase of GoM formation occurred during Late Middle Jurassic time and may have culminated in oceanic crust emplacement (Salvador, 1991). Oceanic crust was first acknowledged in 1955 on the basis of seismic velocities of 6.8-7.2 km/s in the central GoM interior basin (Ewing et al., 1955; Sawyer et al., 1991). Buffler and Sawyer (1985) propose that a period of oceanic crust emplacement during the Middle or Late Jurassic lasted 5-10 million years. Many researchers (Pindell, 1985; Klitgord and Popenoe, 1984; Sawyer, 1991; Bird 1996) suggest that the orientation of second phase rifting was controlled by counter-clockwise motion of the Yucatan crustal block away from North America. The Yucatan block began rotating away at approximately 165 Ma and turned approximately 44° prior to reaching its present position along the southern portion of Mexico in Mid to Late Jurassic time (Bird, 2006).

By Late Jurassic time, passive margin subsidence was occurring and the extension between North and South America ceased (Salvador, 1987, 1991). Lithospheric cooling and sediment loading drove subsidence for the next 145 million years (Buffler and Sawyer, 1985). Many hypotheses have been put forward to explain GoM formation, including:

1. The GoM formed through simple shear extension as exhibited by asymmetrical distribution of crustal types and "differences in the sedimentary record between the northern and southern gulf" (Marton and Buffler, 1993).

2. The GoM opened up through counter clockwise rotation of the Yucatan crustal block aided by several major transform faults in the western and northeastern GoM (Buffler and Sawyer, 1985).

3. The GoM was created by a single transform system from the Florida straits to Mexico

that accommodated counterclockwise motion of the Yucatan block as well as southeast migration of a "Florida straits block" from north Florida to south Florida (Pindell, 1985).

4. The GoM opened after clockwise rotation (24°) of the Yucatan block out of West Texas was accompanied by large transform faults (Hall, 1984).

5. The GoM opened during eastward translation of the Yucatan block from eastern Mexico which was assisted by long northwest trending transfer zones extending all the way to the Caribbean (Klitgord et al., 1984).

6. The GoM formed as a back arc basin as evidenced by a north-south trending subduction zone in central Mexico as well as a relatively brief period of seafloor spreading in the central GoM Interior Basin (Stern and Dickinson, 2010).

The GoM most likely formed through a combination of these mechanisms involving rotation of the Yucatan crustal block, large transforms, tensional grabens, detachment faulting and sporadic volcanism.

The Apalachicola Basin is in the northern EGoM. Basins and arches in the EGoM include, from north to south, the Mississippi Interior Basin, Wiggins Arch, Pensacola Arch, Apalachicola Basin/Desoto Canyon, Middle Ground Arch/Southern Platform, Tampa Embayment, Sarasota Arch and South Florida Basin (Fig. 1). Previous work to determine both the formation of and Mesozoic sedimentation into the Apalachicola Basin and the surrounding EGoM include but is not limited to Addy and Buffler (1984), Wu (1990), Dobson (1990), Dobson and Buffler (1991,1997), MacRae (1993), MacRae and Watkins (1993, 1995,1996), and Mancini et al. (2001).

Most of the basins and arches within the EGoM are northeast trending and are located on thick transitional crust between 20-35 km thick (Dobson and Buffler, 1997). The crust thickens

toward the continent and thins toward the GoM interior basin. Crustal thickness throughout the Apalachicola Basin averages ~35 km (MacRae and Watkins, 1996). The boundaries between continental crust, thick transitional crust and thin transitional crust in the EGoM may be tectonic hinge zones, which are large northwest trending lineaments identified by a change in the dip of basement reflectors (Buffler and Sawyer, 1985; Salvador, 1991; Sawyer et al., 1991; Corso and Austin, 1995).

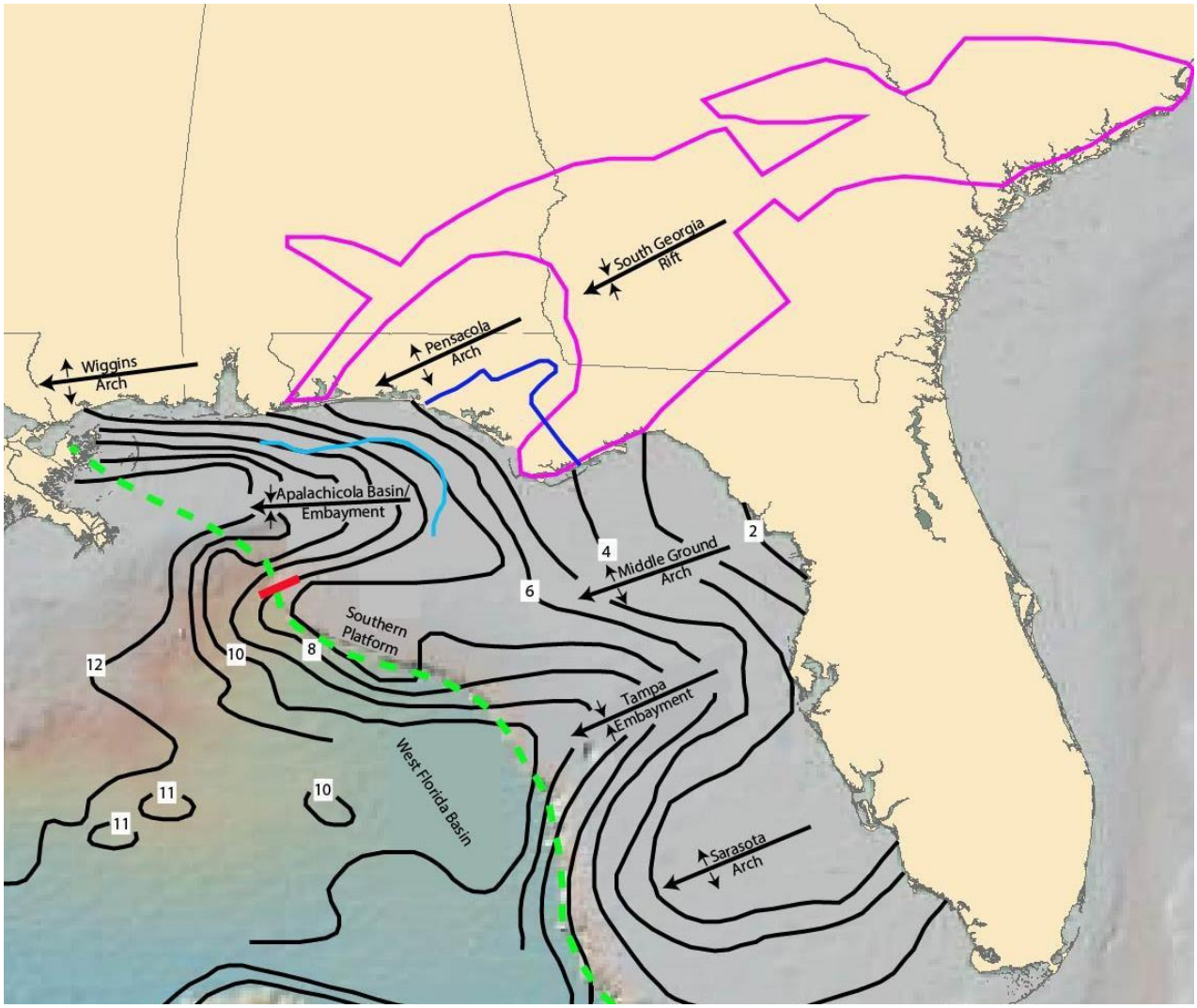

Figure 1: Map of EGOM with depth to basement overlay from Sawyer et al. (1991) (Black Contours). Contour intervals are in kilometers. Basins are marked by plunging syncline symbols and arches are mapped by a plunging anticline symbol. The dark blue line is the landward extent of Apalachicola Embayment from Mitchell-Tapping (1982). The pink line is the outline of the South Georgia Rift from McBride (1991). The dashed green line is the location of the

Cretaceous carbonate shelf after Mancini et al. (2001). The red line is the Desoto Canyon reentrant, north of which the Cretaceous carbonate shelf dips less than 10° and south of which it dips more than 10° (Winkler and Buffler, 1988). The light blue line is the trend of a tectonic hinge zone or step in the dip of basement reflectors after MacRae and Watkins (1993).

A predominant hypothesis regarding the formation of the Apalachicola Basin and other basins in the EGoM is that oblique extension occurred within a set of northwest trending strike slip faults that parallel the Florida coast, creating basins and arches (MacRae and Watkins, 1996). One modification to this model is that sinistral movement along the strike slip faults aided in the translation of the "Florida Straits Block" of South Florida from a position farther north than where it rests today (Pindell and Kennan, 2001).

The Apalachicola Basin is the southwest extension of the onshore Apalachicola Embayment that extends 100 km onshore (Mitchell-Tapping, 1982) (Fig. 1). The eastern (landward) boundary of the Apalachicola Embayment is the limit of observable continuous dipping basement features and coincides with the updip limits of Middle-Upper Jurassic deposits (Miller, 1982; Mitchell-Tapping, 1982). Arden (1974) identifies a 130,000 km^2 area of downwarped, southwest dipping, Late Devonian to Late Triassic age rock extending to the northeast from Apalachicola, Florida into southwestern Georgia that he considers to be one continuous basin. The area has been labelled as the Suwannee River Basin (Braunstein, 1957), the Suwannee Basin (King, 1961), the Southwest Georgia Embayment (Maher and Applin, 1968), the South Georgia Rift (Daniels et al., 1983) and the South Georgia Graben Complex (McBride, 1991) (Fig. 1). The term South Georgia Rift is used in this study.

The western Apalachicola Basin is bounded by a large carbonate shelf known interchangeably as the Cretaceous carbonate shelf, Florida escarpment and carbonate margin. To avoid confusion, the terms used here are the Cretaceous carbonate shelf or the carbonate shelf.

In the western part of the Apalachicola Basin, an area known as the Desoto Canyon Salt Basin is typically associated with a zone of Cenozoic sediment accumulation. This study will only refer to the Apalachicola Basin and the location within the Apalachicola Basin. The exception is the Desoto Canyon Diapir Field, which refers to a specific area of salt tectonics discussed in the Interpretations section. West of the Cretaceous carbonate shelf, the GoM Interior Basin encompasses the deep GoM basin. Lord (1986) identifies the West Florida Basin as the western extension of the more southerly Tampa Embayment. However, Lord does not extend the West Florida Basin north beyond the Southern Platform. The area west of the carbonate shelf bounding the Apalachicola Basin is identified as the GoM Interior Basin.

1.2 Stratigraphic Setting

Basement in this study is acoustic and defined as "all crustal rocks, including Late Triassic-Early Jurassic rift sequences beneath a widespread unconformity that are overlain by Middle Jurassic evaporites or equivalent rocks" (Buffler and Sawyer, 1985). The Base of Salt Equivalent (BSE) marks the top of the basement. The BSE is a 30 million year unconformity from Pliensbachian to Callovian time (Salvador, 1987), during which the EGoM remained emergent (Arden, 1974).

Late Triassic-Early Jurassic Eagle Mills Formation and Equivalent: Late Triassic-Early Jurassic sub-basement sediments include or are the equivalent of the Eagle Mills Formation, consisting of non-marine igneous volcanic rocks and high feldspar content red beds (Salvador, 1987). Deposits are found within offshore grabens and pinchout along graben margins (Arden, 1974; Klitgord and Popenoe, 1984). In the Apalachicola Embayment, below Triassic and Early Jurassic rocks, Paleozoic sedimentary rock, granite and other felsic volcanic rocks exist (Arden, 1974).

Late Middle Jurassic Louann Salt: These deposits represent an early marine transgression into the GoM when shallow hyper saline basins covered large areas of continental Pangea (Salvador, 1991). The ancestral GoM was connected to the Pacific Ocean but not yet to the Atlantic or Caribbean (Salvador, 1991). High rates of evaporation followed, leaving salt deposits as thick as 3-4 km in the GoM Interior Basin (Martin, 1978; 1980). Subsidence allowed shallow water conditions to be maintained throughout Callovian time (Martin, 1978). Subsequent marine transgressions were not restricted, causing deeper water conditions unsuitable for evaporite precipitation (Salvador, 1987). In the Apalachicola Basin, sediment loading and gravity related gliding caused ductile migration of salt from depocenters into the Destin Dome salt anticline in the northeast and the Desoto Canyon Diapir Field (MacRae, 1992) (Fig. 3A). The synchronous Werner Anhydrite, present in the northern GoM, is not found in the northeastern GoM (Dobson and Buffler, 1997).

Previous researchers (Lord, 1986; Salvador, 1987) identify a "salt basin" west of the Desoto Canyon Diapir Field and the Cretaceous carbonate shelf, extending northwest-southeast from the southwestern Apalachicola Basin to an area west of the Sarasota Arch (Fig. 3B). Salvador (1987) describes this salt basin as consisting of salt domes and diapirs, and Lord (1986) maps dense diapirs and pillow structures. Recent discoveries in the Shiloh (DC 269) and Vicksburg (DC 353) wells in this salt basin are associated with turtleback structures and salt rollers.

Early Late Jurassic Norphlet/Smackover Formations: The Oxfordian Norphlet Formation overlies the evaporites, and is a clastic unit that consists mostly of clean eolian, alluvial and wadi sands. The Norphlet Formation sands are a high quality reservoir in Mesozoic petroleum plays, and for this reason, its distribution, thickness, and provenance in the EGoM is

important (Mancini et al., 2001; Lovell and Weislogel, 2010; Hunt, 2013). A facies change accompanies thickness variations, from wadi deposits in the northeast to eolian sands in the south and southwest (Hunt, 2013).

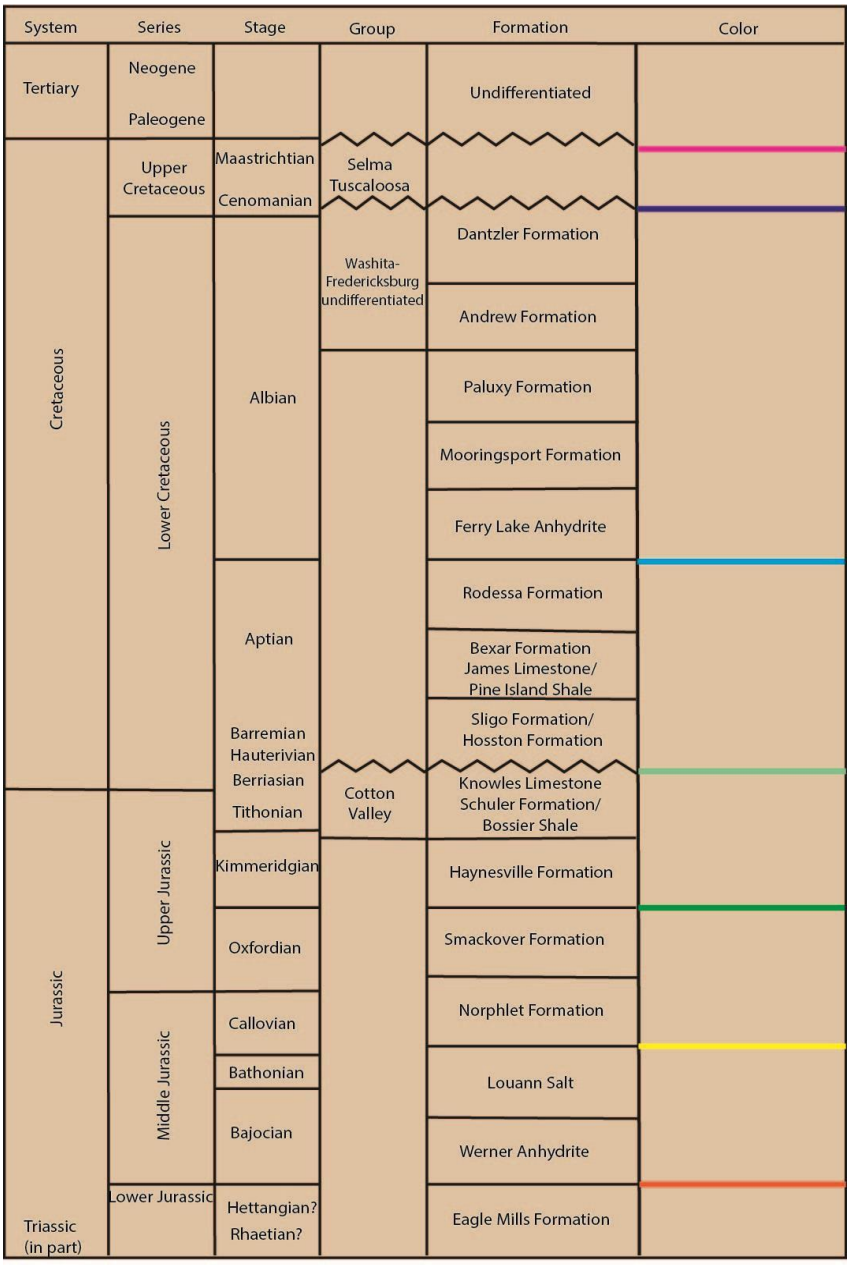

Figure 2: Stratigraphic chart of the EGoM, after Mancini et al. (2001). Colors indicate distinct horizons picked on seismic reflection lines in this study and match the colors in the seismic sections.

Above the Norphlet Formation, subtidal and intertidal carbonate mudstone, wackestone and packstone of the Smackover Formation were deposited by an Oxfordian rise in sea level (Mancini and Benson, 1980; Moore, 1984; Dobson, 1990). The Brown Dense lower member of the Smackover Formation is a high organic content source rock throughout most of the GoM. Mitchell-Tapping (1982) proposes that the lower Smackover Formation was deposited in less than 3 feet of water in a tidal flat environment. In the Apalachicola Basin, the Smackover Formation thickens from northeast to southwest (Dobson and Buffler, 1997). The combined thicknesses of the Norphlet and Smackover Formation varies from 300 m in the northeast to 900 m in the southwest with local accumulations as thick as 1,500 m in the west associated with salt movement (MacRae, 1993).

Late Jurassic-Early Cretaceous Haynesville/Cotton Valley Formations: The Kimmeridgian Haynesville Formation consists of marine shale, sand, and siltstone. Kimmeridgian time represents the first permanent marine transgression in the EGoM since the onset of rifting (Mancini et al., 2001). At this time, the first permanent connection to the Atlantic Ocean was established (Salvador, 1987). The Haynesville Formation is present throughout the Apalachicola Basin, grading from silty sandstone in the northeast to carbonate rocks in the southwest (Dobson and Buffler, 1997). The Tithonian Cotton Valley Formation consists of fluvial sandstone, shale, and carbonate rock (Addy and Buffler, 1984; Wu, 1990; Mancini et al., 2001). The last member is the Knowles Limestone, which is a proven Mesozoic source rock (Mancini et al., 2001). The combined thicknesses of the Haynesville and Cotton Valley formations vary from 900 m in the northeast to 2,300 m in the southwest (MacRae, 1993).

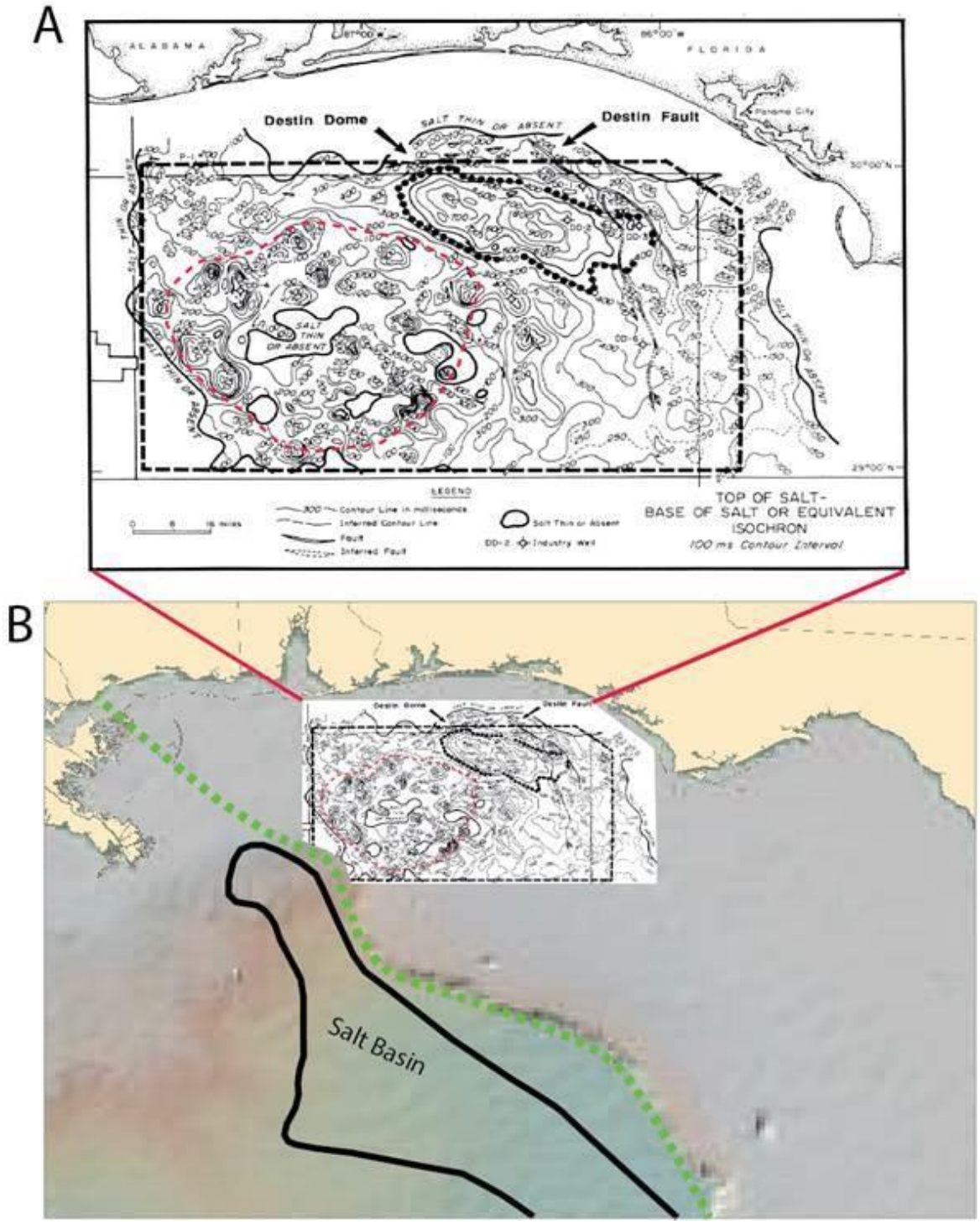

Figure 3 A: Salt isochron throughout the Apalachicola Basin from MacRae and Watkins (1992). Contour intervals are 100 ms. Black dots outline the Destin Dome. The dashed red line outlines the Desoto Canyon Diapir Field with ~15 large diapirs. Autochthonous salt occupies the southeast. B: The black line west of the carbonate shelf outlines a salt basin identified by Lord (1986). The dashed green line illustrates the location of the Cretaceous carbonate shelf.

Early Cretaceous-Cenozoic rock: Along the landward side of the Apalachicola Basin, fluvial deltaic and nearshore clastic sedimentation began during Early Cretaceous time and lasted until the end of Albian time (100 Ma), depositing 300-600 m of sandstone (Addy and Buffler, 1984) directly beneath the Mid Cretaceous Sequence Boundary (MCSB) (Corso and Austin, 1995). At the same time, toward the west, aggradation of the Cretaceous carbonate shelf began (Winkler and Buffler, 1988; Corso and Austin, 1990). The shelf continued to build until a drowning event between 96-93.9 Ma (Late Cenomanian time) (Corso and Austin, 1993, 1995). Lower Cretaceous rock thicknesses vary between 2,300 m in the northeast to 3,500 m in the west with pockets as thick as 3,900 m related to salt evacuation (MacRae, 1993). From about 94 to 30 Ma, the Apalachicola Basin was sediment starved as a result of flooding and the general lack of a fluvial sediment source (Wu, 1990). Since Oligocene time, relatively rapid sedimentation dominated the deeper portion of the Apalachicola Basin (Addy and Buffler, 1984) related to a migration of the eastern lobe of the Mississippi Delta. Beyond the carbonate shelf, fine-grained Early Cenozoic turbidites became coarser during Miocene time (Shaub et al., 1984; Addy and Buffler, 1984). However, **s**hallow water carbonate rock still dominated most of the EGoM (Mancini et al., 2001). Well cross-sections of Wu (1990) and Mancini et al. (2001) identify 1,200 m of Cenozoic section in the northeast. Addy and Buffler (1984) show Cenozoic rocks maintaining a thickness of 1.2-1.5 km westward until the Cretaceous carbonate shelf, where Cenozoic sediments taper to about half of that thickness (Wu, 1990). West of the Cretaceous carbonate shelf, there is 5 km of Oligocene and Miocene sedimentary rock in the GoM Interior Basin (Wu, 1990).

1.3 Tectonic Hinge Zones

Sawyer et al. (1991) identify tectonic hinge zones as an abrupt increase in the dip of basement dipping reflectors related to basin flexure; whereas, MacRae (1993) and Dobson (1997) identify them as a monoclinal step in the BSE related to large northwest trending normal faults. Formation of a hinge zone may be abrupt, forming as a fault boundary (Dobson and Buffler, 1997) or gradually, increasing in basinward dip with the continuation of subsidence.

In the Apalachicola Basin, two tectonic hinge zones are identified, near the eastern and western basin margins (Fig. 4). Dobson (1990) and Sawyer et al. (1991) speculate from seismic interpretations and the location of proposed crustal boundaries of Buffler and Sawyer (1985) (Fig. 5) that the eastern tectonic hinge zone marks the transition between continental crust and thick transitional crust and the western tectonic hinge marks the transition between thin and thick transitional crust. The western tectonic hinge is present along the Cretaceous carbonate shelf, possibly serving as a nucleus for carbonate aggradation. Sawyer et al. (1991) tie the onset of tectonic hinge formation with a change in the nucleus of spreading during rifting. In the GoM, Pindell (2010) interprets a change in the nucleus of spreading in the GoM resulting from a migration of the Yucatan Euler Pole from the EGoM to western Cuba, between Middle Jurassic to Earliest Cretaceous time. It is possible that a combination of Euler pole migration and increasing subsidence rates allowed the tectonic hinge zones to form.

1.4 Cretaceous Carbonate Shelf

The Cretaceous carbonate shelf is the western boundary of the Florida Platform, the wide shallow shelf that contains the Florida peninsula. The carbonate shelf originated during Late Jurassic-Early Cretaceous time (Winkler and Buffler, 1988; Corso and Austin, 1989). In the northern EGoM, margins are similar to those in Louisiana and East Texas with slopes < 10°

(Corso and Austin, 1989). The transition to steep shelf margins with slopes > 10° occurs in the southwest Apalachicola Basin at the Desoto Canyon reentrant (Fig. 1) (Winkler and Buffler, 1988).

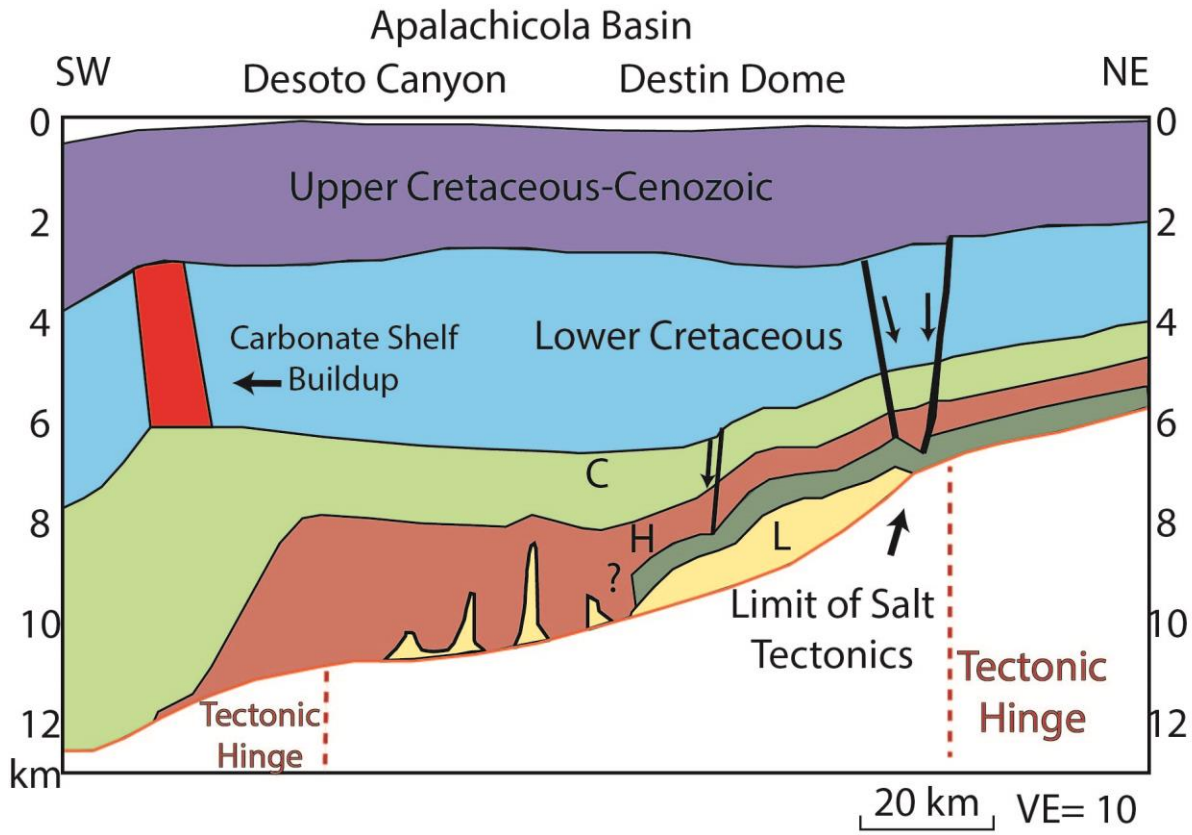

Figure 4: Schematic cartoon dip line through the Apalachicola Basin after Dobson and Buffler (1997). The eastern tectonic hinge zone appears to approximate the extent of salt tectonics. The western tectonic hinge zone parallels the Cretaceous carbonate shelf.

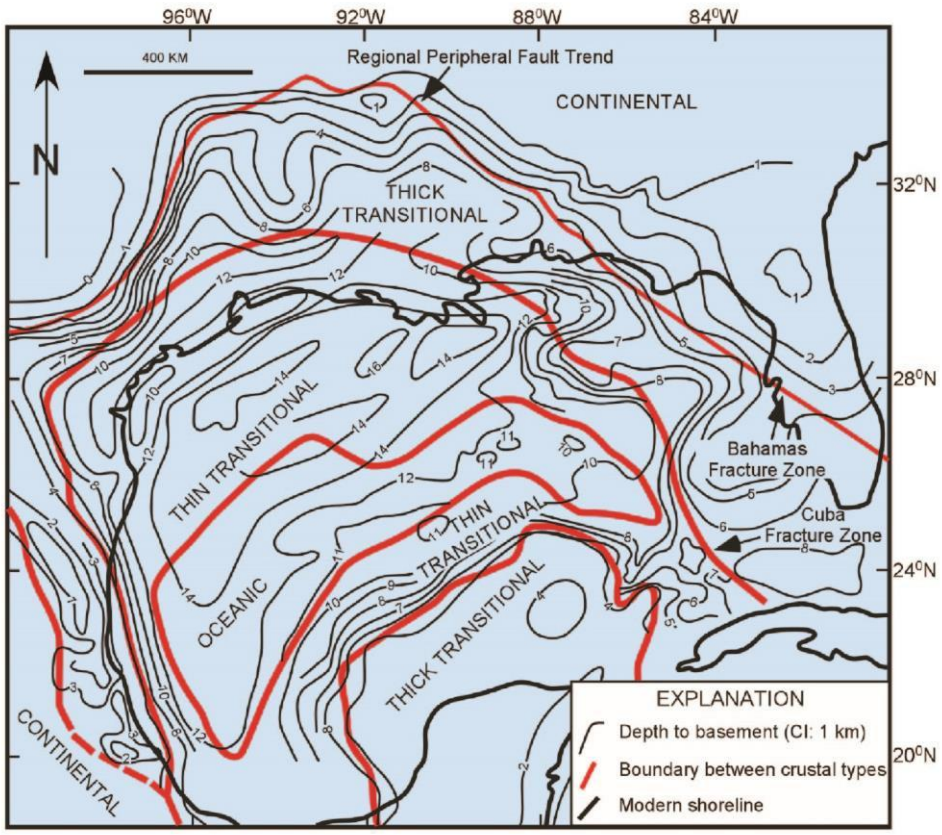

Figure 5: Crustal Type Distribution Map of Buffler and Sawyer (1985), modified from Mancini et al. (2001). The Apalachicola Basin is in the zone of thick transitional crust.

Platform carbonate rocks thrived in shallow water and consist of rudist and stromatolite organisms (Read, 1982). Creation of a carbonate shelf is often the result of declining rates of thermal subsidence (Winkler and Buffler, 1988), enabling reef growing organisms to remain within the photic zone. Bryant et al. (1969) propose that the EGoM carbonate shelf developed as a continuous rim of carbonate rock around the shelf and a restricted semi-lagoonal environment landward of the shelf (Fig. 6). The carbonate shelf formed in one continuous period of carbonate aggradation starting from original rimmed carbonate platforms, lasting from Late Jurassic/Early Cretaceous time to Middle Cretaceous time. By Middle Cretaceous time, sea level rise drowned the shelf (Winkler and Buffler, 1988.) The Mid Cretaceous Sequence Boundary (MCSB) marks the end of carbonate shelf buildup.

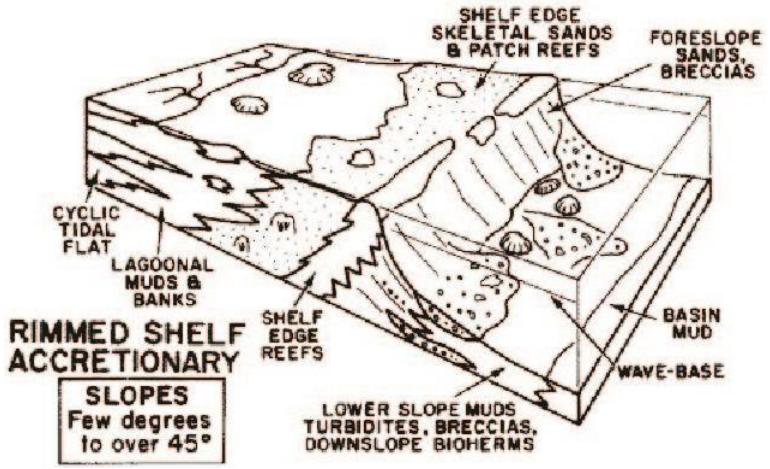

Figure 6: Rimmed carbonate platform (Read, 1982). Low energy restricted environment landward of shelf edge reefs.

The original nucleation of a carbonate shelf can be governed by basement hinge zones, paleo-topography, local sea level and preexisting carbonate buildup (Corso and Austin, 1995). Corso and Austin (1995) determine that the western tectonic hinge served as the nucleus of the Cretaceous carbonate shelf by ruling out other possibilities. Buffler and Sawyer (1988) identify onlapping Lower Cretaceous carbonate rocks onto the western tectonic hinge in the Apalachicola Basin, suggesting that the carbonate shelf and tectonic hinge formed nearly simultaneously during Late Jurassic-Early Cretaceous time.

2. DATA AND METHODS

The principal data set for this project includes 11 Pre Stack Time Migrated (PSTM) lines, 6 Pre Stack Depth Migrated (PSDM) lines (3 within the Apalachicola Basin) donated by Spectrum, and well logs available from the Bureau of Ocean Energy Management (BOEM) and donated by TGS (Fig. 7). Seismic lines were interpreted within the Apalachicola Basin, over the Southern Platform, Tampa Embayment, and GoM Interior Basin (Fig. 7). The seismic data are from 3 separate surveys, Big Wave Phase 2, Desoto Canyon, and Destin Dome. In the Apalachicola Basin, two PSDM lines are processed down to 20 km (lines 32201, 32203) and another to 15 km (line 5040). Over the Southern Platform, PSDM lines are processed to 14 km. In the Tampa Embayment, lines are processed to 16 km. PSTM lines in the Apalachicola Basin are processed down to 7 seconds two way travel time (TWTT). Imaging suffers along the carbonate shelf where seismic velocities can vary laterally from 5200 m/s to 1490 m/s within 200 hundred meters (Gordon et al., 2001). Lack of wells down to the subsalt basement means that velocity profiles used to process PSDM lines are poorly determined near the basement. Therefore, basement structure within these lines may have a depth different than indicated on the seismic lines. Interpretations along PSTM lines may suffer from velocity discrepancies due to lack of well ties used in processing, making apparent geometries different from actual geometries. Wherever possible, seismic interpretations on PSTM lines were verified along the intersection with PSDM. Five lines are positioned in the approximate dip direction of the basin, and the remaining 8 lines are approximate strike lines. Horizons were mapped using Schlumberger's Petrel software, with the aid of well-seismic correlations from wells DD 167 and DC269, and Exxon 3 (Fig. 8), previous interpretations (Addy and Buffler, 1984; Wu et al., 1990; MacRae, 1993; Dobson and Buffler,1997) and characteristic seismic signatures in Mobile Bay (Mancini et al., 2001) and the

Tampa Embayment (Wilson, 2011).

Well control within the Apalachicola Basin is limited. Horizon picks are tied from one seismic reflection line to another. Addy and Buffler (1984) assign average velocities to the sedimentary succession over the Destin Dome. These seismic velocities are used to make thickness observations where PSDM data are not available (Table 1).

Basin restorations were completed using Midland Valley's 2-D Move software along three lines, one PSTM (line 8537) dip line and two PSDM lines (lines 32201 and 32203) (Fig. 7), both oblique to the basin axis.

Velocities m/sec	Formations	Depositional Setting - Paleoenvironment
2375-1750	All Cenozoic Formations	Deep Water to Shallow Water Transition
2525	Selma	Deep Water/ Post MCU Drowning Event
3100	Washita	Shallow Water
4100	Rodessa	Shallow Water
4700	Norphlet Smackover Haynesville Cotton Valley	Coastal to Shallow water with Hypersaline Intervals
4500	Louann Salt	Shallow Hypersaline Marine

Table 1: Average seismic velocities and paleo-environmental conditions around the Destin Dome, after Addy and Buffler (1984). Velocities are from well Exxon 3 (Fig. 7).

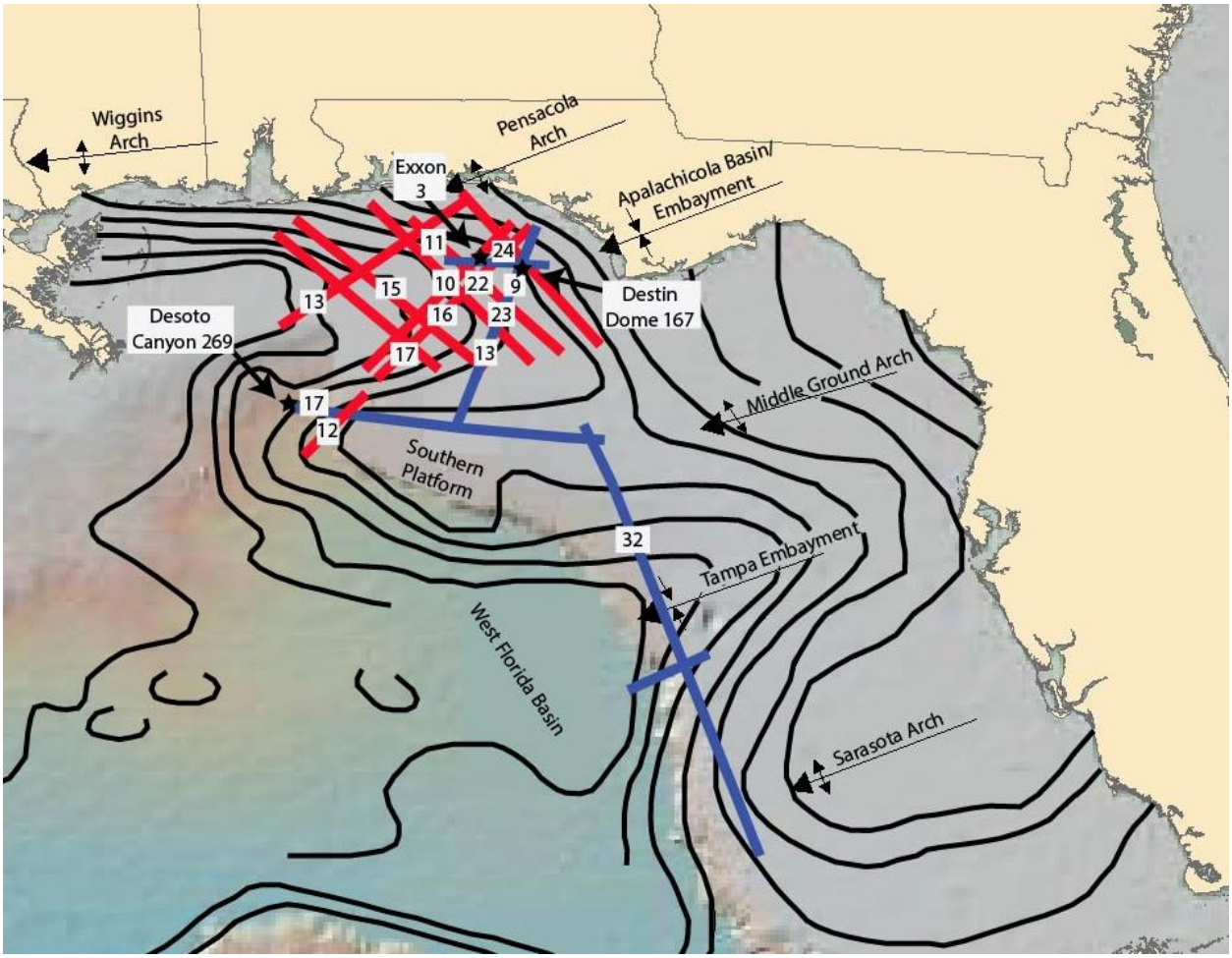

Figure 7: Location of seismic lines and figures. Red lines are PSTM and blue lines are PSDM. Stars indicate the location of wells used to correlate with seismic lines.

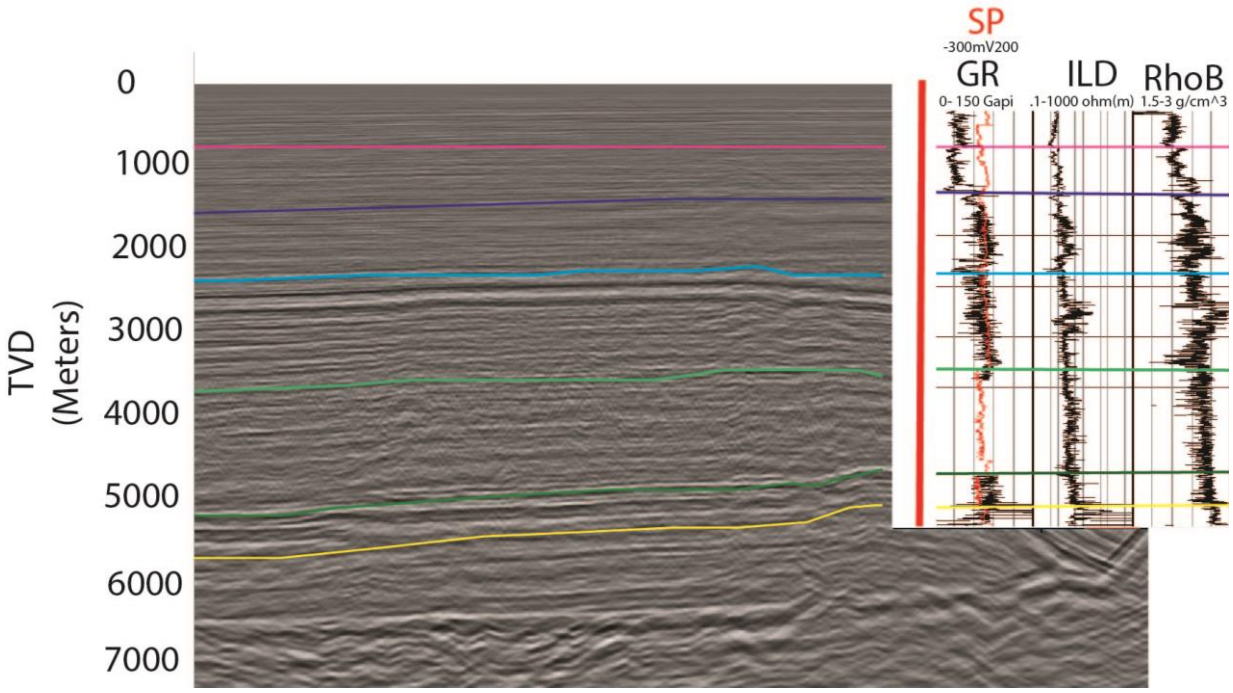

Figure 8: Example of a well to seismic tie. Location of well (Destin Dome 167) is indicated by the red line. The well was drilled down to 17,400 ft (5,303 m) and did not penetrate the BSE. Horizons are identified in Figure 2.

3. INTERPRETATIONS

3.1 Subsalt

Interpretable reflectors below the BSE are visible within a large half graben (Fig. 9), and are likely Late Triassic to Mid Jurassic red beds and volcanic rock based on wells drilled in the Apalachicola Embayment (Well 730 in Liberty County and Well 387 in Apalachicola Bay) (Mitchell-Tapping, 1982).

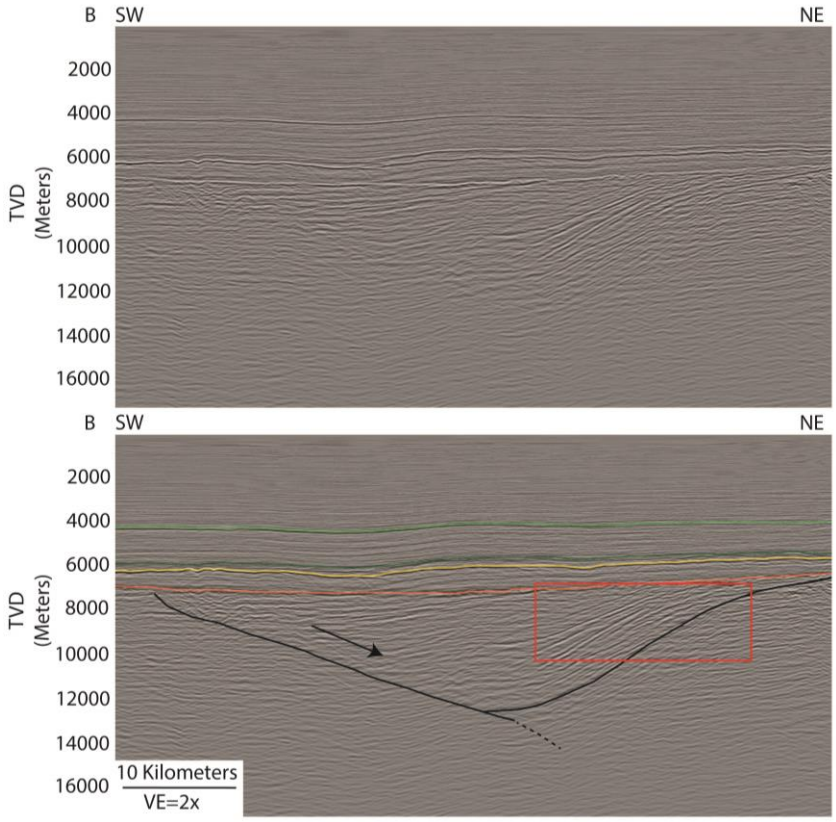

Figure 9: Subsalt, normal fault bounded half graben under the Destin Dome, (location on Fig. 7). A: Uninterpreted. B: Interpreted. The normal fault has an apparent dip to the northeast. Stacked reflectors in the red box flatten and truncate against the normal fault to the southwest.

Along the northeastern edge of the half graben, subsalt dipping reflectors appear robust and stacked (red box, Fig. 9B). Their stacked appearance and common dip (15°) are an indicator of massive volcanism often associated with seafloor spreading. These reflectors thicken and flatten out in the central graben, reaching a depth of between 13,000 and 15,000 m. The half graben contains 5,300 m of rock at its center. Continuity and gradual dip increase of subsalt reflectors northeast of the half graben as opposed to an abrupt truncation of reflectors to the southwest suggest a single normal fault boundary along the southwest border of the graben (Fig. 9). The fault has an apparent dip of 10° NE. This angle is quite shallow and may be attributed to the orientation of the seismic line which is likely not perpendicular to the true orientation of the fault. The clearly defined stacked reflectors are overlain by shallow dipping (≤ 10°) lower amplitude reflectors that may represent a younger (Early to Mid-Jurassic?) stage of graben fill. In the PSTM lines, subsalt reflectors are attenuated and uninterpretable below 6 seconds TWTT (Fig. 10). Elsewhere, subsalt reflectors go from flat lying to dipping towards the basin center in an abrupt transition (Fig. 11) suggesting the presence of faults and other graben structures throughout the basin.

3.2 Base of Salt Equivalent

The BSE is a high amplitude trough made more apparent when underneath a layer of salt (Figs. 9, 10). In the northeastern Apalachicola Basin, the BSE is a prominent angular unconformity (Fig. 10) sitting on top of synrift deposits. The BSE is an irregular, erosional surface.

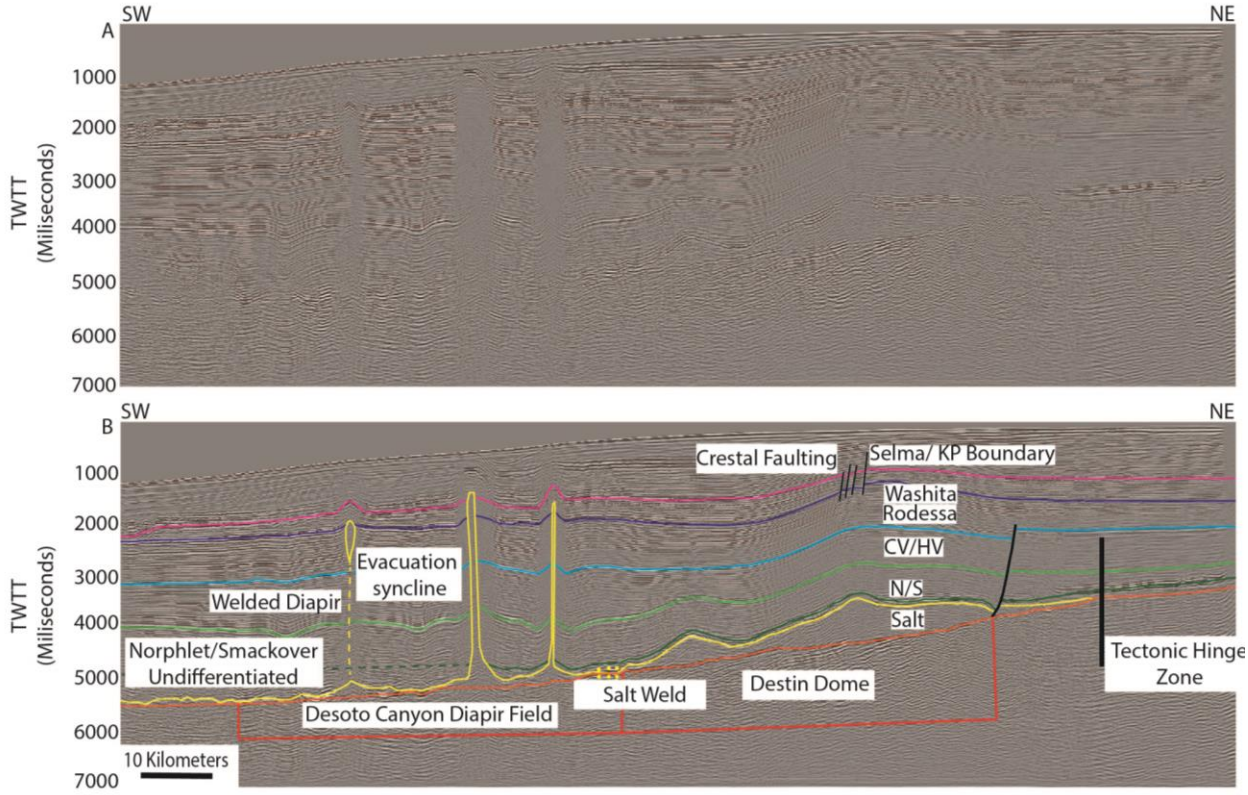

Figure 10: Northeast-southwest trending dip line (location in Fig. 7). A: Uninterpreted. B: Interpreted. Note change in dip of BSE along the Eastern Tectonic Hinge Zone. The line does not extend to the carbonate shelf. Red boxes indicate the locations of the Destin Dome and Desoto Canyon Diapir Field. Within the Desoto Canyon Diapir Field, the Norphlet and Smackover formations are difficult to distinguish from the overlying Haynesville/Cotton Valley formations.

The BSE is often unresolvable near the carbonate shelf (Fig. 12) on PSTM lines due to a massive velocity pull up at the boundary of the carbonate buildup. Along flanking arches, the BSE is heavily eroded, with jagged valleys as deep as 950 m (Fig. 13).

3.3 Callovian Salt

The Callovian age Louann salt is present intermittently throughout the Apalachicola Basin. Salt tectonics in the basin include a series of salt domes and diapirs (Figs. 9, 10), rollers (Fig. 14) and welds (Fig. 10). Autochthonous salt still resides in the southeastern portion of the basin (MacRae and Watkins, 1992) (Fig. 3).

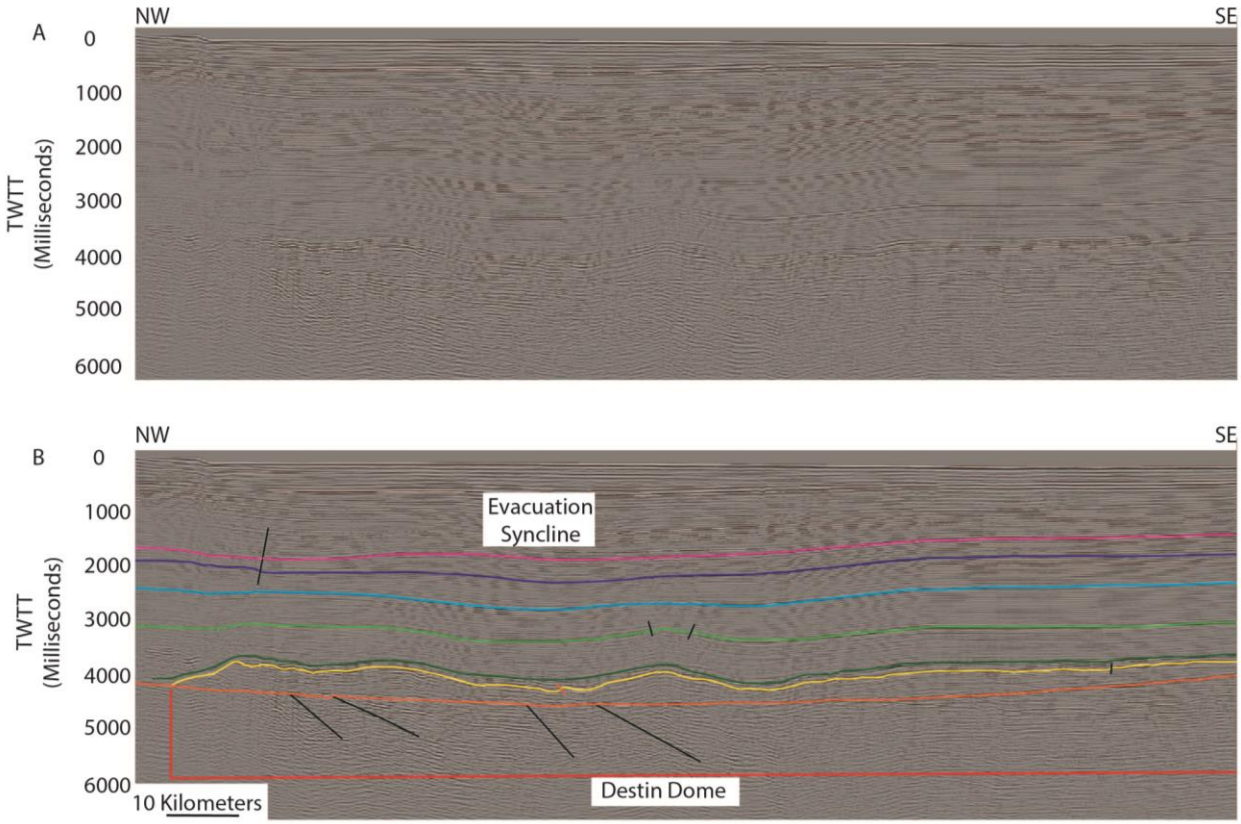

Figure 11: Northwest-southeast strike line through the eastern portion of the Apalachicola Basin (location in Fig. 7). A: Uninterpreted. B: Interpreted. Subsalt dipping reflectors have an apparent dip towards the basin center. Overlying salt along the northwestern tip of the Destin Dome is welded and local synclines are apparent above areas of salt evacuation.

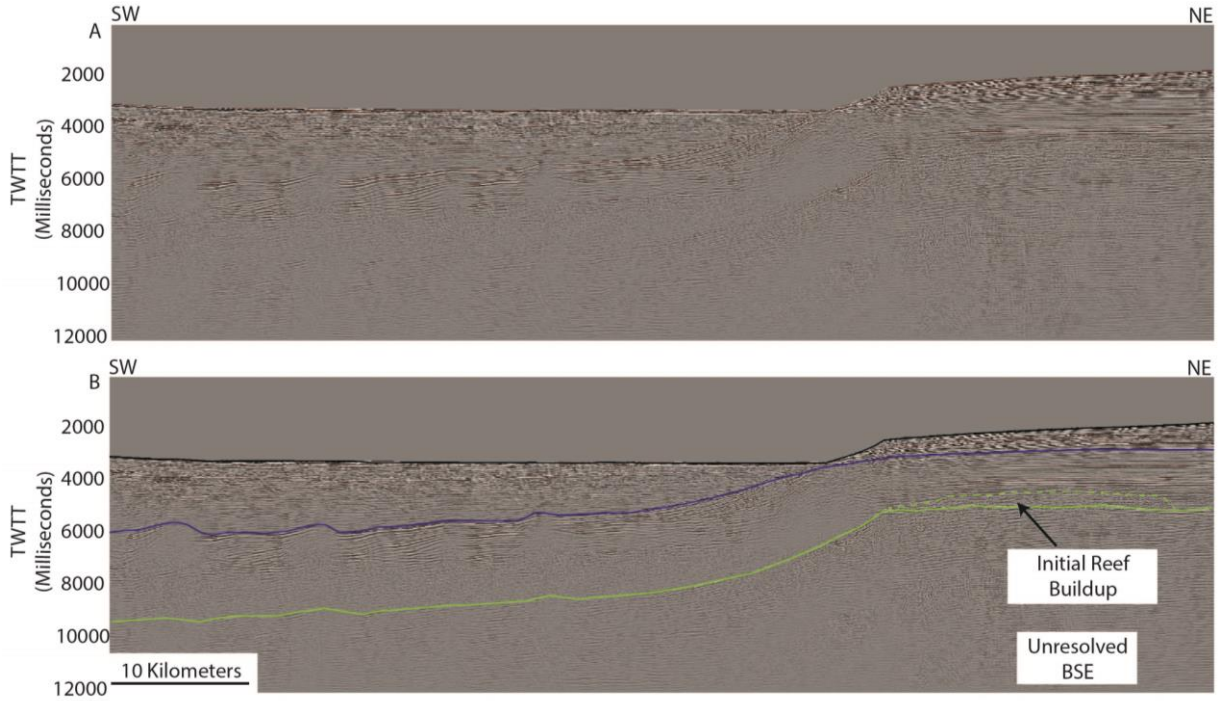

Figure 12: Cretaceous carbonate shelf south of carbonate shelf re-entrant (location on Fig. 7). A: Uninterpreted. B: Interpreted. The BSE is unresolved along this line due to a drastic velocity increase corresponding to carbonate reef buildup and sideswipe. The solid green line marks initiation of the carbonate shelf aggradation and is synonymous with the Knowles Limestone of the Upper Cotton Valley Formation (Fig. 2). The blue line marks the end of carbonate shelf aggradation and is the MCSB.

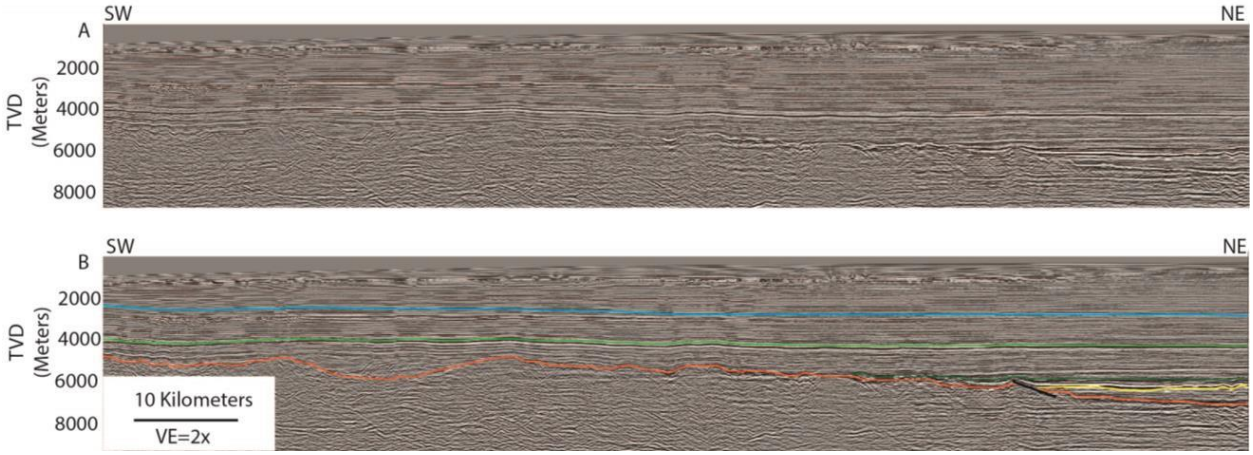

Figure 13: PSDM line illustrating the BSE (orange) along the transition between the Apalachicola Basin and flanking Southern Platform (location on Fig. 7). A: Uninterpreted. B: Interpreted. Louann Salt and Norphlet/Smackover formations onlap onto the BSE near the basin boundary. The BSE is heavily eroded along the Southern Platform and to the east over the Middle Ground Arch.

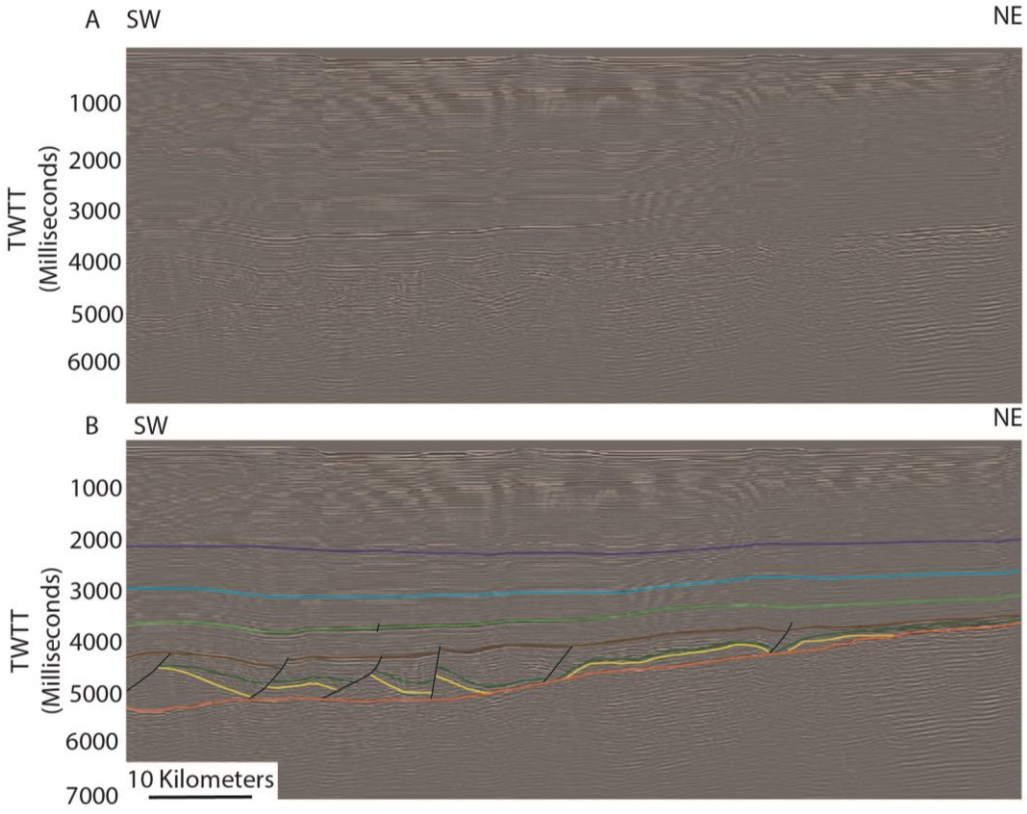

Figure 14: A sequence of salt rollers in the northwestern Apalachicola Basin (location on Fig. 7). A: Uninterpreted. B: Interpreted. Faulting is the result of salt migration. The brown horizon is located within the Haynesville Formation and is used to display fault offset.

Autochthonous salt is at least 700-900 m thick, based on an average seismic velocity of 4.5 km/s (MacRae and Watkins 1993). Salt is thickest (~2 km) along the crest of the Destin Dome (Figs. 3, 10), a large mature salt anticline in the east approximately 80 km long and 35 km wide. Toward the adjoining arches, salt thins and pinches out (Fig. 13). Although the top of salt is a high amplitude continuous peak, internal salt reflectors are chaotic and discontinuous (Figs. 8, 9, 10). A series of salt diapirs (Fig. 10) are intermittently distributed in the Desoto Canyon Diapir Field (Fig. 3). Mitchell-Tapping (1982) identify salt 150 km updip of the eastern tectonic hinge in the Apalachicola Embayment. However, salt structures are not visible in the available data east of the hinge (Fig. 10).

Interpretations over the carbonate shelf suggest a unified salt east and west of the carbonate shelf (Wu, 1990). However, salt is not discernible on the carbonate shelf boundary in this study (Fig. 12). Westward, down slope migration of salt may have been accommodated by normal faulting and/or gravity relating down dip gliding. Vertical migration of salt along the carbonate shelf is unlikely to have occurred due to proximity of dense shelf carbonate rock. An easier migration pathway is west, over the carbonate shelf among unconsolidated slope talus.

3.4 Oxfordian Norphlet/Smackover Formations

In the seismic data, the Norphlet and Smackover formations appear thin and sinuous (Figs. 10, 11). Over the crest of the Destin Dome, the Norphlet and Smackover formations range from 280-290 m to > 600 m thick at its downdip weld. Thickening of these formations on the downdip side of the Destin Dome and small synclines in salt indicate that salt movement was occurring by Oxfordian time. Near salt rollers in the northwestern Apalachicola Basin (Fig. 14), the Norphlet and Smackover formations exhibit thickening and fanning suggestive of growth strata.

Within the Desoto Canyon Diapir Field (Figs. 10, 16), it is difficult to distinguish the Norphlet/Smackover formations from the overlying Haynesville Formation because of seismic attenuation from nearby salt diapirs or a lack of impedance contrast due to a facies change in the lower Haynesville Formation. Both the Norphlet and Smackover formations are likely present at the carbonate shelf edge with combined thicknesses of up to 1,500 m as observed by MacRae (1993). Like the Louann salt, both formations thin and pinch out onto the surrounding arches (Fig. 13). West of the Southern Platform, eolian Norphlet facies extend 100 km or more into the GoM Interior Basin (Hunt, 2013).

Smith (1983) proposes a South American source for the Norphlet Formation because

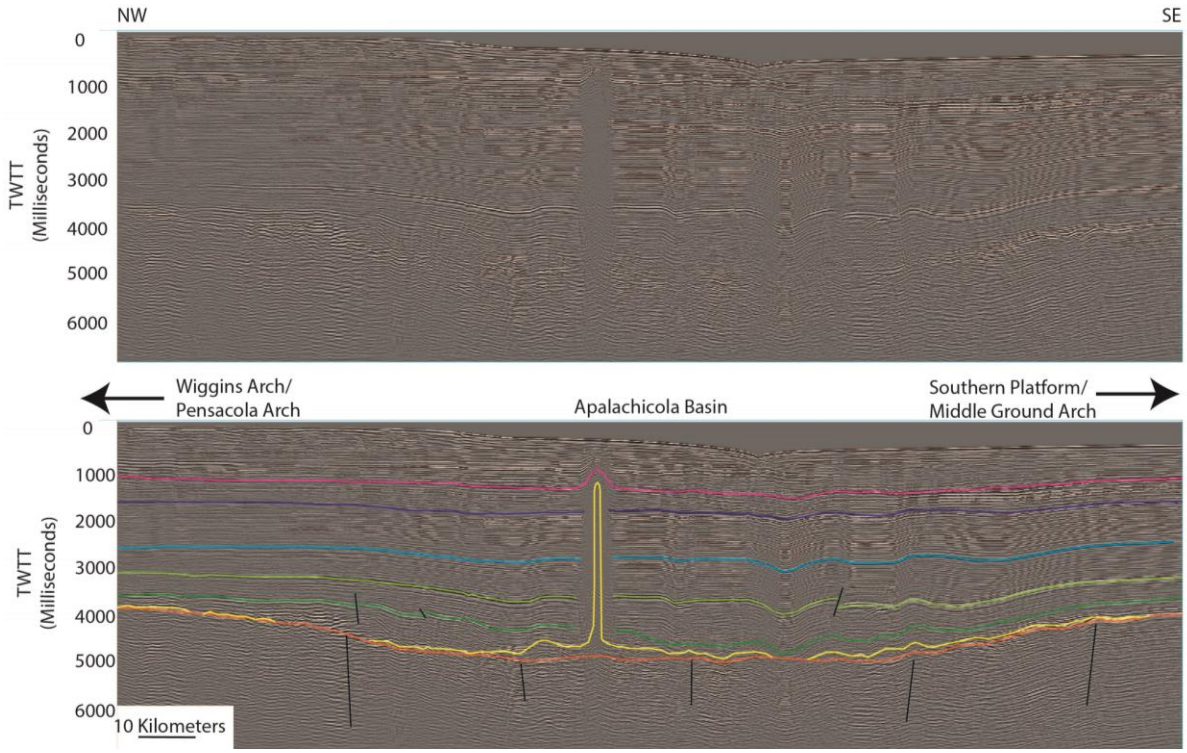

Figure 15: Along strike line within the western portion of the Apalachicola Basin (location on Fig. 7). A: Uninterpreted. B: Interpreted, normal faults. Late Jurassic-Early Cretaceous sediments show thinning and onlap onto surrounding arches. Truncation is apparent in Figure 13 along basin flanks. Basin sag deposits are visible in Jurassic through Late Cretaceous deposits (yellow through pink horizons).

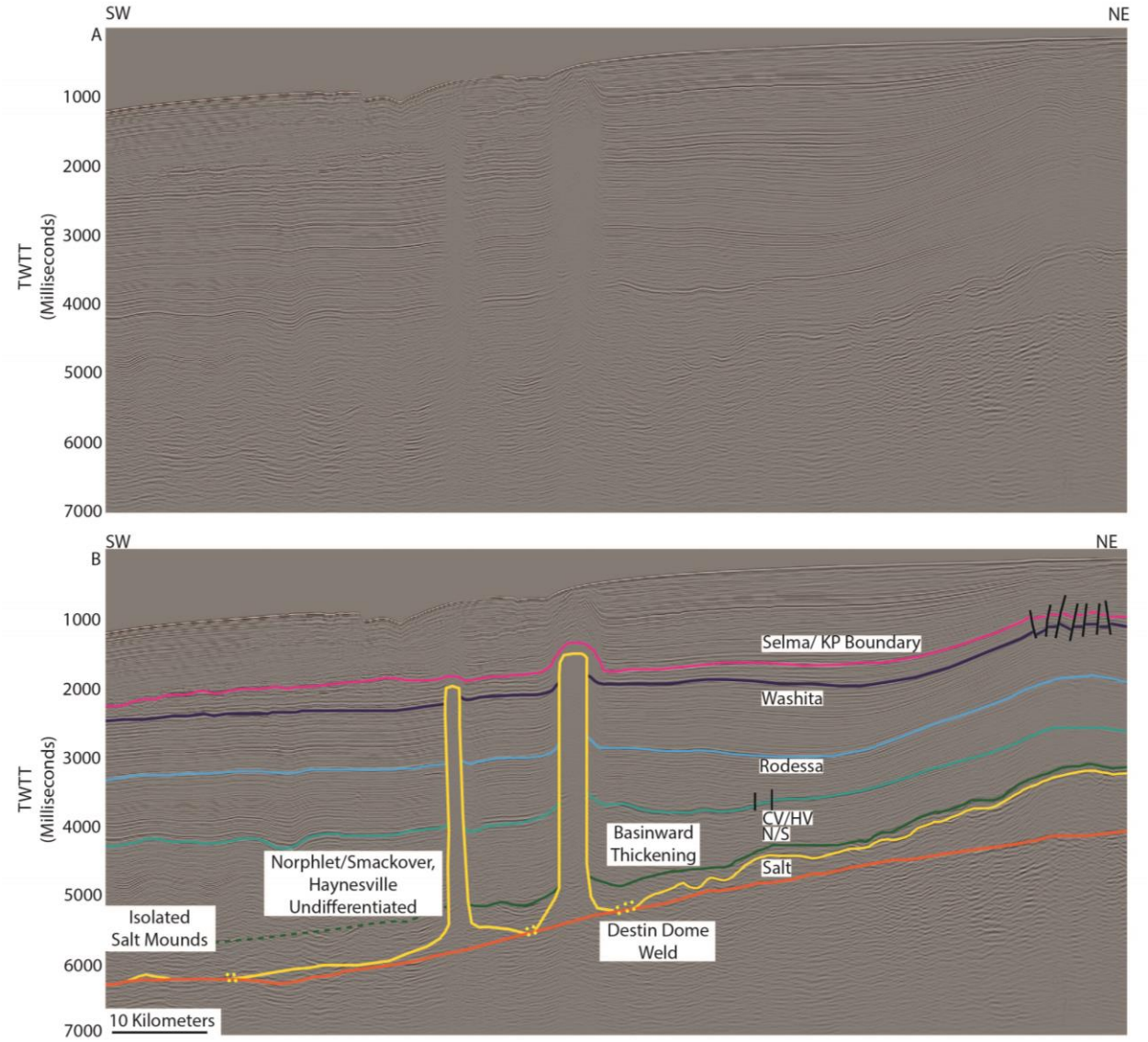

Figure 16: Northeast-southwest trending dip line through the central Apalachicola Basin (location on Fig. 7). A: Uninterpreted. B: Interpreted. The line extends northeast to the crest of the Destin Dome and southwest through the Desoto Canyon Diapir Field.

the gap between North America and South America was small in Middle Jurassic time. However, erosional canyons along the Southern Platform suggest a local source for the Norphlet Formation (Fig. 13). Detrital zircon analysis shows an Appalachian provenance in the western Apalachicola Basin and a Gondwanan provenance toward Florida (Lovell and Weislogel, 2010).

3.5 Kimmeridgian through Berriasian Haynesville/Cotton Valley Formations

The Kimmeridgian Haynesville Formation represents the first marine transgression to inundate both basins and arches. The Haynesville and Cotton Valley formations thin but do not pinch out along the Southern Platform (Fig. 13), indicating that the Apalachicola Basin was first filled to the regional level during Kimmeridgian-Tithonian time. In the seismic data, it is difficult to distinguish the top of the Haynesville Formation from the overlying Cotton Valley Formation due to lack of impedance contrast (Wu, 1990). Thus, the two are grouped together (Fig. 2). Salvador (1987) maps shallow limestone and shale within the northern Apalachicola Basin during the Early Kimmeridgian time and shallow shelf limestone during the Late Kimmeridgian time. A sequence of prograding sigmoidal clinoforms is apparent in the western Apalachicola Basin (Fig. 17), indicating the beginning of carbonate shelf aggradation (Brown and Fisher, 1980). However, these clinoforms are older than the western tectonic hinge, which Corso and Austin (1995) suggest to be the nucleus for Cretaceous carbonate shelf buildup.

Above the Haynesville Formation, the top of the Cotton Valley Formation is the Knowles Limestone, bounded by the MCSB (Fig. 2). The top of the Cotton Valley displays some faulting associated with salt movement (Figs. 15, 16). The thickening of Cotton Valley and Haynesville formations observed in the western Apalachicola Basin may be attributed to accommodation space made available by the evacuation of salt upon deposition of these units and a progressive basin tilt to the west during subsidence (Figs. 10, 16). Along the carbonate shelf, lower Cretaceous carbonate rocks show onlap over the tectonic hinge (Fig. 18) as identified farther north by Winkler and Buffler (1988), suggesting that the western tectonic hinge and the carbonate shelf formed synchronously. Figure 13 identifies a series of attenuated seismic reflections at the base of the Cretaceous carbonate shelf that extend 30 km east of the shelf. This

buildup is likely the "rimmed" carbonate reef buildup defined by Read (1982) and consists of

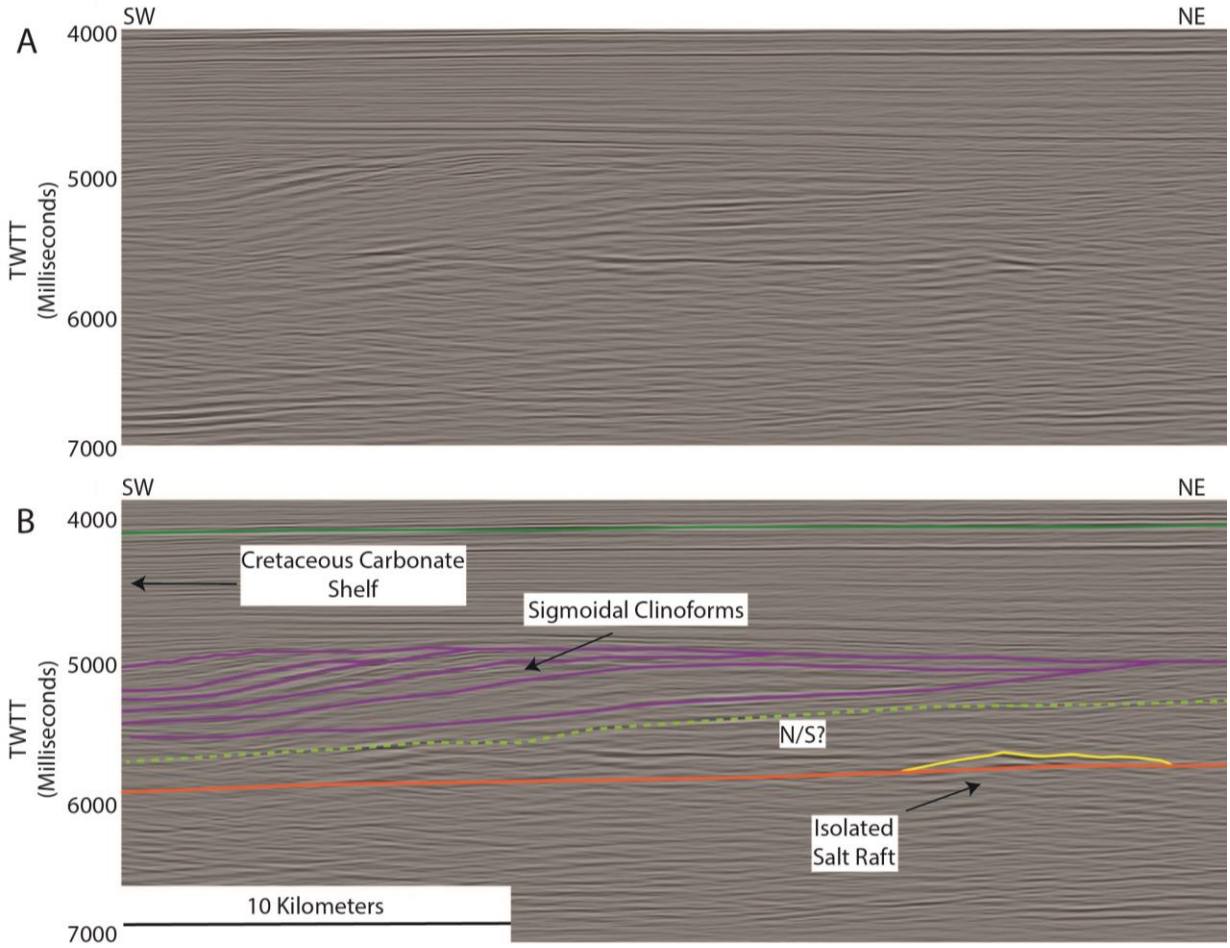

Figure 17: Oxfordian to Kimmeridgian sigmoidal clinoform carbonate rocks of the Haynesville Formation (purple) (location on Fig. 7). A: Uninterpreted. B: Interpreted

the Knowles Limestone. Wilson (2011) identifies similar reefs in the Tampa Embayment.

The combined thicknesses of the Haynesville and Cotton Valley formations varies from 900 m in the northeast to 2,300 m in the southwest (MacRae, 1993). The combined Haynesville/Cotton Valley formations thicken over 200 m from the crest of the Destin Dome to its down dip flank (Figs. 10, 16).

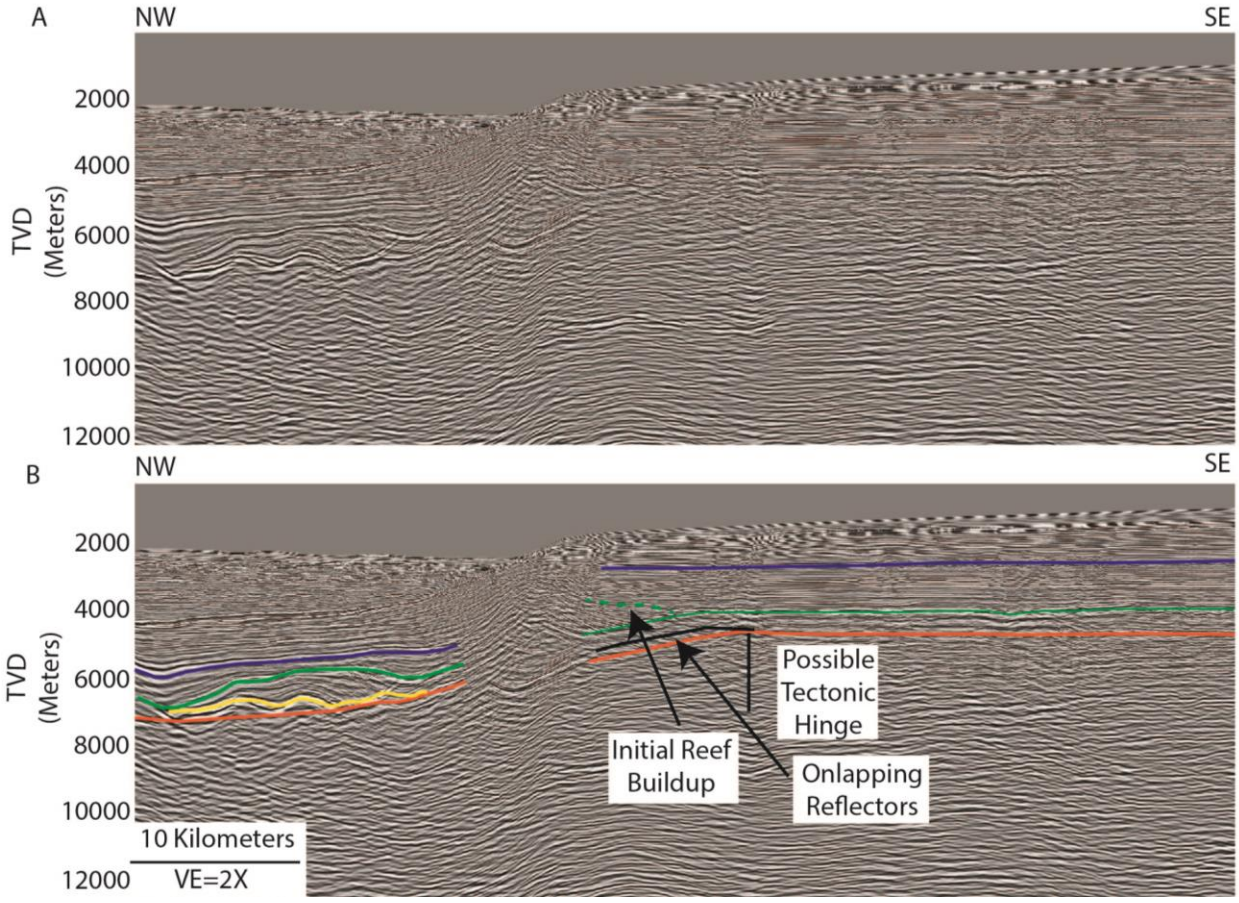

Figure 18: Lower Cretaceous reef buildup along the southern Apalachicola Basin (location on Fig. 7). A: Uninterpreted. B: Interpreted

3.6 Rodessa Formation

The top of the Rodessa Formation represents the end of Albian time (Late Early Cretaceous). Between the top of the Cotton Valley Formation and the top of the Rodessa

Formation lie a series of reef building limestone and shale including the Hosston/Sligo Formation, Pine Island Shale, James Limestone, Bexar Formation and Rodessa Formation. Addy and Buffler (1984) recognize the Rodessa Formation within seismic reflection data over the Destin Dome and trace it throughout the basin and west beyond the Cretaceous carbonate shelf into the deep GoM Basin as part of a larger package known as the Challenger unit. Over the crest of the Destin Dome, the stratigraphic package between top Cotton Valley Formation and Top Rodessa Formation is 2,250 m thick, thickening to 2,870 m at the down dip weld (Figs. 10, 15), indicating continued migration of salt into the Destin Dome. The package varies from 2,460 m, east of the eastern tectonic hinge to 4,100 m in the western Apalachicola Basin (Fig. 10). The overall sag of the basin deposits along strike begins to diminish with the top of the Rodessa Formation (Fig. 15). The top of the Rodessa Formation is a high amplitude continuous reflector. Basinward thickening is not as pronounced as in the Haynesville/Cotton Valley formations.

3.7 Mid Cretaceous Sequence Boundary (MCSB) and the Washita Formation

The interval between the top of the Rodessa Formation and the MCSB includes several Formations; The Ferry Lake Anhydrite, Mooringsport Formation, Paluxy Formation and Washita Formation. The sequence was deposited over 13 million years (113-100 Ma) and consists primarily of marine shale, anhydrite, limestone reef buildup and siliclastic fluvial sediments (Mancini et al., 2001). The MCSB marks the top of the Washita Formation (Figs. 2, 10, 15, 16). The MCSB is an irregular surface, attributed to sea level rise and lack of deposition. Throughout the GoM, the MCSB or its erosional counterpart, the Mid Cretaceous Unconformity, can be traced from shelf to slope and into the GoM Interior Basin (Fig. 12). Thinning of the Washita Formation over the Destin Dome (Fig. 16) indicates that the dome was still growing during Late Early Cretaceous time. Crestal faulting in the Washita Formation indicates that salt migration

was still occurring. The Washita Formation varies in thickness from 800 m, east of the eastern tectonic hinge to 1,000 m in the western Apalachicola Basin (Figs. 10, 17).

3.8 Selma Formation

Within the Apalachicola Basin, Late Cretaceous time is represented by the Tuscaloosa Formation and the Selma Formation, consisting primarily of shale. The top of the Selma Formation is the Cretaceous/Paleogene (K/P) boundary. The crestal faults over the Destin terminate in the Selma Formation. When paired with sediment thinning over the peak of the Destin Dome (Figs. 10, 16), salt migration in the Destin Dome likely ended sometime during Late Cretaceous deposition. Further west, the K/P boundary is a highly eroded surface, appearing jagged and irregular (Figs. 10, 17). The Late Cretaceous package is ~900 m thick northeast of the eastern tectonic hinge and thins basinward to ~500 m.

3.9 Cenozoic

The K/P boundary unconformity marks the base of the Cenozoic and is recognized throughout the deep central GoM and the EGoM (Fig. 16) (Buffler, 1991). The unconformity represents either a rapid submergence drowning event or a fall in sea level leading to subaerial erosion (Addy and Buffler, 1984). The along strike bathymetric profile (Fig. 15) displays the extent of erosion within the basins center. However, since Late Cenozoic time, the western Apalachicola Basin has been part of the eastern lobe of the Mississippi Delta**.** Denne and Blanchard (2013) identify more than 8,000 ft (2,438 m) of Cenozoic section in the southwestern Apalachicola Basin. The influence of Mississippi River sedimentation is observed along strike (Fig. 15) where the Cenozoic section in the southwest is 1.4 times thicker than in the southeast.

3.10 Basin Fill Sedimentation

Time maps were created to document basin fill sedimentation between the Late Middle

Jurassic and Late Paleocene time (Fig. 19). Horizons used for mapping are the BSE, Top Norphlet/Smackover formations, Top Haynesville/Cotton Valley formations, Top Rodessa Formation and Top Selma Formation. Mapping does not extend west beyond the carbonate shelf. Cooler colors represent a greater travel time to the top of each surface and warmer colors represent a lesser travel time.

BSE contours identify the original rifted basin geometry (Fig. 19A). Overall, contours trend northwest-southeast along strike of the basin, and deepen to the southwest, conforming to the northeast-southwest basin axis. The observable BSE is shallowest (4 seconds TWTT) east of the eastern tectonic hinge and shallows further onshore into the Apalachicola Embayment where it is observed at 13,000 ft (4,000 m) (Arden, 1974). The BSE is deepest (6 seconds TWTT) near the carbonate shelf.

Deposition throughout Late Jurassic time continually fills in accommodation space (Figs. 19B, 19C). By Early Cretaceous time, the basin filled to at least 4 seconds TWTT and sedimentation was continuous between Apalachicola Basin, Southern Platform and Wiggins Arch/Pensacola Arch. However, a small basin low (40 km north-south, 42 km east-west) remained in the southwest corner of the Apalachicola Basin (Fig. 19E), which may be attributed to continued basin subsidence or erosional incision as proposed by Harbison (1968) and Denne and Blanchard (2013). Salt tectonics affect depositional contours beginning with the Norphlet and Smackover formations (Fig. 19B), and the Destin Dome can be clearly identified in the northeastern portion of the basin thereafter.

Sedimentation rates were calculated at three points (Fig. 20). The points are labeled southwest Apalachicola Basin, central Apalachicola Basin, and Destin Dome Well 167. Points in the southwest and central Apalachicola Basin were measured using the isopach maps of MacRae

(1993) and well Destin Dome 167 was used for the point in the northeast.

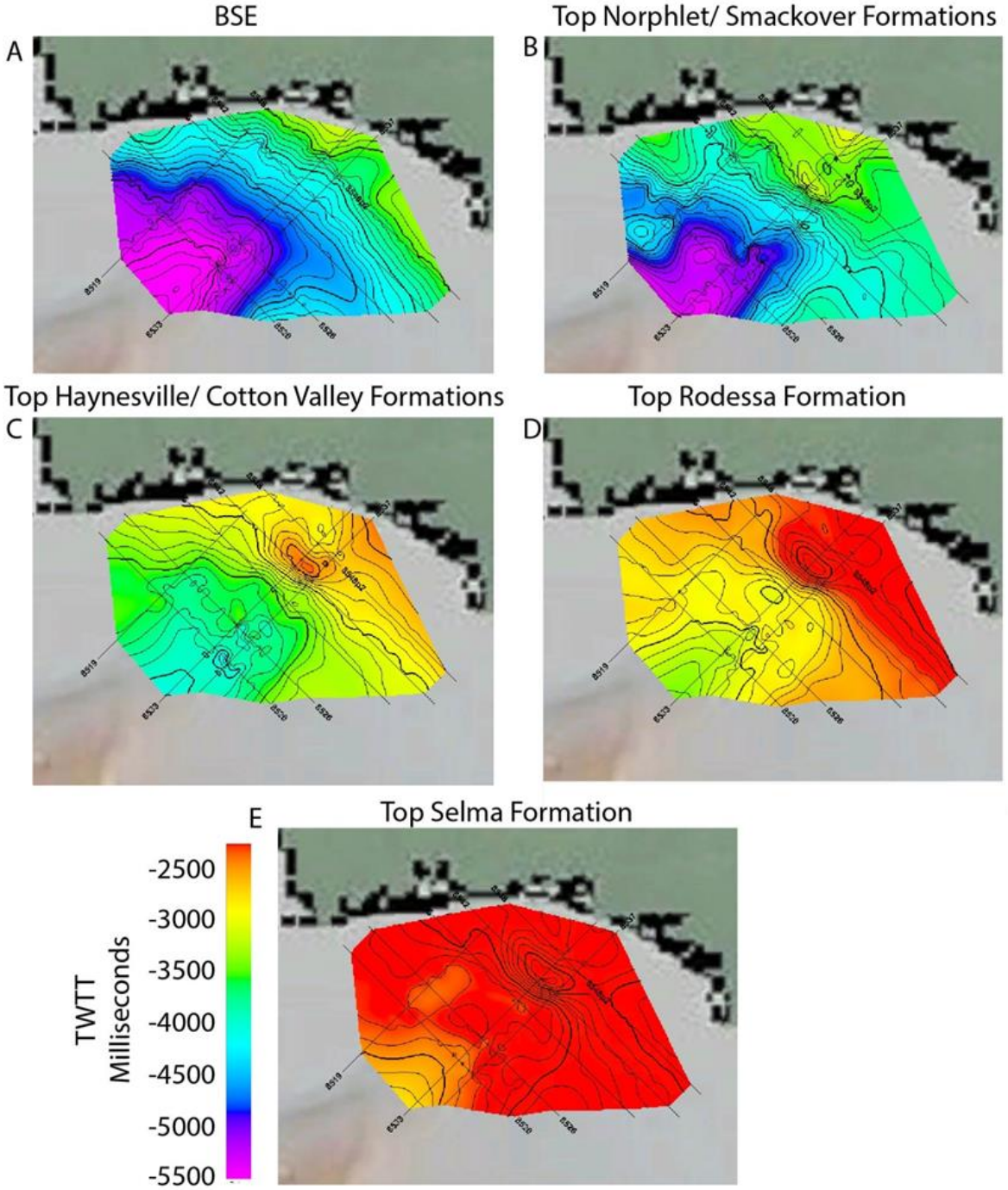

Figure 19: Time maps in TWTT from Middle Jurassic through Late Cretaceous time. Basin contours run northwest-southeast between flanking arches. Salt diapirism caused basin contours to shift orientations by Late Jurassic time. A remaining low may be caused by basin subsidence or erosion.

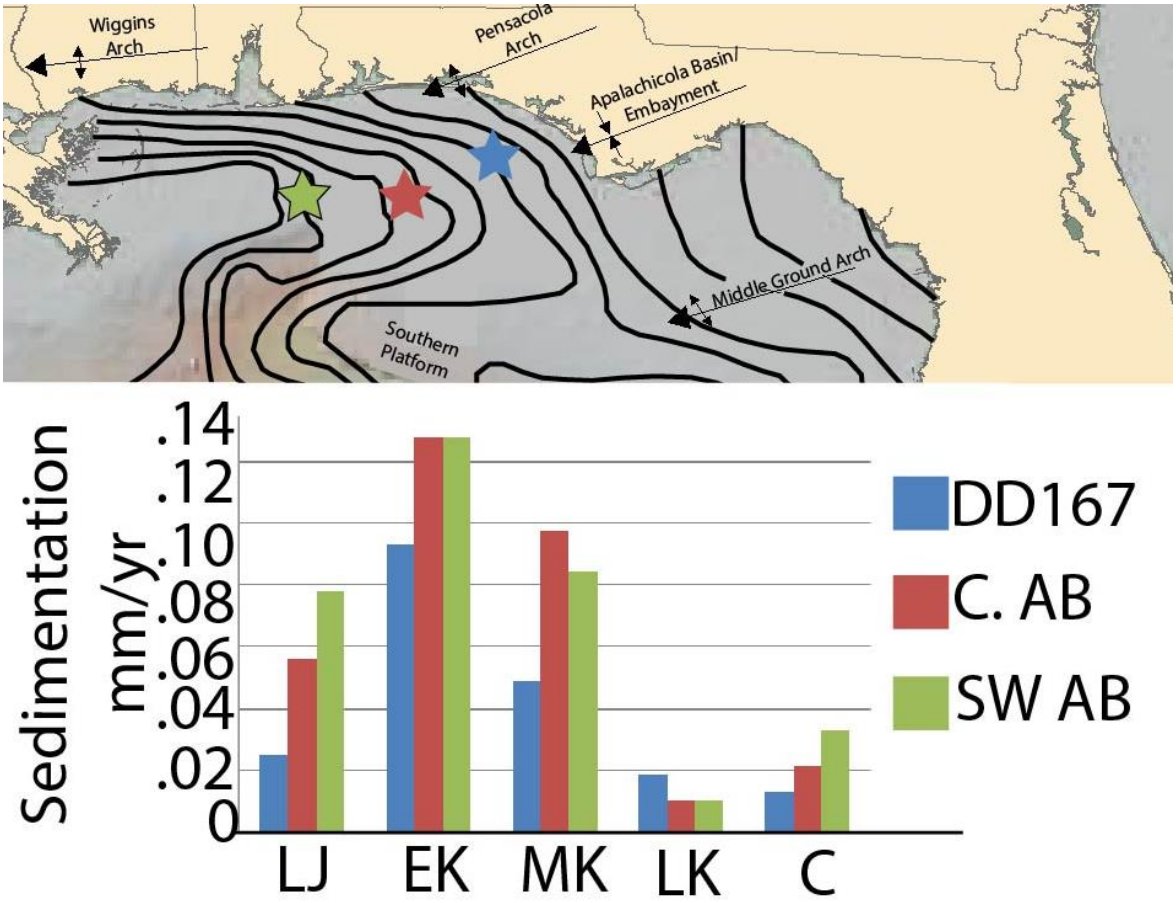

Figure 20: Top: Locations where sedimentation rates were calculated. Bottom: Comparative sedimentation rates. Abbreviations: LJ: Late Jurassic, EK: Early Cretaceous, MK: Middle Cretaceous, LK: Late Cretaceous, C: Cenozoic.

Sedimentation rates were measured by taking sedimentary thicknesses and dividing by the duration of time of their deposition. However, the rates are minimum values because depositional hiatuses and erosion are not included. Sedimentation rates were highest between Late Jurassic and Early Cretaceous time, as high as 0.125 mm/yr in the southwest and center and 0.09 mm/yr over the Destin Dome (Fig. 20). Higher sedimentation rates toward the west are a result of increased depth to basement. Thus, it is reasonable to assume that increased subsidence was occurring along the northeast-southwest trending basin axis. Peak sedimentation rates coincide with the initial filling of the basin to the level of the surrounding arches by Latest

Jurassic to Early Cretaceous time. A sharp decline in sedimentation rates of 80-90% took place from Middle Cretaceous time (~113-100 Ma) to Late Cretaceous time (~100-66 Ma) to less than 0.02 mm/yr throughout the basin, illustrating a period of erosion and low subsidence rates. At the Destin Dome, sedimentation rates were lower (up to 0.09 mm/yr) than in the western basin because of its updip location and because salt migration caused a topographic high to form (Figs. 10, 16).

4. BASIN RESTORATIONS

Basin restorations were completed using Midland Valley's 2-D Move software. The restorations are completed by sequentially backstripping off the top layer of a seismic section and correcting for decompaction of the underlying sediments, resulting in the restored geometry at the time of the base of the removed layer (Rowan, 1993; Gutierrez, 2013). Decompaction is a method to correct for progressive volume loss associated with burial. Backstripping in 2D Move is based on the equation of Sclater and Cristie (1980) that determines the exponential porosity loss with depth.

$$\mathbf{F(z)=f_0 e^{-cz}}$$

z: Present day porosity

$f_{0:}$ Porosity of the rock at the surface

c: constant of compressibility based on lithology lithology

Because well control is limited over the lines to be restored, the default 2D Move porosity values were used based on assigned lithology. MacRae (1993) determines average density values throughout the Apalachicola Basin based on well logs from Pensacola 973, and Destin Dome wells 31, 162, 166, 360, 422, 563 (Table 2), which are used in backstripping. The sea level curve of Haq et al. (1987) is used to help identify the regional level after each decompaction (Fig. 21). Sequential restorations create insights into the: (1) prediction of basin paleogeography and sedimentation from the Late Middle Jurassic to modern time, (2) structural evolution of salt and overlying rocks, and (3) 2-D migration pathways and traps for

hydrocarbons. Sequential restorations make several assumptions (Sclater and Cristie, 1980).

Layer	Density (kg/m^3)
Cenozoic	2300
Upper Cretaceous	2350
Lower Cretaceous	2550
Cotton Valley/Haynesville Fm	2550
Smackover/Norphlet Fm	2700
Louann Salt	2200

Table 2: Average density values throughout the Apalachicola Basin as determined by MacRae (1993) using well logs.

(1) uniform lithological properties for an individual formation, (2) a state of isostatic equilibrium was reached, (3) no sediment movement occurred from out of the plane and (4) salt is an incompressible material.

Exact salt geometries are difficult to determine before the present. Rowan (1993) states "The key to determining the changes in salt thickness and area through time is to calculate independently the evolution of the sub-salt and supra-salt sequences; the resulting space between the restored base-and top-salt at any stage defines the salt geometry at that time". A trial and error approach was used in 2-D Move to identify salt evolution that is compatible with the observations and decompaction of surrounding rocks. Even though some salt is moving in an out of the plane of the restorations, these restored geometries are consistent with those of MacRae and Watkins (1992) over the Destin Dome and, thus, are validated.

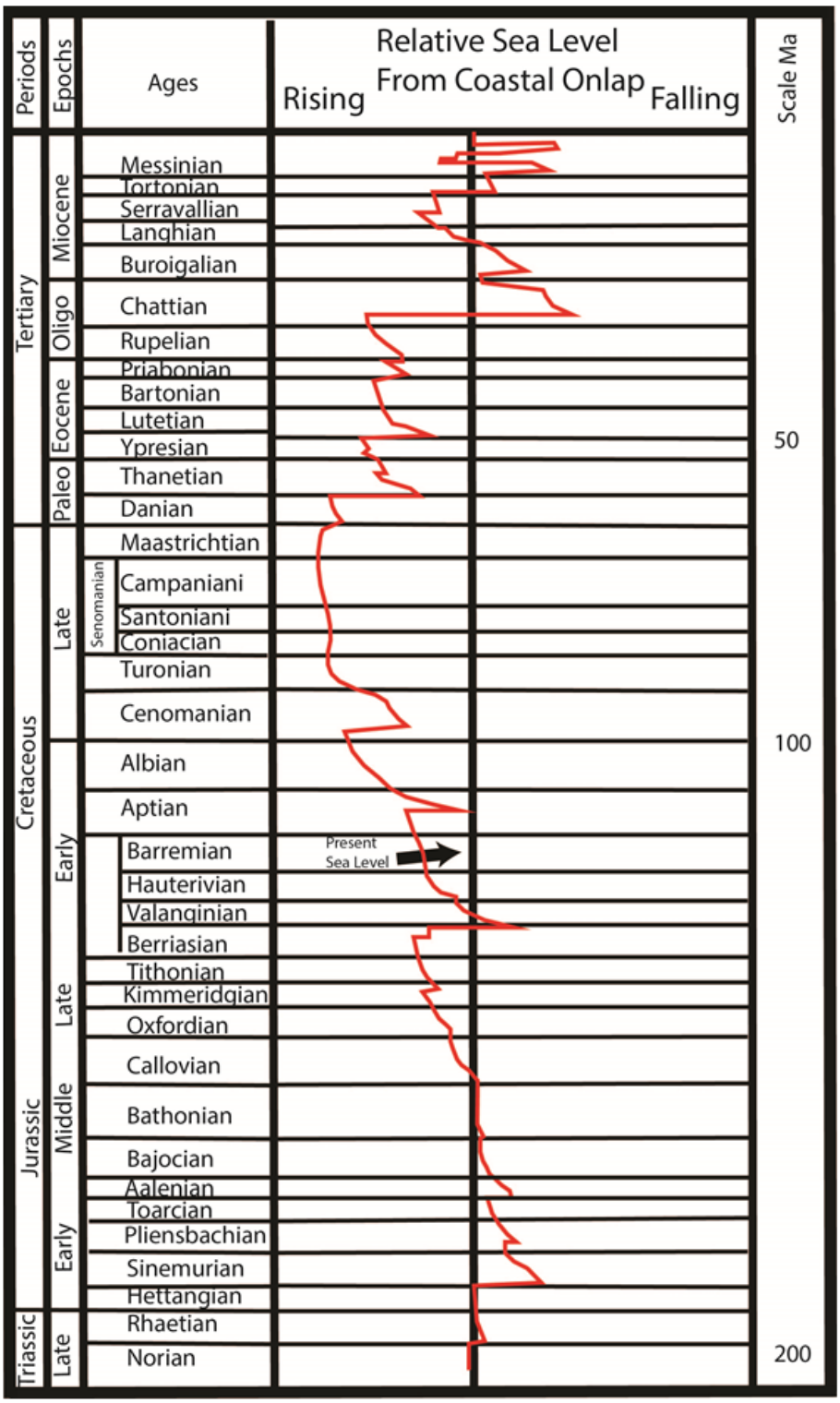

Figure 21: Global sea level curve from Haq et al. (1987) used to identify paleo sea levels.

Based on the availability of seismic reflection data, 3 sections were restored down to the BSE. Line 8533 is a PSTM line oriented in the approximate dip direction of the basin and extending almost to the carbonate shelf. On the western edge of line 8533, the data are ambiguous so the line is shortened. Line 32201 is a PSDM line in the southernmost portion of the basin trending northeast-southwest over the half graben in Figure 10. The line is cropped near the edge of the Southern Platform because Jurassic and early basin fill sediments pinch out at this boundary. Line 32203 is a PSDM line trending northwest–southeast over the crest of the Destin Dome. Although backstripping is performed from youngest to oldest, the results are presented from oldest to youngest to match the evolution of the basin.

Although extension occurred along the lines, the lack of apparent faulting within the given seismic resolution associated with extension plus obscurity within the basement caused by salt migration makes extension related to upper crustal thinning difficult to determine. Extension likely occurred within the upper mantle as well, which cannot be convincingly demonstrated through restorations. Thus, line lengths remain constant throughout the restorations

4.1 Line 8533

Line 8533 is a 50 km long PSTM dip line and intersects major salt structures. The line extends from 3 km northeast of the eastern tectonic hinge, west to within 10 km of the carbonate shelf. Pre-Jurassic structures and horizons are not visible along this line due to signal attenuation below the BSE.

Figure 22A: Callovian (164.7-161.2 Ma) time

Salt filled in the rift basin after deposition of the Late Triassic synrift sediments (Figs. 10, 22A). Seni and Jackson (1983) propose that original salt thickness within a basin can be estimated by uniformly thick undeformed salt elsewhere in the basin. MacRae and Watkins (1993) document tabular undeformed salt approximately 760 m thick, 16 km south of this line and thus, tabular is likely the original geometry of the salt. Salt remains in its autochthonous position throughout this time, building up slowly as sea water incursions evaporate.

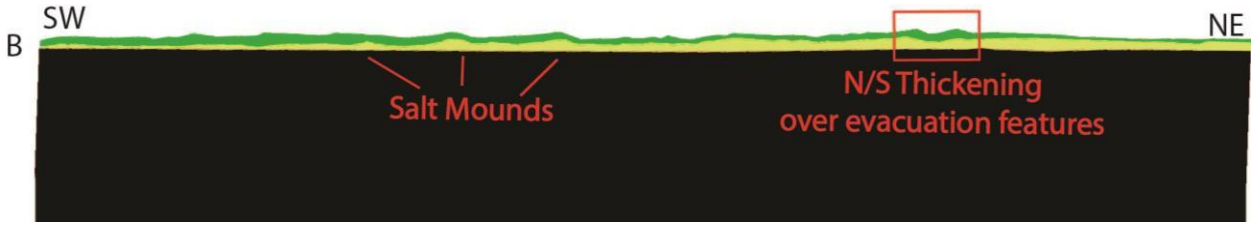

Figure 22B: Early Late Jurassic time (164-157 Ma) time

The Norphlet and Smackover formations began to accumulate during Oxfordian time (Fig. 22B). Small amounts of thickening of these formations over troughs in salt are likely the location of Smackover Formation carbonate mounds similar to those identified by Dobson and Buffler (1997). The mounds and the Norphlet/Smackover formations on top of them sink into and have an onlapping stratigraphic relationship with the overlying salt that creates a small pinchout prospect against the impermeable salt. Deposition of these formations induced initial salt movement. Autochthonous salt deformed into small mounds. In this study, the Norphlet and Smackover formations are undifferentiated from the Haynesville Formation in the western Apalachicola Basin; however, MacRae (1993) recognizes a westward thickening to as much as 1500 m. Down dip thickening is likely the result of basin tilting towards the west as a result of subsidence

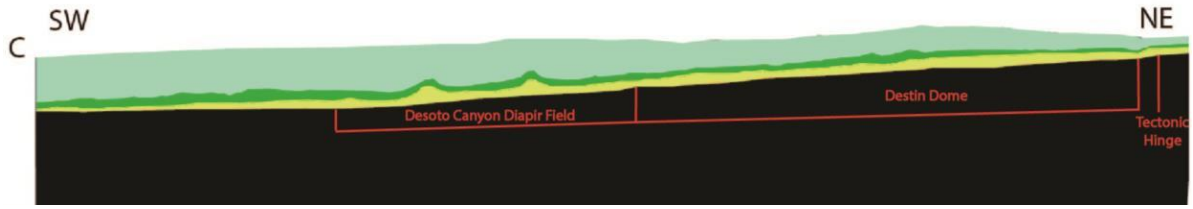

Figure 22C: Late Jurassic-Early Cretaceous time (157-139 Ma) time

MacRae and Watkins (1992) state that the Destin Dome began growing by Middle Cretaceous time. However, a 50% increase in the thickness of the Haynesville/Cotton Valley formations from the crest of the Destin Dome to its basinward tip (Figs. 10, 16, 22C) is consistent with salt movement at the location of the Destin Dome during Late Jurassic and Early Cretaceous time. Distinct thinning of the Haynesville/Cotton Valley formations along the northeast portion of the line that is not present in the Norphlet/Smackover formations suggests that the tectonic hinge formed during this time. The down dip tilt of the basin is more noticeable by this time.

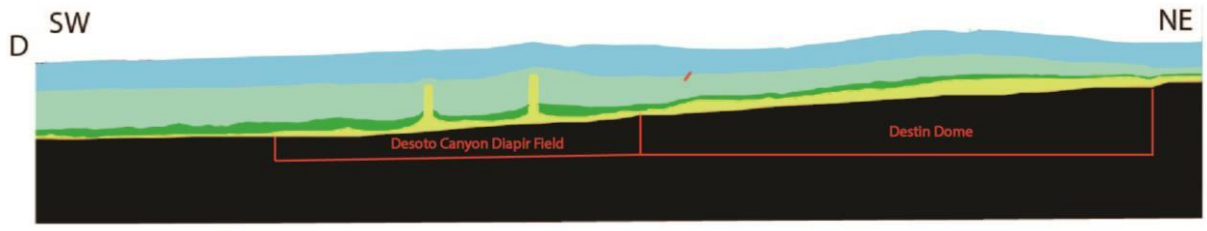

Figure 22D: Early Cretaceous (139-113 Ma) time

The Early Cretaceous Rodessa Formation thickens westward along the line but far less than the Haynesville/Cotton Valley formations (Fig. 22D). High rates of sedimentation in Late Jurassic-Early Cretaceous time (Fig. 20) suggest that salt diapirs emerged from preexisting mounds at this time. The upward penetration rate of diapirs is subject to some interpretation. However, the high sedimentation rates suggest that salt migration was the most rapid during Late Jurassic-Early Cretaceous time. These diapirs narrow slightly from their base upward, which is indicative of sedimentation rates higher than rate of salt rise (Gutierrez, 2013). A slight thinning of the Rodessa

Formation over its crest indicates the Destin Dome assumes a definitive anticlinal shape during Early Cretaceous time. Cumulative hydrocarbon expulsion analyses of Mancini et al. (2001) near the Apalachicola Basin pinpoints the majority of Upper Jurassic sourced oil and gas expelled by 115-120 Ma. Diapirs in the Desoto Canyon Diapir Field had formed viable structural traps by this time.

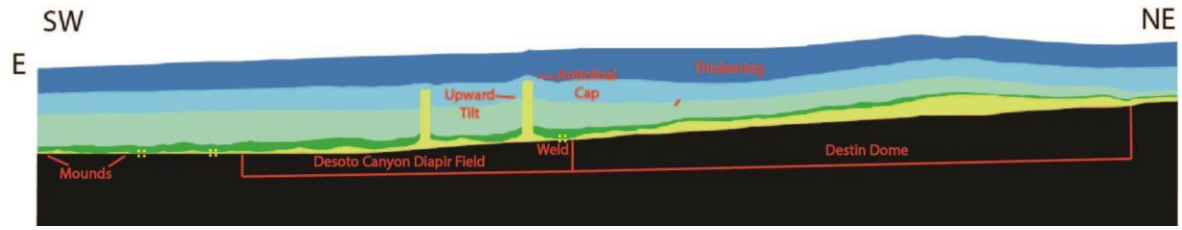

Figure 22E: Late Early Cretaceous-Early Late Cretaceous (113-100 Ma) time

From Late Early Cretaceous time to the MCSB, diapirism continues (Fig. 22E). Where salt diapirs have penetrated, the flanks of surrounding sediments are tilted up. Even where diapirs have not yet penetrated, displaced sediments form an anticlinal cap (Figs. 10, 22E). Basinward tilting likely slowed sharply because sedimentation rates decline (Fig. 19). The Washita Formation (dark blue) maintains a constant thickness across the line, except over the western flank of the Destin Dome where it thickens by 50%. The location of thickening suggests that salt movement within the Destin Dome was internal at this time and that a salt weld located along the southwestern Destin Dome had formed. Other welding in the Desoto Canyon Diapir Field left thin isolated mounds of salt. Similar to the pinchout traps identified in Figure 22B, intermittent welding of the salt in the western Apalachicola Basin created pinchout traps against small salt mounds.

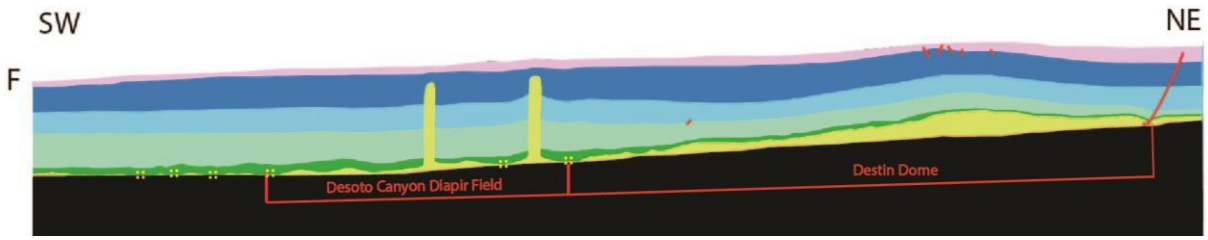

Figure 22F: Late Cretaceous (100-66 Ma) time

Slow sedimentation and erosion occur during Late Cretaceous time. Two to three km west of the eastern tectonic hinge, a listric normal fault forms and cuts down into the Louann salt (Fig. 22F). The fault formed due to a wedge of salt at the landward tip of the Destin Dome, rolling over onto the BSE near the tectonic hinge and cutting off further salt accumulation from the updip direction. The Destin Dome becomes isolated and continues to thicken at its center from salt movement internally. Crestal faulting over the Destin Dome above the MCSB and lack of crestal faulting into Cenozoic time (Fig. 22G) indicates that the Destin Dome finished growing by Late Cretaceous time. Thus, the Destin Dome accumulated over 80-100 million years from Late Jurassic to Late Cretaceous time. Diapirs in Desoto Canyon Diapir Field pierce through the Late Cretaceous Selma Formation, continuing to grow during the Cenozoic.

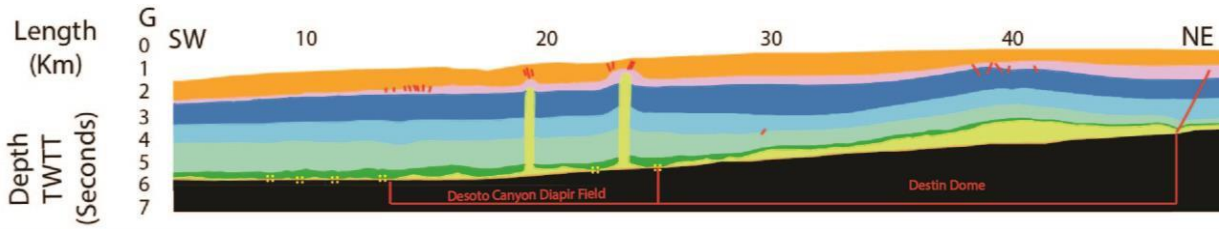

Figure 22G: Cenozoic (66-0 Ma) time

The modern jagged appearance of the K/P boundary along the top of the Selma Formation in the southwestern Apalachicola Basin indicates that erosion dominated by the end of Mesozoic time (Fig. 22G). During Oligocene to Miocene time, terrestrial sediments began to buildup in the southwestern Apalachicola Basin (Fig. 22G) (Addy and Buffler, 1984). Small normal faults over the top of the salt diapirs indicate that the diapirs were still building well into Cenozoic time. Oil maturation within the Lower Cretaceous Washita Limestone facies occurred around 44 Ma (Mancini et al., 2001). The slow sedimentation from Late Cretaceous to Late Cenozoic time

suggests that the diapirs reached a height close to that of modern day prior to 44 Ma, and would be viable traps for oil expulsed at this time.

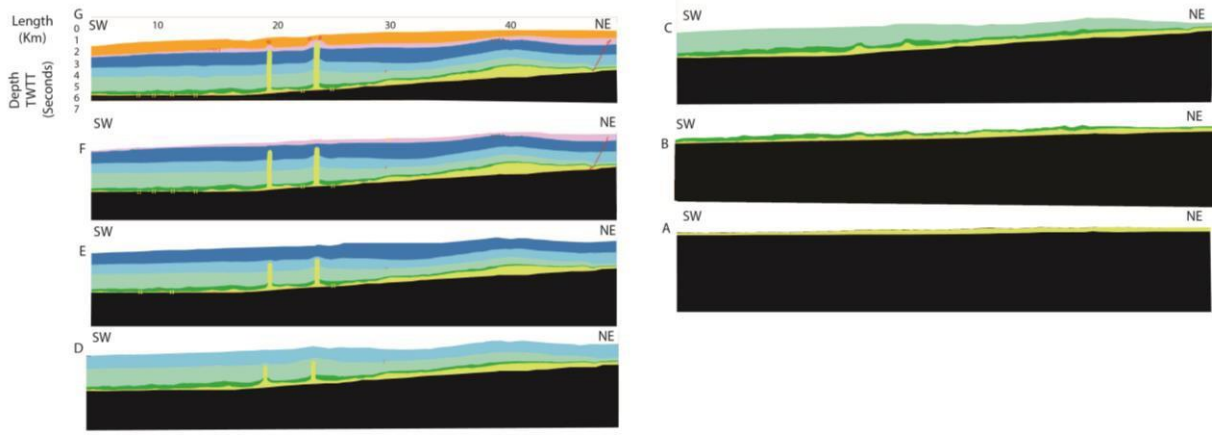

Figure 22: Restoration of line 8533 from Callovian time to the present. Length is in meters and depth is in TWTT. See figure 7 for location of line.

The complete restoration is shown in Figure 22 from the deposition of Callovian salt to the modern basin configuration. Tracing salt over the location of the two diapirs from the Callovian to modern, an apparent decrease in the elevation of their bases, midpoints, and crests suggests the diapirs formed by downbuilding. In this method, the crest of the diapirs is stationary while the base and the salt stock extend downward with subsidence. This mechanism of growth is based on subsidence and the constant density of salt, which becomes comparatively lower and lower as sediment is piled on top of neighboring stratigraphy. Cutting off of the Destin Dome from salt to both the northeast and southwest may have prevented it from following a similar trend of growth. It is possible that faulting along the BSE, not overburden caused salt migration into the Destin Dome area. Such faults however, would be nearly horizontal and therefore difficult to determine on seismic data.

Lines 32201 and 32203 are PSDM lines oriented northeast-southwest and northwest-southeast. Restoration of these lines enabled the calculation of subsidence values from Callovian

time to the present. Because the evolution of stratigraphy along the lines is similar to line 8533, only a brief summary of the important stages is given.

4.2 Line 32201

Line 32201 is a 110 km long PSDM seismic reflection line trending northeast-southwest. The line extends to 10 km west of the eastern tectonic hinge and ends along the northwestern flank of the Southern Platform.

Figure 23A: Late Triassic-Early Middle Jurassic time. Dark blue color indicates early graben fill, and light blue represents a younger stage of graben fill. A listric normal fault bounds the half graben to the southwest.

Triassic synrift volcanic and siliclastic rocks fill in a northeast trending half graben 5,300 m deep at its center and 60 km long in the northeast-southwest direction (Figs. 9, 23A). Two distinct sequences fill the half graben. The first sequence consists of high amplitude stacked reflectors beginning in the northeast (dark blue) discussed in the Observations section,steepening toward the center of the graben, then flattening, narrowing and truncating against the listric normal fault to the southwest (Figs. 9, 23A). This may be the Eagle Mills Formation. The second sequence is deposited on top, containing individual reflectors that lack the robust high amplitude seen to the northeast (dark blue). The northeast trending normal fault that bounds the half graben is truncated by the BSE.

This line trends along the southeastern tip of the Destin Dome, oblique to the primary direction of subsidence. Salt accumulation here is far less than along line 8533 (Fig. 22) that runs over the crest of the Destin Dome in the predominant dip direction of the basin. Salt maintains a

tabular shape throughout Early Late Jurassic time (Fig. 23B). In the southwest, the salt and Norphlet/Smackover formations thin and pinch out near the Southern Platform border (Figs. 23B, 23C). The combined Haynesville/Cotton Valley formations do not thin noticeably along the boundary with the Southern Platform (Fig. 23D) although Applegate et al. (1985) note that the Cotton Valley Formation pinches out along the highest part of the Middle Ground Arch. Along this line, the northeastern border of the Destin Dome is 15-18 km from the eastern tectonic hinge,

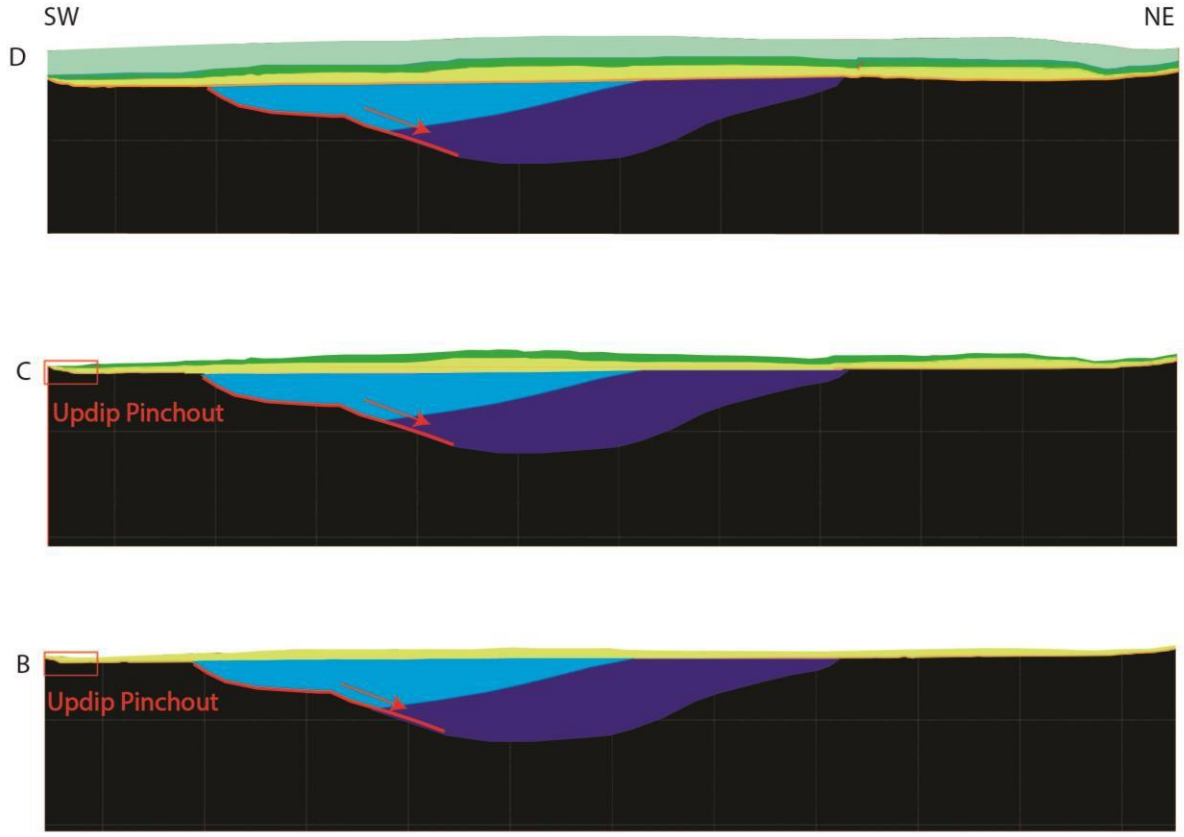

Figure 23B, C, D: B: Latest Middle Jurassic (166-164.7 Ma). C: Early Late Jurassic (164-157 Ma.) D: Late Jurassic to Early Cretaceous (157-139 Ma) suggesting that the hinge did not control the updip limit of the Destin Dome as may be inferred from a dip line perspective, such as Figure 22C.

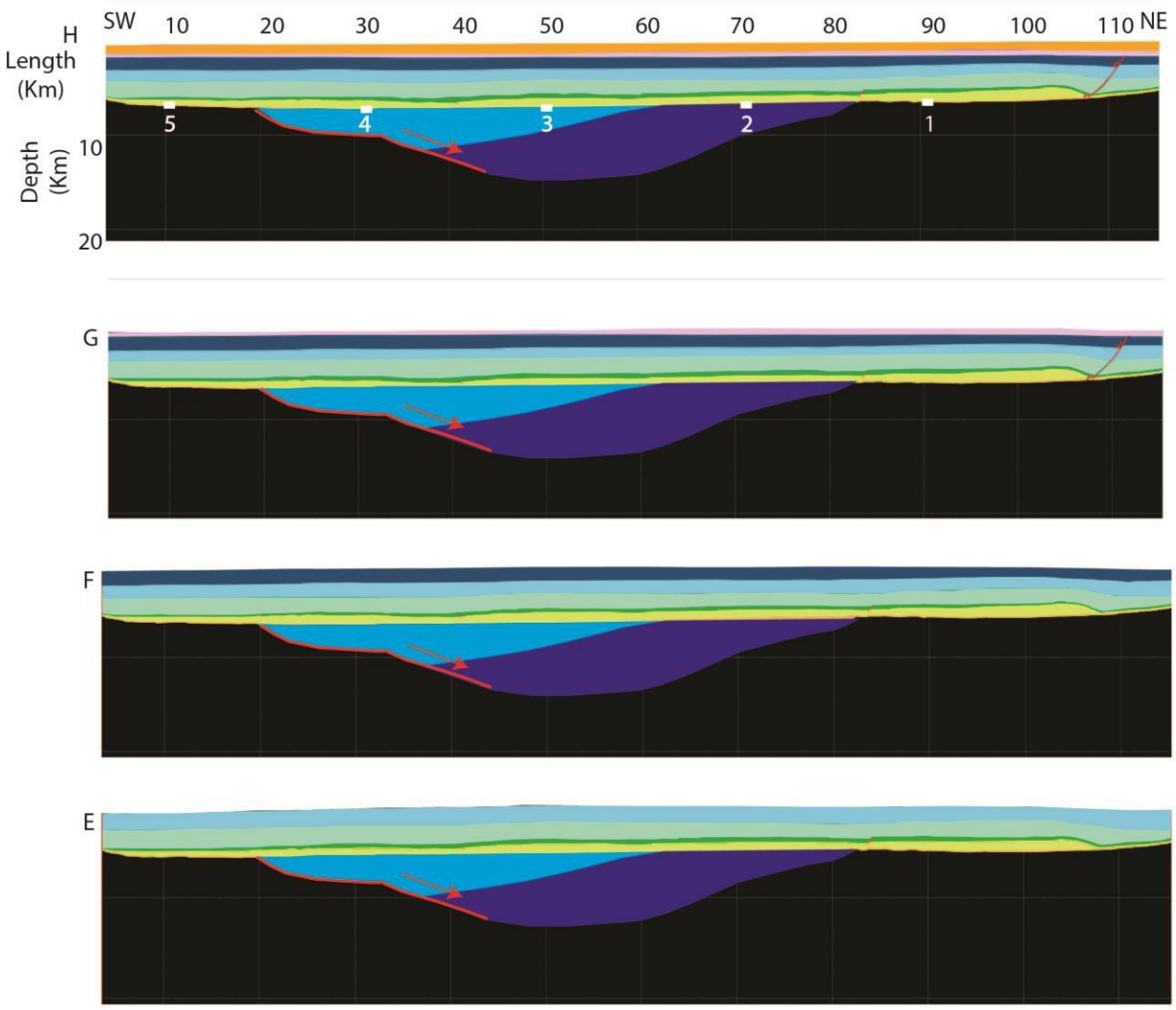

Figure 23E, F, G, H: E: Early Cretaceous time (139-113 Ma). F: Late Early Cretaceous to Early Late Cretaceous (113-100 Ma). G: Late Cretaceous (100-66 Ma). H: Cenozoic (66-0 Ma)

The decompacted Rodessa Formation (Fig. 23E), Washita Formation (Fig.23F), Selma Formation (Fig. 23G) and Cenozoic sediments do not fluctuate more than 300 m in thickness from northeast to southwest, except near the landward tip of the Destin Dome. The large wedge of salt marking the dome's tip eventually rolls over in a similar manner to the salt rollers in Figure 13 (Figs. 23G, 23H). This relatively homogeneous line is distal from the majority of salt migration and extreme variations in subsidence along dip, making it clear that since Late Jurassic time, salt and subsidence have completely influenced the paleogeography of the Apalachicola Basin. The

effect of the Triassic-Early Jurassic half graben on basin morphology is thoroughly eradicated prior to the deposition of salt in Middle Jurassic time (Fig. 23B). Figure 23 displays the complete restoration of line 32201. The slight synclinal nature of the line after Callovian time (Fig. 23B) is attributed to salt accumulation. White numbered boxes in Figure 23H indicate locations where subsidence was measured after each step from Callovian time to modern time.

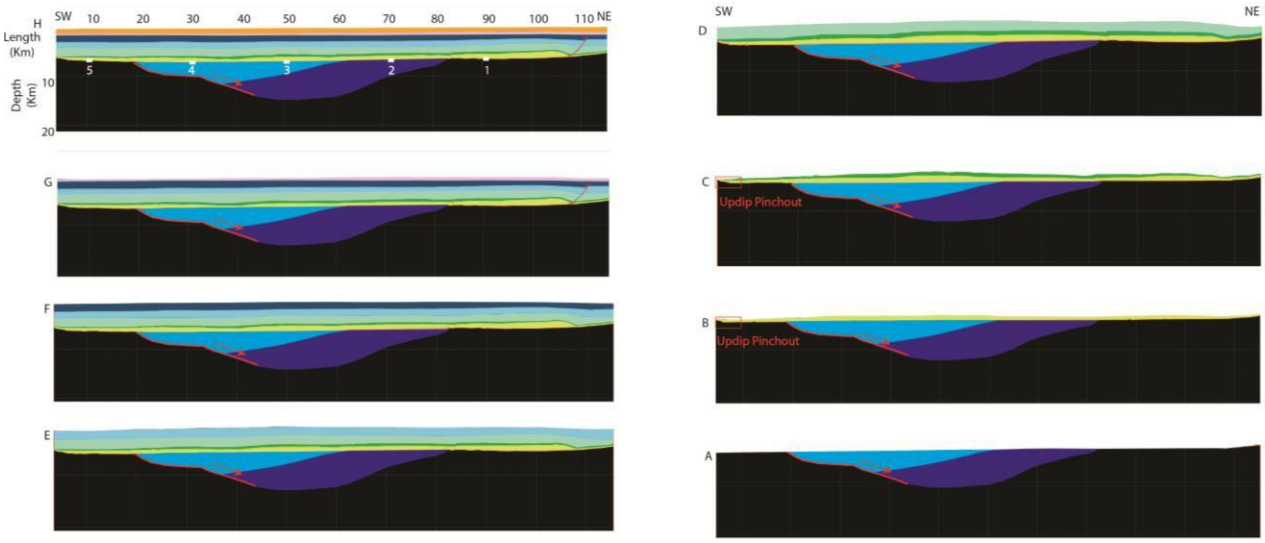

Figure 23: Restoration of line 32201 from Late Triassic time to the present. White numbered boxes in Figure 23H indicate locations where subsidence was measured. For location of line see Figure 7.

4.3 Line 32203

Line 32203 is a 70 km long northwest-southeast trending PSDM line that extends from the southeastern tip of the Destin Dome, west to the dome's crest. The southeastern edge of the line is 5 km southwest of the eastern tectonic hinge although the hinge is not shown. The half graben in Figure 10 likely continues under line 32203, although the seismic resolution is poor enough that it remains unobserved. Undulations in salt (Fig. 24B) clearly indicate allochthonous salt movement by Early Late Jurassic

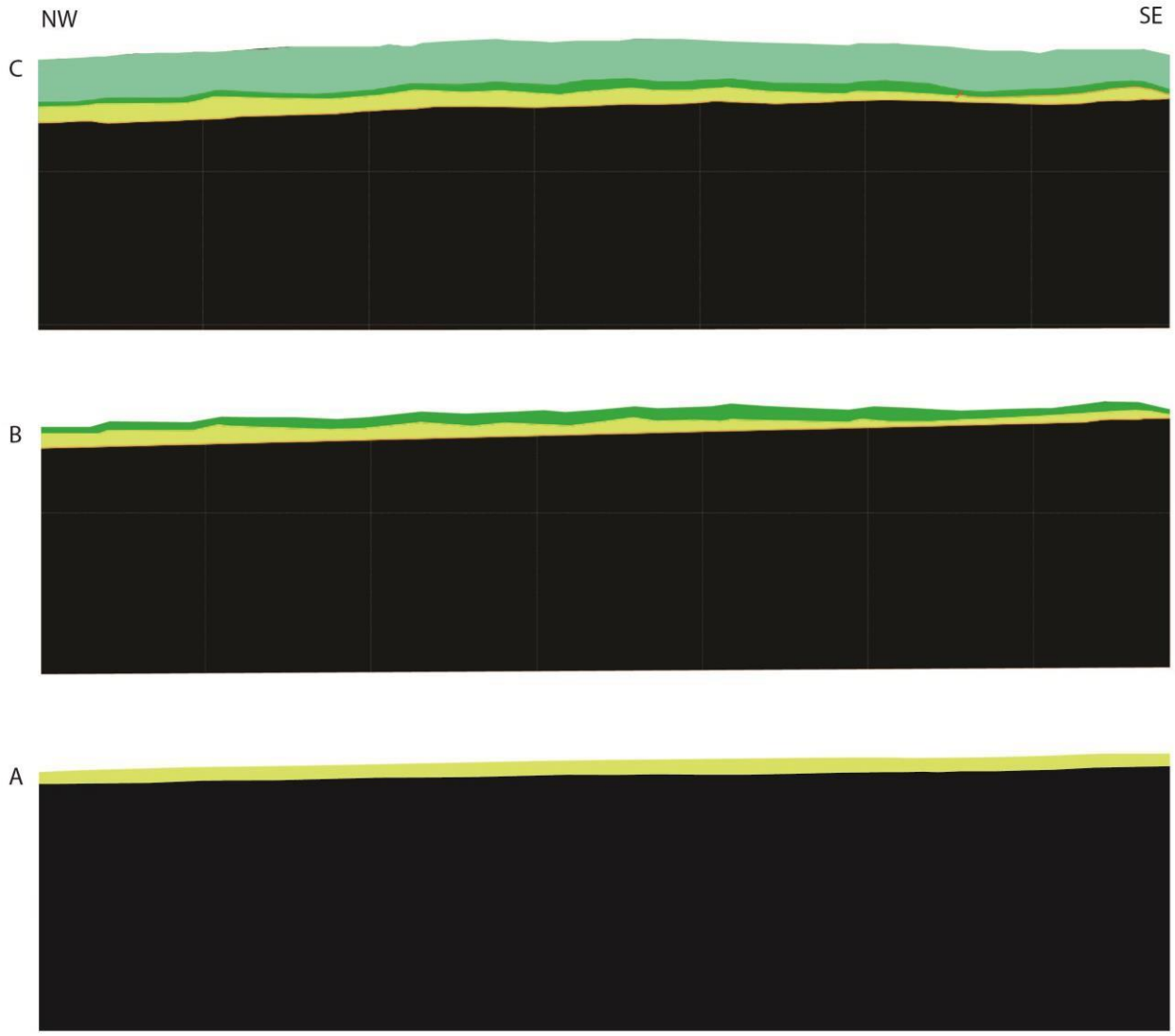

Figure 24A, B, C: A: Latest Middle Jurassic (166-164.7 Ma). B: Early Late Jurassic (164-157 Ma).C: Late Jurassic to Early Cretaceous (157-139 Ma).

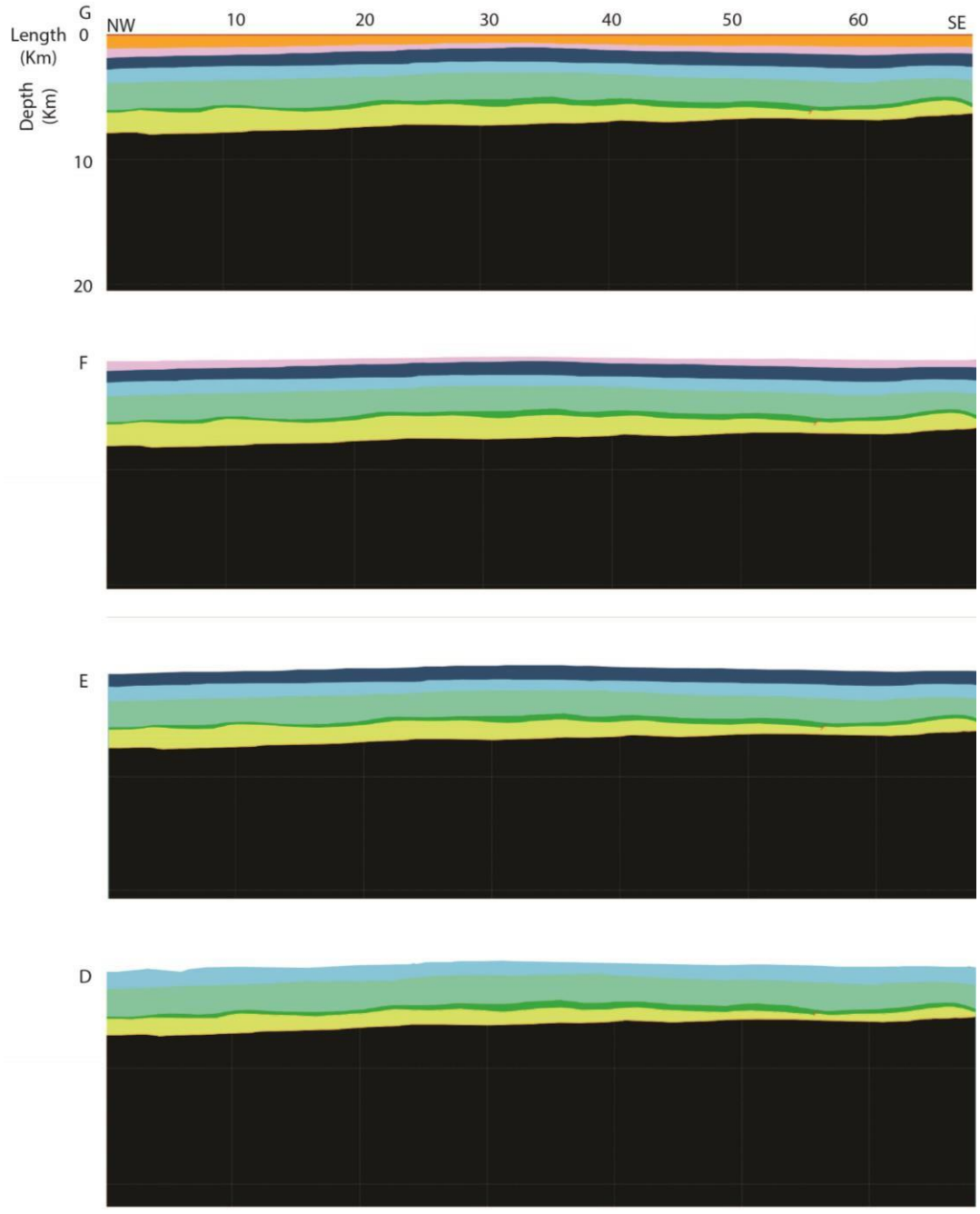

Figure 24D, E, F, G: D: Early Cretaceous (139-113 Ma). E: Late Early Cretaceous to Early Late Cretaceous (113-100 Ma). F: Late Cretaceous (100-66 Ma). G: Cenozoic (66-0 Ma).

Along this orientation, salt accumulates continuously throughout Cretaceous time (Figs. 24D, 24E, 24F). Because this cross-section is farther landward than the other two lines, this line is shallower. Only 4-6 km of overburden overlie the central Destin Dome (Fig. 24G) at its crest.

Downdip, sedimentary overburden is as much as 9-9.5 km as mapped by MacRae (1993).

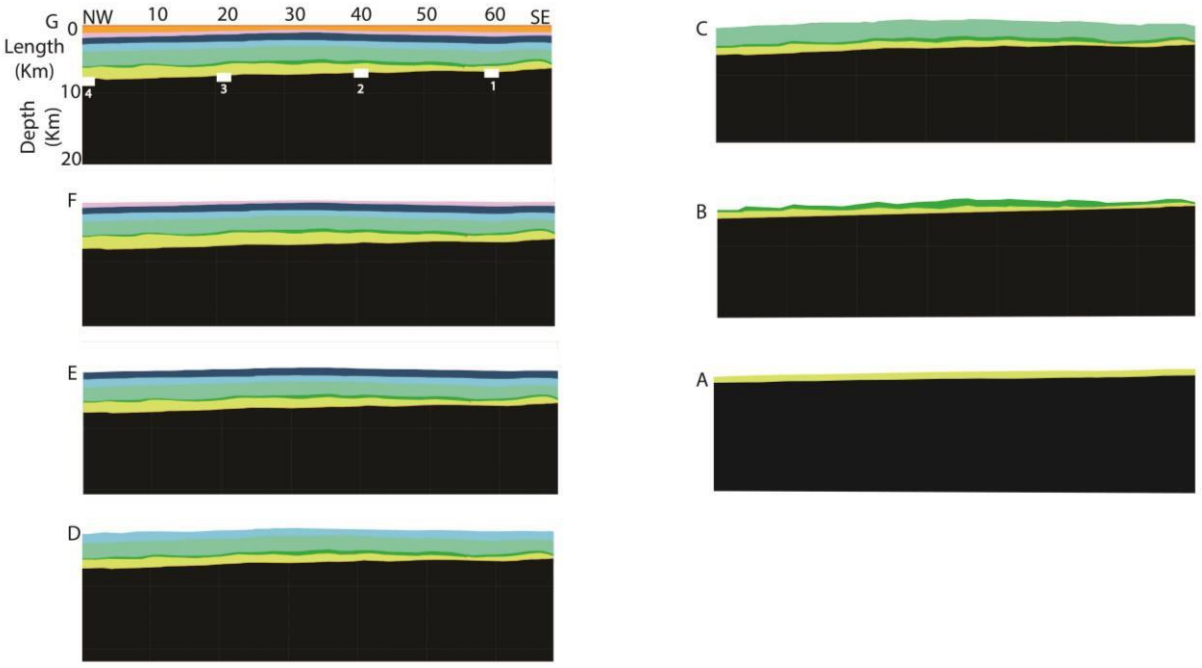

Figure 24: Restoration of line 32203 from Late Triassic time to present. White numbered boxes in figure 24G indicate locations where subsidence was measured. For location of figure, see Figure 7.

4.4 Subsidence

One assumption made prior to measuring subsidence is that the basement was at the surface prior to the formation of the basin (Dunbar and Sawyer, 1987). The erosional nature of the BSE suggests that this is the case. The total subsidence is the modern depth to basement. Total tectonic subsidence (TTS) is defined as the sediment unloaded depth to basement (Buffler and Sawyer, 1985). TTS isolates that part of subsidence of a basin not caused by sediment and water loading (Steckler et al., 1980). To differentiate TTS from total subsidence, it is necessary to know the densities of each formation to properly backstrip them. Subsidence values were calculated using restorations of PSDM lines 32201 and 32203 (Figs. 23, 24). Density values used are listed in Table 2. After backstripping each layer and its subsequent decompaction, the elevation of the BSE was

measured. The amount of elevation change between one time period and the next is divided by the duration of the time period to obtain a subsidence rate during each period. TTS is then the sum of all elevation changes.

In the EGoM, the BSE is used as a surface upon which to calculate TTS (Dunbar and Sawyer, 1987; Driskill et al., 1988; MacRae and Watkins, 1996). Upper crustal rifting in Triassic and Early Jurassic time was likely intermittent and slow (Salvador, 1991), suggesting the crust had time to cool and reequilibrate. The low density of faulting within the basement suggests that the majority of TTS was accommodated by lower crustal thinning during a second phase of rifting in Middle Jurassic through Early Cretaceous time. Therefore, the subsidence measurements from restorations down to the BSE are viable.

Along line 32201, subsidence was measured in 5 locations from northeast to southwest, every 20 km, starting from 20 km southwest of the eastern tectonic hinge to just northeast of the Southern Platform border (Fig. 22). TTS totaled 4 km in the axis of the basin at location 2 under the northeast portion of the Destin Dome (Fig. 25A). Locations 3, 4 and 5 are near the Southern Platform and have 3 to 3.5 km of TTS. The smallest measurements are at location 1 in the northeast with a total of 2.7 km.

Along line 32203, subsidence was measured at 4 locations, every 20 km starting from 10 km northwest of the eastern tectonic hinge to the crest of the Destin Dome (Fig. 25B). The amount of subsidence was 3 km at location 4 along the peak of the Destin Dome in the axis of the basin (Fig. 25B). TTS decreases to the northeast from location 3 (2.85 km) to location 2 (2.65 km) to location 1 (2 km). The decrease in subsidence from southwest to northeast is consistent with northeast-southwest directed extension during Early Late Jurassic to Early Cretaceous time.

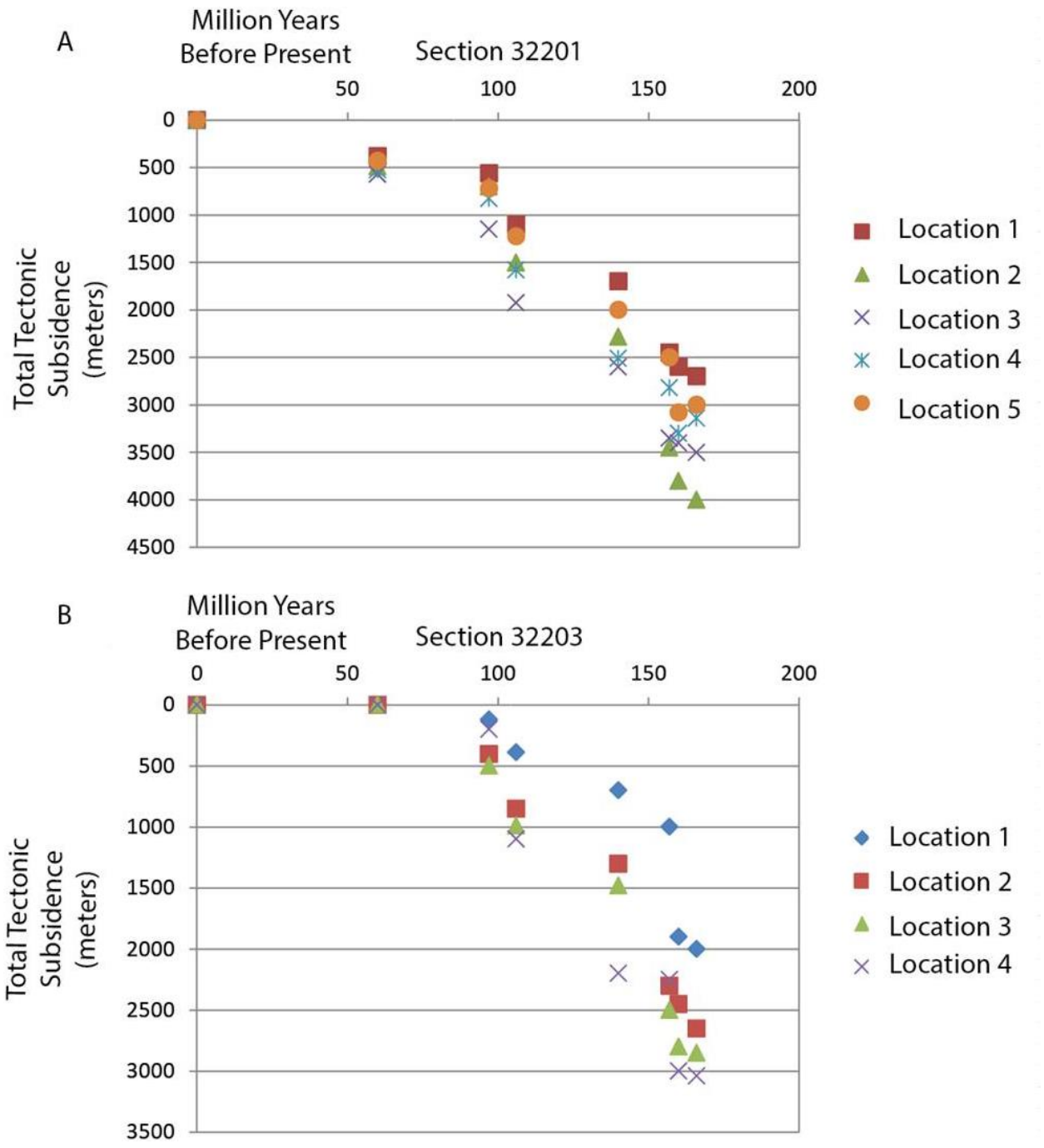

Figure 25: Subsidence measurements along lines 32201 (A) and 32203 (B) between 165 Ma and the present. Figures 23 and 24 show the locations of subsidence measurements.

A near exponentially declining relationship defines TTS rates between synrift subsidence, early postrift subsidence and late postrift subsidence. During synrift subsidence in Late Middle to Early Late Jurassic time, TTS rates near the Destin Dome were as high as .06 mm/yr. During late

synrift to early postrift subsidence in Late Jurassic to Early Cretaceous time, TTS rates dropped to 0.045 mm/yr. During late postrift subsidence from Mid Cretaceous to Cenozoic time, TTS rates dropped to nearly 0 mm/yr.

Driskill et al. (1988) estimates that Jurassic subsidence accounts for 40-43% of TTS within the Mississippi Interior Salt Basin and Wiggins Arch, and that Cretaceous subsidence accounts for another 43% of the TTS. Using location 2 on line 32201 to make similar estimates in the Apalachicola Basin, 43% of TTS occurred over 26 million years during the Early Late Jurassic-Early Cretaceous time (166-140 Ma). The bulk of the Cretaceous (140-70 Ma) accounts for the next 43% and took 2.7 times as long. The remaining 14% occurred over the next 70 million years to the present. These percentages of TTS are almost identical to those of Driskill et al. (1988) in the Wiggins Arch and Mississippi Interior Salt Basin suggesting that these structures formed synchronously with the Apalachicola Basin.

Dunbar and Sawyer (1987) estimate TTS values based on observed bathymetry, observed basement depth and a carbonate based density model. Their subsidence values are plotted in Figure 26A and range from less than 2 km in the northeast of the basin to 6 km at the carbonate shelf. However, the sparsity of their data set in the EGoM make for a challenging comparison. Measurements from the 2 lines in this study are placed over the contours of Dunbar and Sawyer (1987) for comparison (Fig. 26A).

MacRae (1993) also created subsidence contours within the Apalachicola Basin based on observed densities from wells. However, their subsidence values are not in agreement with those of this study and are 1-1.5 km less at each location (Fig. 26B). The values of MacRae (1993) are also not consistent with those of Driskill et al. (1988) who use wells in the Apalachicola

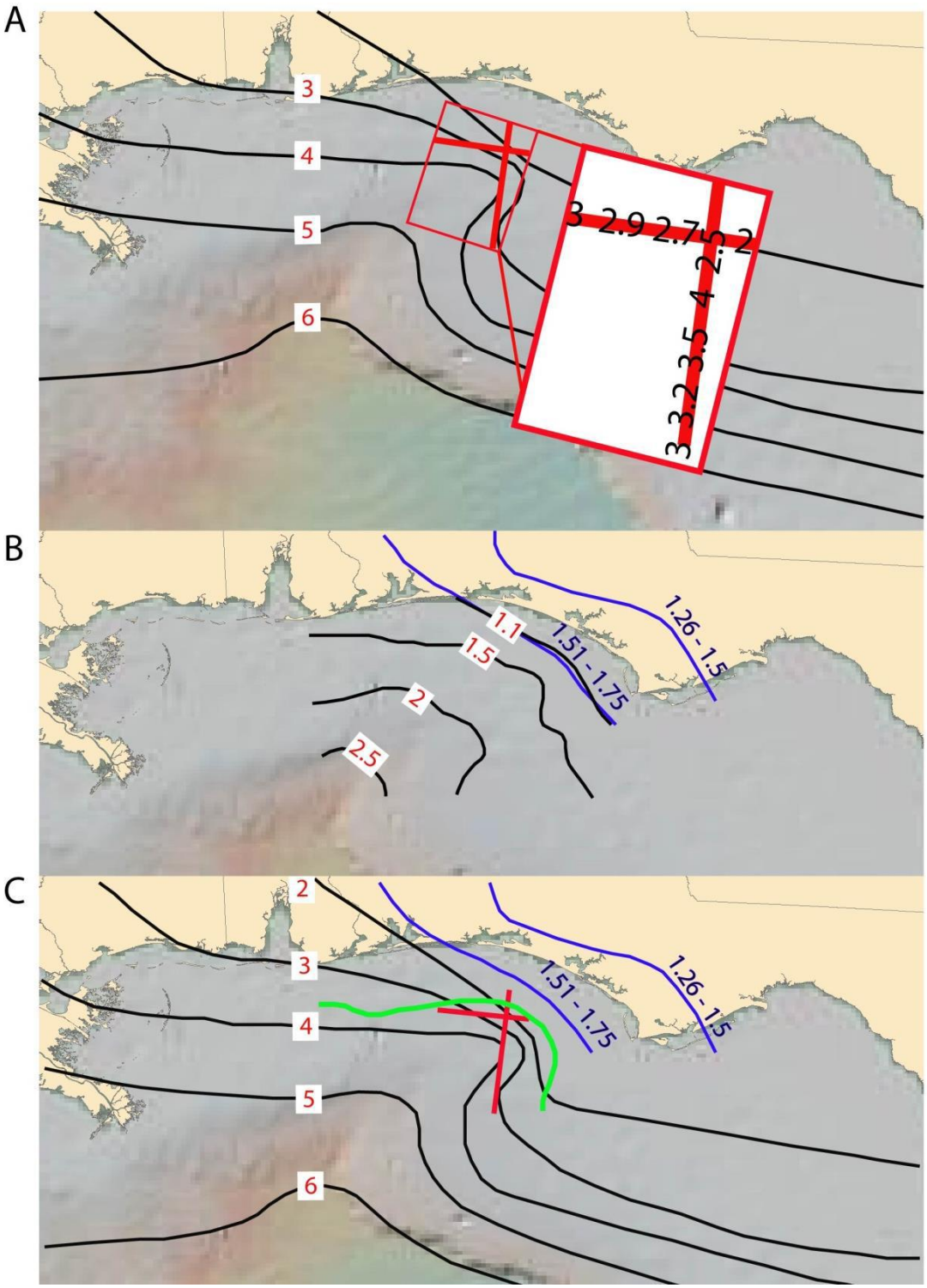

Figure 26: A: The black lines are TTS values in kilometers marked with red numbers from Dunbar and Sawyer (1987). The two boxed red lines identify locations where ITS values are measured in this study, and the inset is a zoomed in view of the red lines. B: The black lines marked with red numbers are TTS values of MacRae (1993). The blue

lines indicate assigned TTS values of Driskill et al. (1988). C: Black contour lines of Dunbar and Sawyer (1987) modified to include subsidence values of this study. The contours are compatible with those of Driskill et al. (1988). The green line is the location of the eastern tectonic hinge (MacRae and Watkins, 1993).

Embayment (Fig. 26B). Errors such as incorrect depth conversion and lack of abundant well data may account for the inconsistent values.

Figure 26C modifies the subsidence contours of Dunbar and Sawyer (1987) slightly to match those within this study. The product is compatible with onshore values of Driskill et al. (1988) (Fig. 26C). The resultant subsidence map is a reasonable approximation of TTS values in the Apalachicola Basin.

Within their crustal classification of the GoM, Buffler and Sawyer (1985) divide continental crust types along subsidence boundaries (Fig. 5). Dobson (1990) and Sawyer et al. (1991) suggest crustal type boundaries coincide with tectonic hinge zones. Researchers use tectonic hinge zones as crustal boundaries because of the close proximity of the western tectonic hinge zone with the Cretaceous carbonate shelf, apparent control of the updip extent of salt tectonics by the eastern hinge zone, the truncation of Triassic basins near the western hinge zone, and the apparent shift in the trend of basement features on either side of the western hinge zone - from approximately perpendicular to the carbonate margin on the landward side to approximately parallel to it on the basinward side (Buffler, 1989; Sawyer et al., 1991; Buffler and Thomas, 1994).

New subsidence contours derived from basin restorations (Fig. 26C) show that the eastern tectonic hinge zone lies nearly 20 km east of the 3 km subsidence boundary, which marks the thick transitional crust to continental crust transition in the northeastern Apalachicola Basin, and up to 30 km south of it in the northern central Apalachicola Basin. To the south, in

the Tampa Embayment, the western tectonic hinge is located up to 50 km landward of the carbonate shelf, much farther east than in the Apalachicola Basin. Restoration 2 suggests that the eastern tectonic hinge zone did not constrain the updip limit of salt tectonics.

The above observations imply that tectonic hinge zones are not likely to represent discrete crustal boundaries. The size of tectonic hinge zones in the EGoM is also questionable. Previous researchers (Corso, 1987; Dobson, 1990; Corso and Austen, 1991; Sawyer et al., 1991) consider unique tectonic hinge zones to extend between individual basins in the EGoM. However, the offset between the carbonate shelf and the western tectonic hinge zone in the Apalachicola Basin verses that in the Tampa Embayment suggests that they are not one continuous tectonic hinge zone.

The tectonic hinge zones may instead represent basement faulting or flexure as suggested by Dobson and Buffler (1997). This could have occurred at the local level with movement on smaller faults causing rotation of basement reflectors in certain areas and not in others. This would explain why no researcher has been able to map a continuous tectonic hinge zone trend throughout the EGoM. The northwest overall trend of both identified tectonic hinge zones in the Apalachicola Basin suggests that they formed along an inherited northwest trending tectonic fabric associated with the Paleozoic formation of Pangea. Paleozoic lineaments with a similar trend to the tectonic hinge zones are postulated by Thomas (1976). Restoration 2 (Fig. 22C) identifies the formation of the eastern tectonic hinge during Late Jurassic-Early Cretaceous time and onlapping Early Cretaceous rocks onto the western tectonic hinge (Fig. 18) suggest that it also formed around this time. Reactivation of the Paleozoic lineaments may have been caused by migration of the Euler pole around which the Yucatan Crustal Block rotated during Late Jurassic-Early Cretaceous time.

5. ORIGIN OF THE APALACHICOLA BASIN

5.1 Basin Boundaries

MacRae and Watkins (1993, 1995) speculate that east-northeast trending, steeply dipping normal faults mark boundaries between the Apalachicola Basin and the surrounding arches. Changes in the dip of subsalt reflectors below the BSE suggest that northeast trending normal faults are present near the Southern Platform and Pensacola Arch/Wiggins Arch boundary (Figs. 11**,** 14). Figure 13 identifies a 750 m step up in the BSE between the Apalachicola Basin and the Southern Platform due to offset along a small normal fault with apparent northeast dip. This offset does not account for the entire elevation difference between the Apalachicola Basin and Southern Platform, which at its crest is 1500 meters higher than the Apalachicola Basin along its flanks.

The transition between the Apalachicola Basin and the GoM Interior Basin is not clear in this study and others due to lack of clarity within the seismic data along the carbonate shelf. Wu (1990) interprets extremely thin continuous salt between the Apalachicola Basin and the GoM Interior Basin, suggesting the two basins are linked. Gordon et al. (2001) identify steeply dipping normal faults that may extend down to the BSE, isolating the two basins. MacRae (1993) and MacRae and Watkins (1996) propose that the basin extent is limited between two transform faults of Late Triassic to Middle Jurassic age, which parallel the Cretaceous carbonate shelf. In this scenario, the basins were never linked. Figure 18 displays a continuously dipping BSE reflector over the carbonate shelf in the southwestern Apalachicola Basin. The reflector is difficult to correlate underneath the crest of the shelf but is identifiable on the shelf's western side. There is no apparent fault displacement. Salt extends up the northwestern side of the shelf

but is not present closer than 10 km west of the crest (Fig 18). These two observations, along with the conclusion by Wilson (2011) that the southern Tampa Embayment and the West Florida Basin are part of one larger basin suggests that Early Mesozoic rifted basement also continues west of the carbonate shelf near the Apalachicola Basin. Thus, the salt basin of Lord (1986) (Fig. 3) west of the carbonate shelf and salt within the Apalachicola Basin were likely linked, at least until formation of the western tectonic hinge in Late Jurassic-Early Cretaceous time.

Although data within this project does not extend into the onshore portion of the Apalachicola Basin known as the Apalachicola Embayment, previous researchers (Mitchell-Tapping, 1982) identify the continuation of initial rift basin fill salt and the Norphlet and Smackover Formations at least 100 km inland based on well data. It is possible that the Apalachicola Basin and the South Georgia Rift System were linked. Transform faults near the northeastern portion of the Apalachicola Basin are proposed by McBride (1987) and may have served to offset the South Georgia Rift System and the Apalachicola Basin.

5.2 Cretaceous Carbonate Shelf

The criteria for rimmed carbonate platforms of Read (1982) includes linear trends of shelf edge reefs, a marked increase in slope into deep water, and foreslope sandstone, breccia and turbidites grading seaward in hemipelagic muds. West of the carbonate shelf in the Apalachicola Basin, a sequence of Middle Cretaceous deep marine carbonate and clastic rocks transition into Middle–Late Cretaceous fine grained hemipelagic mudstone and carbonate rock, and into Tertiary and Miocene fine grained turbidites and hemipelagic mudstone parallel to the carbonate shelf (Shaub et al., 1984; Addy and Buffler, 1984). A marked increase in slope into deep water is present, South of the reentrant in the central and southern EGoM (Fig. 27a).

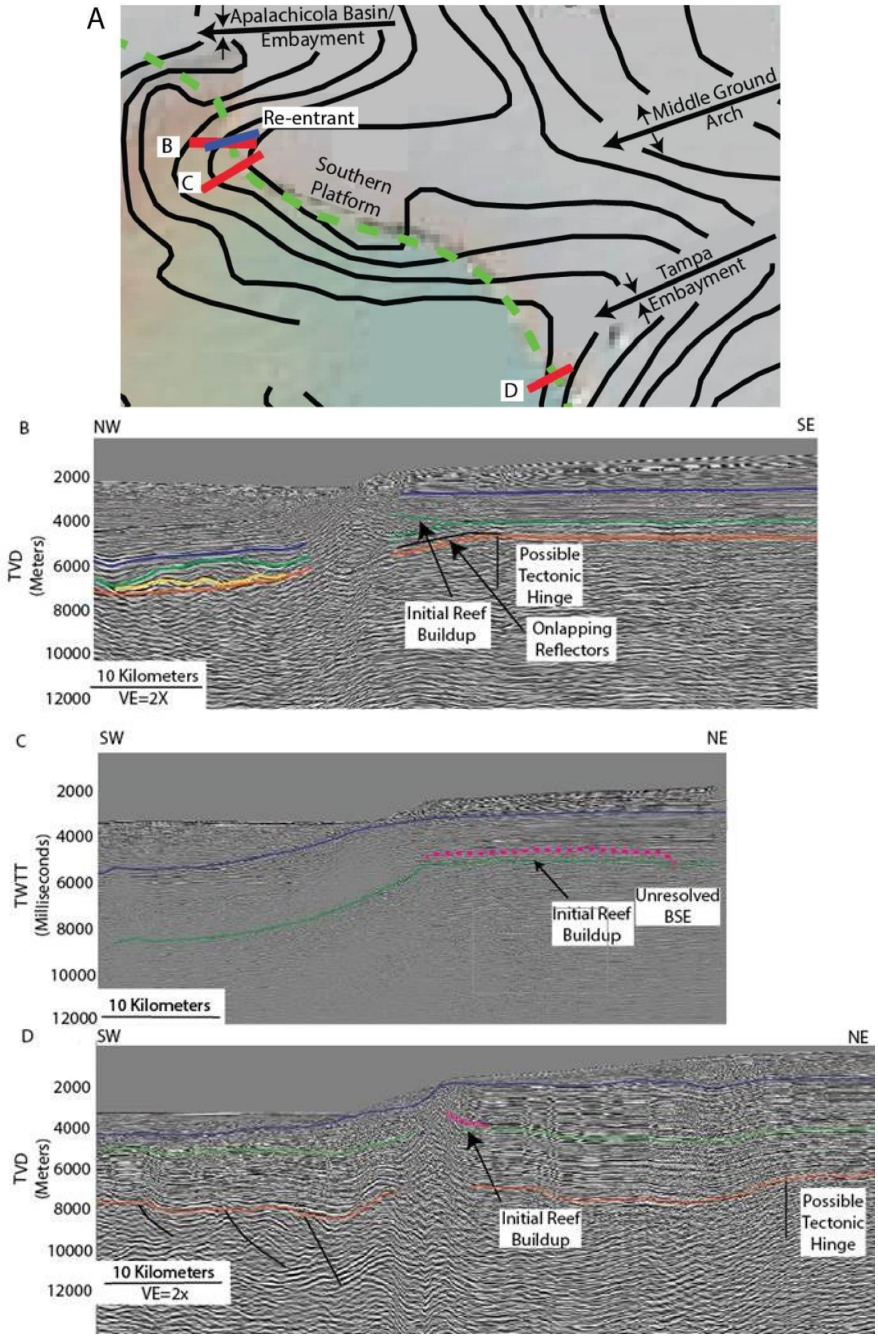

Figure 27: A: Location of figures. Blue line is shelf re-entrant. B: East-west line in the southern most Apalachicola Basin. The green line marks the Early Cretaceous beginning of carbonate shelf aggradation and the dark blue line identifies the MCSB. A thin wedge of salt extends up the carbonate shelf but is truncated against the slope. The initial rimmed carbonate reef buildup is identified in pink. C: Northeast-southwest line over the northern Southern Platform. D: Northeast-southwest line over the Tampa Embayment carbonate shelf. Note the significant offset in the Tampa Embayment between the tectonic hinge zone and the Cretaceous carbonate shelf.

Addy and Buffler (1984) state that lack of coherent reflections at the base of Lower Cretaceous carbonate shelf may represent a high energy rudist reef. Jumbled, incoherent reflections mark the base of the Lower Cretaceous at the carbonate shelf boundary in the southwestern Apalachicola Basin (Figs. 27B, 27C). An examination of the carbonate shelf reveals such reef facies are laterally continuous throughout the southwestern Apalachicola Basin and northern portion of the Southern Platform. Wilson (2011) identifies the same reef trend within the Tampa Embayment (Fig. 27D). These observations reveal that the criteria for rimmed carbonate platforms are met in the southern Apalachicola Basin and extending south to the southwestern Tampa Embayment, perhaps unbroken. North of the shelf reentrant (Fig. 27A), the rudist reef may still be present (Addy and Buffler, 1984), implying a gradual transition from rimmed carbonate shelf to a gently sloping carbonate shelf of isolated patch reefs such as those of Louisiana and East Texas.

The western tectonic hinge zone accredited with nucleation of the carbonate shelf (Corso et al., 1989) is 10 km east of the carbonate shelf in the Apalachicola Basin (Fig. 27B). However, in the Tampa Embayment the tectonic hinge is ~30 km or more east of the carbonate shelf (Fig. 27D), implying a different location of shelf nucleation in the Tampa Embayment. One possible alternative is a separate deep basement involved fault, which would extend into Cretaceous rock (Dobson and Buffler, 1991, 1997). A sequential illustration of development of the Cretaceous carbonate shelf in the Apalachicola Basin is described below (Fig. 28).

A. Salt is deposited and extends from the Apalachicola Basin west beyond the location of the future Cretaceous carbonate shelf as evidenced by thin salt west of the shelf, extending updip (Figs. 18, 28A). Wu (1990) identifies 1-2 km of Late Jurassic sediment underneath the

Cretaceous carbonate rock across the Apalachicola Basin. Jurassic carbonate buildups of the upper Haynesville Formation appear landward of the future carbonate shelf (Fig. 17). The Jurassic carbonate buildups form prior to the western tectonic hinge and are not associated with the Cretaceous carbonate shelf.

B. A tectonic hinge forms during Latest Jurassic to Early Cretaceous time (Fig. 28B). Simultaneously or shortly thereafter, salts move away from the tectonic hinge zone. Salt may have moved by gravity related gliding associated with increased dip, differential sedimentation from the shallow shelf into the sediment starved GoM Interior Basin or Cretaceous normal faulting along the carbonate shelf.

C. Without salt, the platform stabilizes enough for carbonate aggradation to occur (Fig. 28C**)**. Carbonate shelf buildup occurs from Earliest Cretaceous to Cenomanian time when a drowning event ceased further buildup (Wu, 1990), represented by the MCSB.

D. A depositional hiatus between Middle Cretaceous and Oligocene time followed (Addy and Buffler, 1984). Rapid deposition occurred in Oligocene time (Fig. 28D), dumping more than 5 km of sediment on the basinward side of the shelf (Wu, 1990). Cenozoic sediments are not continuous from the Apalachicola Basin to the GoM Interior Basin (Fig. 12); they extend to and are truncated at the shelf edge (Fig. 28D). Patterns of onlap are likely associated with the toe of the prograding Mississippi River deltaic fan.

5.3 Basin Forming Mechanism

Wilson (2011) states that the Tampa Embayment to the south of the Southern Platform/Middle Ground Arch, displays a near perfect steer's head geometry (Fig. 29). The steer's head geometry represents a simple thermal model of basin formation based on two layer lithospheric stretching described by White and McKenzie (1988) (Fig. 30). Within this model,

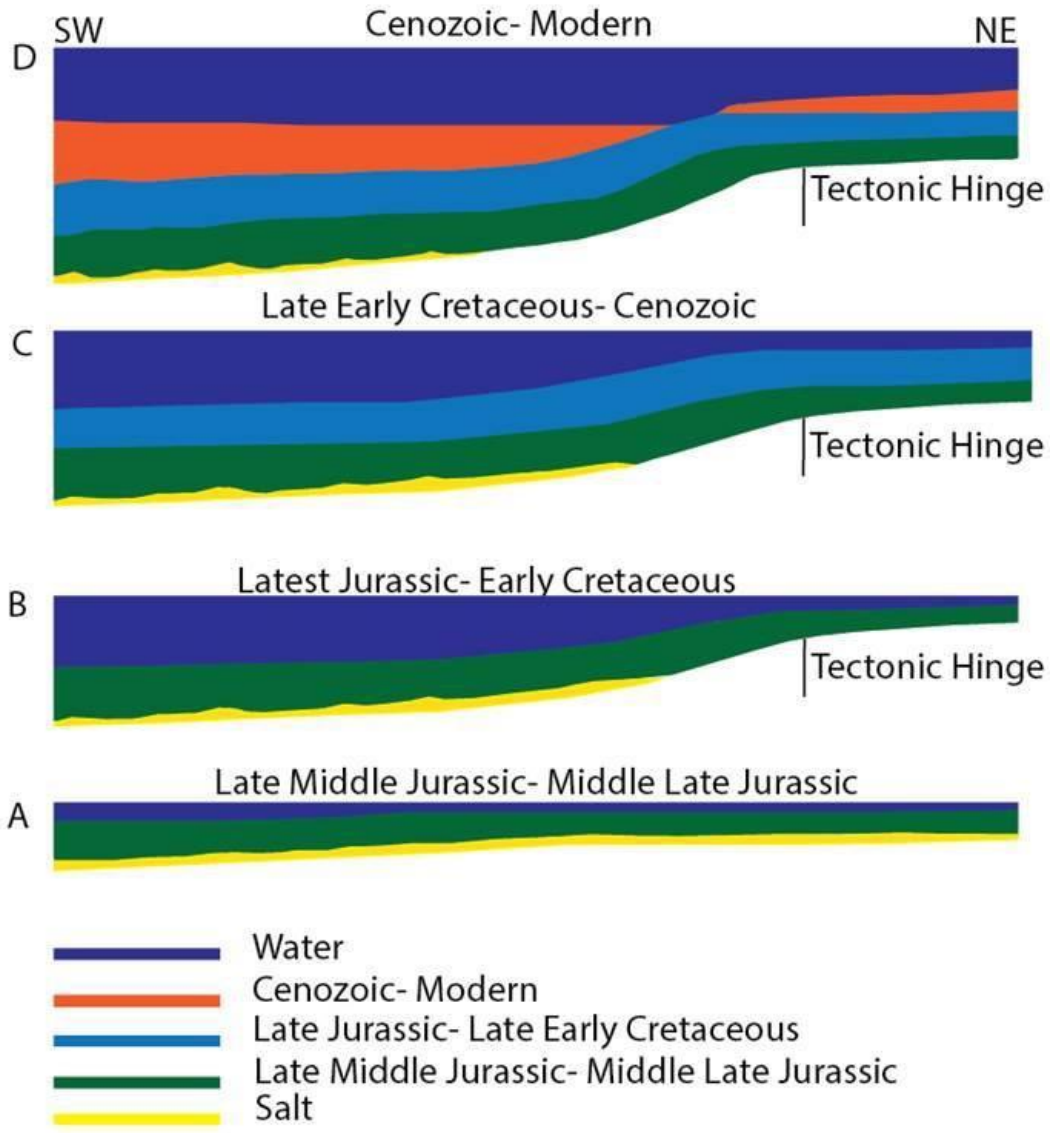

Figure 28: Cartoon illustration of the formation of the Cretaceous carbonate shelf, see text for explanation.

extension between the crust and lithospheric mantle is appropriated differently, although the total amount of stretching is the same within both regions. Crustal stretching is concentrated in the center of the basin and is represented by a series of grabens. Crustal stretching decreases sharply along basin flanks. Stretching of the lithospheric mantle occurs over a fractionally wider region than the crust. Uplift occurs along basin flanks due to thinning of the lithospheric mantle, the first reaction to which is local uplift. Early post-rift stratigraphic onlap results from the decay of

the thermal anomaly that created initial uplift. Characteristic features of a basin with steer's head geometry include the early post rift stratigraphic onlap onto basin flanks, thickening of stratigraphic packages into the basin center and exponentially decreasing rates of subsidence over time, initially instantaneous and related to faulting, then relating to decay of the thermal anomaly in the upper mantle lithosphere and finally, once the thermal anomaly is abated, related to sedimentary loading.

The Apalachicola Basin also displays the basic steer's head geometry (Fig. 15) and contains its defining characteristics. Figure 13 displays the onlapping relationship between Callovian and Oxfordian age sediments onto the neighboring Southern Platform. An eroded surface of the BSE cuts jagged valleys over the Southern Platform (Fig. 13) suggesting rapid uplift and erosion. Sedimentary packages thicken toward the basin center (Fig. 15) in areas with minimal salt influence. Rapid synrift and early postrift subsidence in Late Jurassic and Early Cretaceous time are clearly distinguished from late postrift subsidence in the Mid Cretaceous to Cenozoic according to TTS measurements (Fig. 25).

The large half graben in Figure 9 is located along the central basin axis. The half graben boundary fault extends down to 13,000 m or deeper with up to 5,300 m of graben fill. Other dipping subsalt reflectors below the BSE on PSTM lines (Figs. 11, 15) suggest that there are several grabens filling an area between basin bounding arches.

5.4 Comparison with the Tampa Embayment

To further compare rifting and rift timing between the Apalachicola Basin and the Tampa Embayment, a composite illustration was created running northwest-southeast from the base of the Apalachicola Basin to the central portion of the Sarasota Arch (Fig. 31). The composite was created with PSDM seismic lines in the Tampa Embayment and PSTM lines in

the Apalachicola Basin. An approximation of thicknesses in the Apalachicola Basin

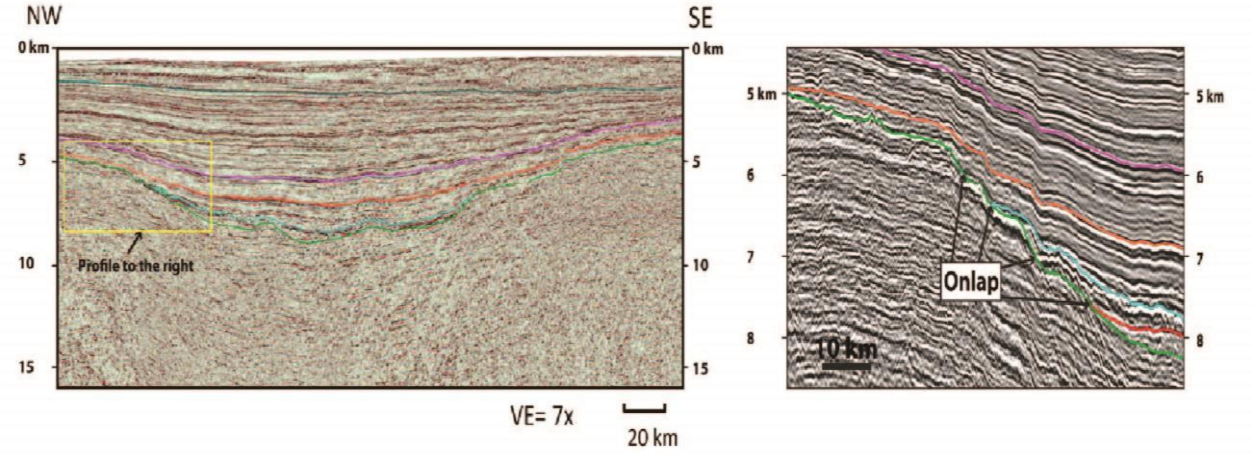

Figure 29: Along strike section through the Tampa Embayment from Wilson (2011), identifying a similar geometry to the Apalachicola Basin.

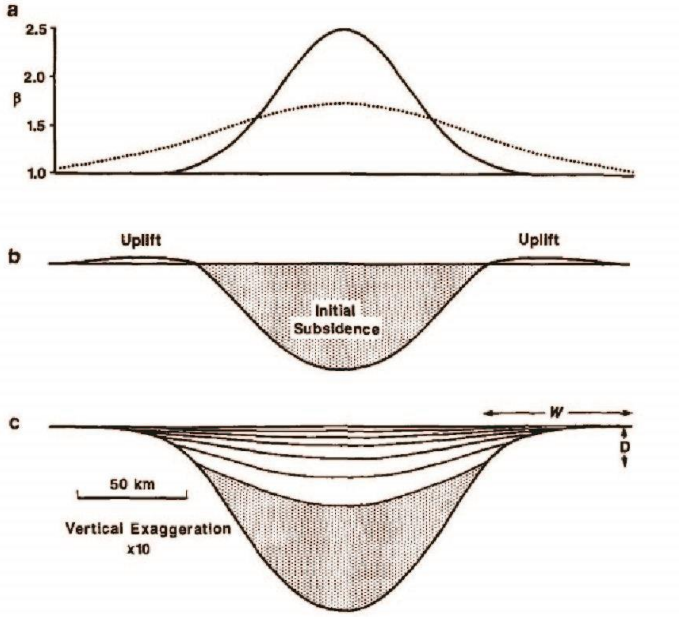

Figure 30: White and McKenzie (1988) steer's head geometry model of basin formation. A: Lateral variation in lithospheric mantle extension factor (dashed line) compared with crustal extension factor (solid line). B: Initial rift configuration showing uplifted flanks. C: Thermal subsidence as well as basin flank onlap. Lines overlying initial subsidence are 25 million year intervals showing an exponentially declining rate of subsidence.

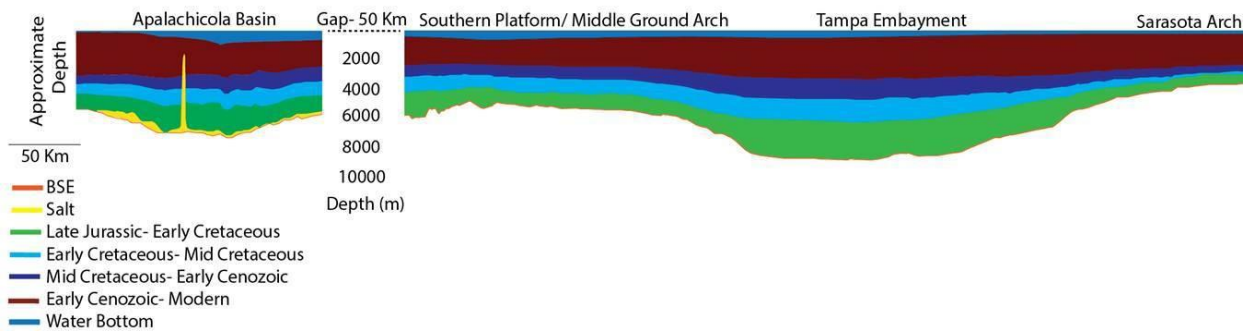

Figure 31: Regional composite line between the Apalachicola Basin and Sarasota Arch.

was created using the isochore maps of MacRae (1993) and Denne and Blanchard (2013).

Initial progradation of the Haynesville and Cotton Valley formations from both basins over the Southern Platform indicates that they were both structural lows filled in by Late Jurassic time (Fig. 31). Although in this section, the Apalachicola Basin appears shallower than the Tampa Embayment, the deepest BSE in the Tampa Embayment east of the carbonate shelf is close to 10,000 m, while in the Apalachicola Basin it is closer to 12,000 m. Because the total extension factors in each basin (β) are similar (between 1.5 and 3 out to the carbonate shelf) (Dunbar and Sawyer, 1987), the discrepancy in BSE elevation can be attributed to the increased input of clastic sediments in the Apalachicola Basin from the Mississippi and Apalachicola Rivers during Cenozoic time. The apparent rugosity of the BSE over the Southern Platform is much greater close to the Apalachicola Basin (Fig. 31), indicating the Southern Platform was exposed to a greater degree of erosion further north. Basement involved faulting in the Tampa Embayment offsets the Lower Cretaceous Cotton Valley Formation (Dobson and Buffler, 1997), later than any observed basement involved faulting in the Apalachicola Basin and suggesting upper crustal extension lasting beyond that within the Apalachicola Basin. The implication here is that the Tampa Embayment continued to develop after the Apalachicola Basin, suggesting that basins in the EGoM are younger in the southeast and older in the northwest.

5.5 Evolution of the Apalachicola Basin

Triassic sedimentary rock within grabens in the onshore Apalachicola Embayment suggest a Late Triassic origin of rifting. The half graben in Figure 9 is likely one of several grabens formed within the Apalachicola Basin during this early phase of rifting. Two distinct sequences of graben fill beneath the BSE (Fig. 9) suggest that Late Triassic-Early Jurassic faulting contained an element of reactivation and may have consisted of brief intermittent pulses of extension. Basement involved faulting is generally truncated at the BSE, although previous researchers (Hunt, 2013) have identified basement involved faulting continuing into overlying salt near the Destin Dome area, suggesting a Late Triassic to Late Middle Jurassic age of initial rifting. Above Upper Middle Jurassic salt, faults are small and cannot be distinguished from faults caused by salt movement. Graben topography was filled prior to Middle Jurassic time, as salt was deposited in a tabular geometry on top (Fig. 9). The data within this study are insufficient to identify the orientation of initial rifting, although Macrae and Watkins (1996) identify multiple northeast-southwest trending normal faults in the basement and suggest rifting occurred in the northwest-southeast direction. Onlap of salt and upper Jurassic sediments onto neighboring arches indicates that basin flank uplift and the steer's head geometry in the Apalachicola Basin and the Tampa Embayment was established by Late Middle Jurassic time. This model of rifting requires both brittle upper and lower crustal thinning as well as rising of the asthenosphere causing elevated crustal temperatures. Very rapid local subsidence accompanied graben formation and high rates of salt deposition, allowing for a thick buildup of salt. Figure 30B presents the basic basin geometry at this time.

By Late Jurassic to Early Cretaceous time, sedimentary packages began to thicken to the southwest accompanied by a basinward tilt (Fig. 22C). This implies that the basin became

elongated towards the west. Total extension estimates of Dunbar and Sawyer (1987) increase along the axis of the basin from northeast to southwest from $\beta = 1.5$ to 3 at the carbonate shelf. Lack of observed normal faults dissecting Upper Jurassic-Lower Cretaceous stratigraphy suggests that westward extension was accommodated by thinning of the lower crust. The thick transitional crust that the Apalachicola Basin occupies formed during this time.

This time period is coincident with or slightly following the initiation of Yucatan rotation away from North America (Buffler and Sawyer, 1985; Pindell, 1985; Salvador, 1987) and an Euler pole rotation from Florida to modern Cuba (Pindell, 2010). The Yucatan block may have been caught between broad transtensional zones across Mexico and Florida. However, the proposed steer's head two layer stretching model does not require the presence of large scale transform faults to create the sequence of basins and arches in the EGoM. The two observed tectonic hinge zones formed during this time and appear to trend northwest (Fig. 26C), with an orientation similar to transform faults described by Klitgord et al. (1984), Macrae and Watkins (1996).

The second phase of rifting, which includes lower crustal thinning and basin elongation to the west, may not actually be distinct from the first, rather a continuation of rifting with a gradual shift in orientation. The shift in orientation may be attributed to migration of the euler pole around which the Yucatan rotated (Pindell, 1985). High rates of subsidence continued throughout Early Cretaceous time (Fig. 25) as the thermal anomaly declined.

Subsidence and sedimentary thickening to the southwest created a local compressional load along the originally tabular salt in the Apalachicola Basin, forcing salt updip into the areas of the Destin Dome and the Desoto Canyon Diapir Field. Although gravity related sliding is typically identified as the primary factor in horizontal salt migration, lateral variations in

overburden thickness can result in differential loading of salt (Macrae and Watkins, 1992). Diapirs in the central Apalachicola Basin grew down through the process of downbuilding, their constant and relatively low density creating a positive buoyancy gradient as surrounding sediments are compressed and decline. The crest of these diapirs remains static over time, while the body stretches and fills in accommodation space created through subsidence. The Destin Dome on the other hand was cut off from the mother salt by a weld to the southwest and a fault to the northeast, preventing it from achieving the same vertical growth.

Lack of faulting makes it difficult to constrain the end of rifting. Wilson (2011) identifies basement involved faulting in the Tampa Embayment into Early Cretaceous time. Diminishing basin sag deposits throughout Cretaceous time (Fig. 15), paired with declining TTS rates, imply that the rift related thermal anomaly was waning greatly by Late Cretaceous time and had become minor by Cenozoic time. TTS measurements (Fig. 25) suggest that between 100-50 Ma, subsidence became almost completely dependent on sedimentary loading.

6. CONCLUSIONS

1. Basin restorations suggest that since Late Jurassic time, the two major controls on basin paleogeography are salt movement and subsidence. A massive differential sediment load between the northeastern and southwestern Apalachicola Basin enabled updip migration of salt into the large Destin Dome and the surrounding diapir field. The Destin Dome was growing for approximately 80-100 million years, from Early Late Jurassic to Late Cretaceous time. Diapirs in the Desoto Canyon Diapir Field continue to grow into Cenozoic time. Comparison of restorations with expulsion of Upper Jurassic and Lower Cretaceous sourced hydrocarbons indicates that structural traps against salt were in place prior to expulsion of Late Jurassic sourced hydrocarbons, making them viable.

2. Late Jurassic to Early Cretaceous subsidence was rapid and accommodated ~42% of overall subsidence. Subsidence rates declined quickly during the next 140 million years, with rates approaching zero by modern time. Total tectonic subsidence values range between 2 km near land and 6 km near the Cretaceous carbonate shelf. The timing of subsidence in the Apalachicola Basin is nearly identical with subsidence in the Mississippi Interior Salt Basin and the Wiggins Arch, suggesting they formed simultaneously.

3. Sedimentation rates closely follow thermal subsidence rates. Over the southwestern Apalachicola Basin sedimentation rates declined rapidly from a high of 0.125 mm/yr during Late Jurassic-Early Cretaceous time to a low of 0.02 mm/yr during Late Cretaceous time.

4. The eastern tectonic hinge zone is 20-30 km offset of the thin to thick transitional crust boundary in the Apalachicola Basin in some places, indicating that hinge zones do not mark crustal boundaries in the EGoM. The formation of the tectonic hinge zones may be linked to some preexisting regional tectonic lineament.

6. Lack of large normal faults at the carbonate shelf combined with salt extending up the majority of the western portion of the carbonate shelf suggests that the large salt basin to the west of the carbonate shelf and that of the Apalachicola Basin were once unified.

7. The Apalachicola Basin has a steer's head geometry that incorporates a two layer stretching model that explains uplifted rift flanks, onlap of early postrift sediments, erosion of the BSE along neighboring arches, increasing stratigraphic thicknesses towards the basin center and rapidly decreasing subsidence. The Tampa Embayment displays a similar geometry.

7. REFERENCES

Addy, S. K., and R. T. Buffler, 1984, Seismic stratigraphy of the shelf and slope, northeastern Gulf of Mexico: American Association of Petroleum Geologists Bulletin, v. 68, p. 1782-1789.

Applegate, A. V., and J. M. Lloyd, 1985, Summary of the Florida petroleum production and exploration, onshore and offshore through 1984: Florida Geological Survey, Information Circular, n. 101, p. 1-69.

Arden, D. D. Jr., 1974, Geology of the Suwannee basin interpreted from geophysical profiles: Gulf Coast Association of Geological Societies Transactions, v. 24, p. 223-230.

Barker, S., and Mukherjee, S. S., 2011, Interpretation of the basement step – some observations and implications in the Gulf of Mexico [abs]: American Association of Petroleum Geology Search and Discovery Article, no.90124, http://www.searchanddiscovery.com/abstracts/html/2011/annual/abstracts/Barker.html>

Barnett, R.S., 1975, Basement structure of Florida and its tectonic implications: Gulf Coast Association of Geological Societies Transactions, v.25, p. 122-142.

Bartok, P., 1993, Pre-breakup geology of the Gulf of Mexico-Caribbean: its relation to Triassic-Jurassic rift systems of the region: Tectonics, v. 12, p. 441-459.

Bird, D.E., Burke, K., Hall, S.A., and Casey, J.F., 2005, Gulf of Mexico tectonic history: Hotspot tracks, crustal boundaries, and early salt distribution: American Association of Petroleum Geologists Bulletin, v. 89, p. 311–328.

Buffler, R. T., and D. S. Sawyer, 1985, Distribution of crust and early history, Gulf of Mexico basin: Gulf Coast Association of Geological Societies Transactions, v. 35, p. 333–344.

Buffler, R. T., 1991, Seismic stratigraphy of the deep Gulf of Mexico basin and adjacent margins, *in* A. Salvador (ed.), The Gulf of Mexico Basin: The Geology of North America, v. J: Geological Society of America, Boulder, Colorado, p. 353-387.

Brown, L.F., and Fisher, W.L., (1980). Seismic stratigraphic interpretation and petroleum exploration: American Association of Petroleum Geologists Continuing Education Course Note Series 16.

Brun, J. and X. Fort, 2011, Salt tectonics at passive margins: geology versus models: Marine and Petroleum Geology, v. 28, p. 1123-1145.51

Bryant, W.R., Meyerhoff,A. A., Brown, N. K., Jr., Furrer, M. A., Pyle, T. E., and Antoine, J. W., 1969, Escarpments, reef trends and diapiric structures, eastern Gulf of Mexico: American Association of Petroleum Geologists Bulletin, v. 53, n. 12, p. 2506-2542.

Buffler, R. T., 1989, Distribution of crust, distribution of salt, and the early evolution of the Gulf of Mexico basin, *in* Gulf of Mexico salt tectonics, associated processes and exploration potential (abs.): Tenth Annual Research Conference Program and Abstracts, Gulf Coast Section of the SEPM, p. 25–27.

Buffler, R. T., and W. Thomas, 1994, Crustal structure and evolution of the southeastern margin of North America and the Gulf of Mexico basin, *in* R. C. Speed, ed., Phanerozoic evolution of North American continent–ocean transitions: Boulder, Colorado, Geological Society of America, The Geology of North America, v. CTV-1, p. 219–264

Chowns, T.M., and C.T. Williams, 1983, Pre-Cretaceous rocks beneath the Georgia coastal plain—regional implications: United States Geological Survey Professional Paper 1313-L, 42 p.

Corso, W. P., Austin, J. A., and R. T. Buffler, 1989, The early Cretaceous platform off northwest Florida: controls on morphologic development of carbonate margins: Marine Geology, v. 86, p. 1-14.

Corso, W. P., and J. A. Austin, 1995, Tectonic control of Early Cretaceous carbonate platforms in the Gulf of Mexico, 27th Annual Offshore Technology Conference Proceedings, Offshore Technology Conference7690, p. 495-505.

Debalko, D. A., and R. T. Buffler, 1992, Seismic stratigraphy and geologic history of Middle Jurassic through Lower Cretaceous rocks, deep eastern Gulf of Mexico: Gulf Coast Association of Geological Societies Transactions, v. 42, p. 89-105.

Dickinson, W.R., and Gehrels, G.G., 2008, U-Pb ages of detrital zircons in relation to paleogeography: Triassic paleodrainage networks and sediment dispersal across southwest Laurentia: Journal of Sedimentary Research, v. 78, p. 745–764.

Dobson, L. M., 1990, Seismic stratigraphy and geologic history of Jurassic rocks, northeastern Gulf of Mexico [Master's thesis]: University of Texas at Austin, Austin, Texas, 165 p.

Dobson, L. M., and R. T. Buffler, 1997, Seismic stratigraphy and the geologic history of Jurassic rocks, northeastern Gulf of Mexico: American Association of Petroleum Geologists Bulletin, v. 81, p. 100-120.

Doyle, L. J., and Holmes, C. W, 1985, Shallow structure, stratigraphy and carbonate sedimentary

processes of the West Florida upper continental slope: American Association of Petroleum Geologists Bulletin, v. 69, p. 1133-1144.

Driskill, B.W., Nunn, J.A., Sassen, R., and Pilger Jr, R.H., 1988, Tectonic subsidence, crustal thinning and petroleum generation in the Jurassic trend of Mississippi, Alabama and Florida: Gulf Coast Association of Geological Societies, v. 38, p. 257-265

Dunbar, J., and D.S. Sawyer, 1987, Implications of continental crust extension for plate reconstruction: an example from the Gulf of Mexico: Tectonics, v. 6, p. 739-755.

Freeman-Lynde, R. P., 1983, Cretaceous and Tertiary samples dredged from the Florida Escarpment, eastern Gulf of Mexico: Gulf Coast Association of Geological Societies Transactions, v. 33, p. 91-99.

Galloway, W.E., 2008, Depositional evolution of the Gulf of Mexico sedimentary basin: *in* Miall, A.D., ed.: The Sedimentary basins of the world v.5, The Sedimentary Basins of the United States and Canada, p. 505-549.

Gordon, M. B., Schneider, R. V., Hightower, S. L., Denman, H. E., and S. F. Scholz, 2001, Prestack depth imaging in the Eastern Gulf of Mexico, Part 2: Interpretation of the Mid-Cretaceous sequence boundary and underlying geologic events: The Leading Edge, v. 20, p. 396-399.

Hall, S., Shepherd, A., Titus, M., and Snow, R., 1984, Magnetics, *in* Buffler, R. T., Locker, S. D., Bryant, W. R., Hall, S. A., and Pilger, R. H., Jr., eds.. Gulf of Mexico: Woods Hole, Massachusetts, Marine Science International, Ocean margin Drilling Program Regional Atlas Series, Atlas 6, sheet 3.

Hall, S. A., and I. J. Najmuddin, 1994, Constraints on the tectonic development of the eastern Gulf of Mexico provided by magnetic anomaly data: Journal of Geophysical Research, v. 99, p. 7161–7175.

Haq, B. U., Hardenbol, J., and P. R. Vail, 1987, Chronology of fluctuating sea levels since the Triassic: Science, v. 235, p. 1156-1167.

Harbison, R. N., 1968, Geology of De Soto Canyon: Journal of Geophysical Research, v. 73, p. 5175–5185.

Hunt, B., 2013, Regional Norphlet Facies Correlation, Analysis and Implications For Paleostructure and Provenance, Eastern Gulf of Mexico [Master's Thesis]: The University of Alabama, Tuscaloosa, Alabama, 102 p.

Ibrahim, A. K., Carye, J., Latham, G., and R. T. Buffler, 1981, Crustal structure in Gulf of Mexico from OBS refraction and multichannel reflection data: American Association of Petroleum Geologists Bulletin, v. 65, p.1207-1229. 53

Imbert, P., Cramez, C., Talwani, M., and Jackson, M., 2001, Seaward-dipping reflectors in the eastern Gulf of Mexico: Implications for basin opening: Geological Society of America Abstracts with Programs, v. 33, no. 6, p. 157–158.

Jackson, M.P.A., and Talbot, C.J. (1986) External shapes, strain rates, and dynamics of salt structures: Geological Society of America Bulletin, v. 97, p.305-323

Jackson, M. P. A., and Vendeville, B. C., 1994, Initiation of salt diapirism by regional extension: global setting, structural style, and mechanical models*:* The University of Texas at Austin, Bureau of Economic Geology Report of Investigations No. 215, 39 p.

Jee, J.L., 1993, Seismic Stratigraphy of the Western Florida Carbonate Platform and History of Eocene Strata [Ph.D. Dissertation]: The University of Florida, Gainesville, Florida, 236 p.

Klitgord, K. D., Popenhoe, P., and H. Schouten, 1984, Florida: a Jurassic transform plate boundary: Journal of Geophysical Research, v. 89, p. 7753-7772.

Klitgord, K.D., Hutchinson, D.R.., and Schouten, H., 1988, U.S. Atlantic continental margin; Structural and tectonic framework, *in*, Sheridan, R.W., and Grow, J.A., eds., The Atlantic Continental Margin, U.S.: Geological Society of America, The Geology of North America, V. I-2, p. 19-55.

Ladd, J.W., R.T. Buffler, J.S. Watkins, J.L. Worzel, and A. Carranza, 1976, Deep seismic reflection results from the Gulf of Mexico: Geology, v. 4, p. 365-368

Lord, J., 1986, Seismic stratigraphic investigation of the West Florida Basin [Master's thesis]: Rice University, Houston, Texas, 207 p.

Lovell, T., and A. Weislogel, 2010, Detrital zircon U-Pb age constraints on the provenance of the Upper Jurassic Norphlet Formation, eastern Gulf of Mexico: Implications for paleogeography: Gulf Coast Association of Geological Societies Transactions, v. 60, p. 443-460.

MacRae, G., 1993, Mesozoic development of the Desoto Canyon Salt Basin in the framework of the early evolution of the Gulf of Mexico [Ph.D. dissertation]: Texas A&M University, College Station, Texas, 140 p.

MacRae, G., and J.S. Watkins, 1996, Desoto Canyon Salt Basin: tectonic evolution and salts structural styles, *in* Jones, J. O., and R. L. Freed, (eds.), Structural Framework of the Northern Gulf of Mexico, Gulf Coast Association of Geological Societies Special Publication, p. 53-61.

Mancini, E. A., Badali, M., Puckett, T. M., Parcell, W. C., and J. C. Llinas, 2001, Mesozoic carbonate petroleum systems in the northeastern Gulf of Mexico: Gulf Coast Section of

the Society for Sedimentary Geology Foundation 21st Annual Research Conference Proceedings, p. 423-451.

Martin, R.G., 1978, Northern and eastern Gulf of Mexico continental margin: stratigraphic and structural framework, in A.H. Bouma, G.T. Moore, and J.M. Coleman, eds., Framework, facies, and oil-trapping characteristics of the upper continental margin: American Association of Petroleum Geologists Studies in Geology 7, p. 21-42.

Marton, G., and R. T. Buffler, 1993, Application of simple shear model to the evolution of passive continental margins of the Gulf of Mexico basin: Geology, v. 21, p. 495-498.

May, P.R., 1971, Pattern of Triassic-Jurassic dikes around the North Atlantic in the context of the pre-drift positions of the Continents: Geological Society of America Bulletin, v. 82, p. 1285-1292.

Mickus, K., Stern, R.J., Keller, G.R., and Anthony, E.Y., 2009, Potential field evidence for a volcanic rifted margin along the Texas Gulf Coast, Geology, v. 37, p. 387-390.

Miller, J.A., 1982, Structural control of Jurassic sedimentation in Alabama and Florida: American Association of Petroleum Geologists Bulleting, v. 66, p. 1289-1301.

Mitchell-Tapping, H.J., 1982, Exploration analysis of the Jurassic Apalachicola embayment of Florida: Gulf Coast Association of Geological Societies Transactions, v. 32. p. 413-425.

Mitchum, R.M., Jr., 1978, Seismic stratigraphic investigation of west Florida slope, Gulf of Mexico, in Framework, facies, and oil-trapping characteristics of upper continental margin: American Association of Petroleum Geologists Studies in Geology, v. 7, p. 193-223.

Mutter, J.C., Talwani, M., and Stoffa, P.L., 1984, Evidence for a thick oceanic crust adjacent to the Norwegian margin: Journal of Geophysical Research, v. 89, p. 483–502.

Moore, C.H., 1984, Regional patterns of diagenesis, porosity evolution, and hydrocarbon production, upper Smackover of the Gulf rim: Gulf Coast Section of the Society for Sedimentary Geology Foundation 3rd annual Bob F. Perkins Research Conference, p. 283-307.

Obid, J. A., 2006, Sequence and seismic stratigraphy of the Jurassic strata in the northeastern Gulf of Mexico [Ph.D. dissertation]: University of Alabama, Tuscaloosa, Alabama, 253 p.

Perez Gutierrez, C.M., 2013, Structural Kinematics and Salt Evolution in the “Kuzam” Area; Offshore Southeast Gulf of Mexico: Implications for Petroleum Prospectivity [Master’s thesis], Colorado School of Mines, Golden, Colorado, 189 p.

Pindell, J. L. 1985, Alleghenian reconstruction and subsequent evolution of the Gulf of

Mexico, Bahamas, and Proto-Caribbean, Tectonics, 4(1), 1–39.

Pindell, J. and L. Kennan, 2001, Kinematic evolution of the Gulf of Mexico and Caribbean: Gulf Coast Section of the Society for Sedimentary Geology Foundation 21st Annual Research Conference Proceedings, p. 193-220.

Read, J.F., 1982. Carbonate platforms of passive (extensional continental margins: types, characteristics and evolution: Tectonophysics, v. 81, no. 3, p. 195-212

Rowan, M. G., 1993, A systematic technique for the sequential restoration of salt structures: Tectonophysics, v. 228, p. 331-348.

Salvador, A., 1987, Late Triassic-Jurassic paleogeography and origin of Gulf of Mexico Basin: American Association of Petroleum Geologists Bulletin, v. 71, p. 419-451.

Salvador, A., 1991, Origin and development of the Gulf of Mexico Basin, in A. Salvador, (ed.), The Gulf of Mexico Basin: The Geology of North America, v. J: Geological Society of America, Boulder, Colorado, p. 389-443.

Sawyer, D., and Harry, D., 1991, Dynamic modeling of divergent margin formation: application to the U.S. Atlantic margin: Marine Geology v. 102, p. 29-42.

Sawyer, D. S., Buffler, R. T., and R. H. Pilger Jr., 1991, The crust under the Gulf of Mexico Basin in A. Salvador, (ed.), The Gulf of Mexico Basin: The geology of North America, v. J: Geological Society of America, Boulder, Colorado, p. 53-72.

Shaub, F.J., Buffler, R.T., and Parsons, J.G., 1984, Seismic stratigraphic framework of deep central Gulf of Mexico Basin: American Association of Petroleum Geologists Bulletin, v. 68, p. 1790-1802.

Smith, D.L., 1983, Basement Model for the Panhandle of Florida, Gulf Coast Association of Geological Societies Transactions, v. 33, p. 203-208

Tew, B.H., Mink, R.M., Mann, S.D., Bearden, B.L., and Mancini, E.A., 1991, Geologic framework of Norphlet and pre-Norphlet strata of the onshore and offshore eastern Gulf of Mexico area: American Association of Petroleum Geologists Bulletin, v. 75, p. 1539-1562.

Thomas, W. A., 1976, Evolution of Ouachita-Appalachian continental margin: Journal of Geology, v. 84, p. 323-342.

Watkins, J.S., J.W. Ladd, R.T. Buffler, F.J. Shaub, M.H. Houston, and J.L. Worzel, 1978, Occurrence and evolution of salt in deep Gulf of Mexico, *in* A.H. Bouma, G.T. Moore, and J.M. Coleman, eds., Framework, facies, and oil-trapping characteristics of the upper continental margin: American Association of Petroleum Geologists Studies in Geology, v. 7, p. 43-65.

Watts, A.B., Karner, G.D., Stecker, M.S., 1982, Lithospheric Flexure and Evolution of Sedimentary Basins: Philosophical Transactions of the Royal Society of London, v. 305, No. 1489, pp. 249-281.

Wernicke, B., and Burchfiel, B.C., 1982, Modes of extensional tectonics: Journal of Structural Geology, v. 4, p. 105-115.

White, N., and D. McKenzie, 1988, Formation of the "steer's head" geometry of sedimentary basins by differential stretching of the crust and mantle: Geology, v. 16, p. 250-253.

Wilson, J.T., 1965, A new class of faults and their bearing on continental drift: Nature, v. 207, p. 343-347.

Wilson, K. L. 2011, The origin and development of the Tampa Embayment: implications for the tectonic evolution of the Eastern Gulf of Mexico [Master's thesis]: The University of Alabama, Tuscaloosa, Alabama, 57 p.

Winkler, C.D., and R.T. Buffler, 1988, Paleogeographic evolution of early deep-water Gulf of Mexico and margins, Jurassic to middle Cretaceous (Cenomanian): American Association of Petroleum Geologists Bulletin., v. 72, p. 318-346.

Wu, S., Vail, P. R., and Cramez, C., 1990, Allochthonous salt, structure, and stratigraphy of the north-eastern Gulf of Mexico. Part 1: Stratigraphy: Marine and Petroleum Geology, v. 7, p. 318-333.

Wu, S., Bally, A.W., and Cramez, C., 1990, Allochthonous salt, structure and stratigraphy of the north-eastern Gulf of Mexico. Part II: Structure: Marine and Petroleum Geology, v. 7, p. 334-370.